ABSTRACT

Trellis and Tree Search Algorithms for Equalization and Multiuser Detection

by

Abdulrauf Hafeez

Chair: Wayne E. Stark

This thesis deals with the detection of digital signals in the presence of inter-symbol interference (ISI) and/or multiple-access interference. We develop a new fractional maximum likelihood sequence estimation (MLSE) receiver which is suitable for wireless communication systems with excess signal bandwidth and fast time-varying channels. We investigate the effect of the receive filter and the branch metric on decision feedback sequence estimation (DFSE) and M-algorithm receivers, which are reduced-complexity alternatives to MLSE. The analysis leads to the classification of these receivers on the basis of the presence of untreated interference components, referred to as bias, which dominate the error-rate performance of the receiver. Bias arises in a DFSE or M-algorithm receiver due to a mismatch between the receive filter and the branch metric. We show that an unbiased receiver comprises a front-end filter matched to the overall channel or the transmit filter response followed by the appropriate noise-whitening or zero-forcing filter and a reduced trellis or tree search algorithm. Receivers with just a matched filter followed by a reduced trellis or tree search algorithm belong to the class of biased receivers.

We compare various trellis-based receivers on the basis of the distance of a given error sequence, which characterizes the probability of the associated error event. We show that whitening filter DFSE receivers maximize the error distance among unbiased DFSE receivers and truncated-memory MLSE receivers with pre-filtering. For matched filter DFSE

receivers. we describe bias compensation methods employing hard as well as soft tentative decisions, which significantly enhance performance in most cases without adding much complexity. Union bounds on the error probability of the various receivers are derived and evaluated using a modified generating function approach.

We derive an optimum forward-recursive soft-output algorithm which operates on the standard matched filter statistics and has complexity that grows exponentially with the channel memory only. We also derive a reduced-state soft-output algorithm which provides good symbol reliability estimates with reduced complexity. The performance of the various algorithms is compared for equalization of ISI and multiuser detection for direct-sequence code-division multiple-access systems via simulation and analytical examples.

To my dear parents, aunts, uncles and siblings.

ACKNOWLEDGEMENTS

I wish to thank God and all the people who have helped to make it possible for me to complete my graduate studies and this thesis. My gratitude goes to Wayne Stark, my thesis advisor, for his support and encouragement during the course of the study. I am also grateful to him for the invitation to accompany him to his sabbatical at Ericsson Inc., RTP, from which I benefited in many ways.

I gratefully acknowledge the support of Professor Alexandra Duel-Hallen of North Carolina State University in allowing me an office space and the use of research facilities in the department of Electrical and Computer Engineering at NCSU for more than a year. I benefited greatly from informal discussions with Dr. Gregory Bottomley and Dr. Karl Molnar of Ericsson Inc. and Prof. Alexandra Duel-Hallen and fellow student Ayman El-ezaby of NCSU. I also benefited from the company of several colleagues and fellow students here.

I wish to thank all the professors who I took courses with. I also appreciate the efforts of the doctoral committee in reading and evaluating this thesis. I wish to thank the Ministry of Science and Technology, Government of Pakistan for the Science and Technology scholarship award which made this endeavor possible. I also wish to thank the Army Research Office (grant number DAAH04-95-I-0246) and Ericsson Inc. for additional financial support.

Finally, I am deeply indebted to my family, especially my late father, my late uncles and my dear aunts, sisters and brothers. Without their unrelenting patience and encouragement, I would not have been able to complete this task.

TABLE OF CONTENTS

LIST OF TABLES

LIST OF FIGURES

Figure

LIST OF APPENDICES

CHAPTER 1

Introduction

Bandwidth efficient data transmission over wireline and wireless channels is made possible by the use of equalization techniques to compensate for the inter-symbol interference (ISI) introduced by the channel. In wireline channels like telephone lines, time dispersion results from non-ideal amplitude and phase characteristics of the medium and causes adjacent transmitted pulses to interfere with each other. In radio and undersea channels, the signal traverses several paths with differing amplitude and delay responses to reach the receiver. This phenomenon, known as multipath propagation, causes ISI. The problem of ISI also occurs in magnetic and optical recording channels due to non-ideal characteristics of the inductive read head. The medium is not always responsible for causing ISI. Bandwidth efficient design of signals, known as partial-response signaling, generally introduces controlled ISI to enable high-rate transmission.

Many wireline and wireless communication systems suffer from the impairment of multiple-access interference (MAI) in varying degrees. In code-division multiple-access (CDMA) systems, users share a common physical channel to transmit/receive non-orthogonal signals which interfere with each other. In hybrid time-division multiple-access/frequency-division multiple-access (TDMA/FDMA) systems, users reusing the frequency of the desired user in nearby cells cause co-channel interference. In twisted-pair local subscriber lines, crosstalk between users occurs due to the coupling of signals in adjacent wires. The problem of MAI can be alleviated by means of a multiuser detection technique. Such techniques have gained popularity especially in the case of direct-sequence CDMA (DS-CDMA) systems and are being considered for the next generation wireless systems as a key to improve capacity. Co-channel interference cancellation techniques are also being considered for the TDMA/FDMA

system based on the digital advanced mobile phone system (D-AMPS) standard.

The mitigation of ISI has been a prolific area of research for several decades [34]. Several techniques have been developed for equalization of ISI for pulse-amplitude modulated (PAM) systems which have been adopted for related problems, including MAI suppression. Maximum likelihood sequence estimation (MLSE) [6,13,22,40,43] is an optimal detection technique for channels with memory and additive noise. It minimizes the probability of sequence error for *a-priori* equiprobable sequences. The technique was first proposed by Forney [13] for optimum equalization of linear finite ISI channels with additive white Gaussian noise (AWGN). Later, other authors discovered applications of the MLSE algorithm to related problems. Verdú [43] derived an optimum multiuser detector for DS-CDMA systems by noting that the MAI in a DS-CDMA system can be viewed as cyclo-stationary ISI in a single-user system. The detector finds the joint maximum likelihood sequence of symbols for all users.

Maximum *a-posteriori* symbol-by-symbol detection (MAPSSD) is an optimal detection technique for channels with memory and additive noise which minimizes the probability of symbol error [1,3,23,28,42]. Conventional implementation of a MAPSSD receiver, compared to an MLSE receiver, has the added benefit of obtaining symbol *a-posteriori* probabilities (APP) which are useful for concatenated systems. Central to an MLSE (MAPSSD) receiver is a non-linear processor called the Viterbi algorithm (optimum soft-output algorithm). For a channel with delay response with finite length L (measured in symbol periods) and input alphabet size $\mathcal{A}$, the Viterbi algorithm employs a trellis with $\mathcal{A}^L$ states or nodes. The size of the trellis and the computational complexity of the algorithm become prohibitive if the channel has a long delay response. The algorithm can not be implemented for channels with infinite delay response. The same is true for an optimum soft-output algorithm (OSA). Thus, several low-complexity linear and non-linear techniques have been considered for equalization [34] as well as for multiuser detection [44]. Some of the most powerful complexity reduction techniques are non-linear techniques which are derived from an MLSE or MAPSSD receiver. These include decision feedback sequence estimation (DFSE) [7,8,10,11,17,19,20,39,50], truncated memory MLSE (TM-MLSE) [12,26,35,49], the M-algorithm [2,48,51] and Bayesian conditional decision feedback estimation (BCDFE) [18,25]. This thesis deals with analysis and derivation of MLSE and MAPSSD receivers and some of their most prominent reduced-complexity derivatives. New techniques are de-

veloped for applications in equalization and multiuser detection. Existing techniques are compared to each other and to the new techniques via analysis and simulation. Most work in this thesis is focussed on MLSE and related receiver structures. For this purpose, Chapter 2 sets up the system models for a single-user ISI system and a multiuser DS-CDMA system and describes optimum equalization and multiuser detection methods based on the MLSE technique. The notation developed there is followed throughout the thesis.

In wireless communication systems, the channel is generally considered as comprising a time-invariant transmit pulse-shaping filter and a time-varying and dispersive transmission medium. Forney's MLSE receiver comprises a front-end filter matched to the overall channel impulse response (the standard matched filter), followed by a symbol-rate sampler and a discrete-time noise-whitening filter to whiten the filtered noise affecting the statistics. The Viterbi algorithm operates on the whitened statistics to search for the most likely sequence transmitted using the Euclidean distance metric. Ungerboeck [40] derived an alternative MLSE formulation where the Viterbi algorithm operates directly on the statistics obtained after standard matched filtering, using a modified metric. In a time-varying environment, both receivers require an adaptive front-end filter which is not desirable for implementation purposes. Moreover, if the signal bandwidth is greater than the data rate, sampling at the symbol rate results in high sensitivity to the sampler timing phase [34]. Many narrowband communication systems utilize excess signal bandwidth. To handle these problems, Hamied *et al.* [22] proposed a receiver with a non-adaptive front-end filter matched to the transmit filter response (transmit matched filter), followed by a fractional-rate sampler and a fixed noise-whitening filter. However, due to the presence of nulls in the Nyquist band of practical pulse-shaping filters like the square-root raised cosine filter, the noise-whitening filter has a long slowly-damped delay response and any practical length truncation results in significant distortion. In Chapter 3, we derive a new fractional MLSE receiver that does not need a noise-whitening filter. The receiver is insensitive to the sampler timing phase. It exploits the knowledge of the pulse-shaping filter at the receiver and requires only one-step prediction for the medium response coefficients. These features make the receiver attractive for systems with excess signal bandwidth and fast time-varying media.

DFSE and TM-MLSE are trellis-based techniques where the complexity is controlled by reducing the memory of the trellis in the Viterbi algorithm. On the other hand, the M-algorithm is a tree-based technique where the complexity is reduced by pruning the tree

(representing sequence hypotheses) to maintain a given number of branches at each step. In TM-MLSE [12,35], the tail of the delay response of the channel is canceled by means of linear pre-filtering. In DFSE [7,8] and the M-algorithm [2], the tail of the delay response is canceled by feeding back past decisions taken from survivor paths in the trellis or tree. This manner of conditional decision feedback has been shown to alleviate the problem of error propagation that limits the conventional decision feedback equalizers. DFSE and M-algorithm receivers have been proposed to operate with whitened as well as standard matched filter statistics. It has been noted that the receive filter has a profound influence on the performance of these receivers [37,48,50]. However, this effect has not been quantified and understood.

In Chapter 4, we examine the effect of the receive filter and the branch metric on a generalized receiver comprising a front-end filter followed by a general transversal processing filter and a reduced trellis or tree search algorithm with conditional decision feedback. We consider two different formulations for the branch metric — in one case the front-end filter is the standard matched filter while in the other case, it is the transmit matched filter. The latter formulation is desirable for fractional equalization in the presence of excess signal bandwidth. A first error event analysis of the generalized receiver indicates that a proper combination of the processing filter and the branch metric is necessary to avoid *bias* (untreated interference components). The presence of bias severely limits the error-rate performance of a DFSE or M-algorithm receiver for most channels of interest. The various receivers are thus classified as biased and unbiased. Bias occurs in a DFSE or M-algorithm receiver due to a mismatch between the processing filter and the branch metric. We show that the processing filter must either be the appropriate noise-whitening filter (WF) or the zero-forcing filter (ZF) in order to achieve unbiasedness. Thus, the well-known DFSE and M-algorithm receivers with the whitening filter (WF-DFSE and WF-MA, respectively) belong to the class of unbiased receivers, while the receivers with just the matched filter (MF-DFSE and MF-MA) belong to the class of biased receivers.

The error-rate performance of the various DFSE and TM-MLSE receivers can be characterized by a parameter called the *error distance*. The error distance, in our case, does not merely mean the distance between two hypothesized signal sequences as in Forney [13], but it also includes the effect of noise enhancement. The distance of a given error sequence for a DFSE receiver depends on the type of filtering and the branch metric. The distance is max-

imized by the MF-DFSE receiver with the standard matched filter, while it is smaller for WF-DFSE and ZF-DFSE. This is due to the fact that the standard matched filter maximizes the output signal-to-noise ratio (SNR) by collecting all the energy of the pulse transmitted at a given time in the corresponding output sample. The noise-whitening filter spreads out the signal energy into several output samples in the process of whitening noise. The linear zero-forcing filter decorrelates all interfering signal components but enhances (and correlates) noise in the process. The reduced trellis-search algorithms which follow these filters recover part of the SNR that is spread out but are unable to recover all of it. Unfortunately, the drawback of MF-DFSE is that the reduced trellis search algorithm, in this case, is unable to resolve some anti-causal interfering signal components which generally dominate the error performance. Since the noise-whitening filter removes only the anti-causal signal components, which is necessary for unbiasedness, it maximizes the error distance among unbiased DFSE receivers. ZF-DFSE and TM-MLSE perform additional signal decorrelation and have lower error distance and thus inferior error-rate performance than WF-DFSE. The analysis ignores the effect of error propagation on DFSE receivers which, however, is small for most channels of interest. We obtain upper bounds on the symbol error probability of the various trellis based receivers assuming no error propagation and describe a generating function method to evaluate the union bounds.

Despite the unbiasedness and excellent error distance properties of WF-DFSE, its applicability is limited by the requirement of the noise-whitening filter. In applications where the noise at the output of the front-end filter is white, the algorithm can be employed without noise-whitening. However, the error performance in this case is highly sensitive to channel phase. While the best performance is obtained if the channel has minimum-phase, the performance may be rather poor if the channel has maximum or mixed phase. An all-pass filter is needed to get the minimum-phase channel. Computation of the additional processing filter requires channel inversion and/or factorization operations. This may not be desirable for applications involving time-varying channels and channels with deep spectral nulls. MF-DFSE is suitable for such applications. However, its performance is severely limited by the presence of bias as described earlier.

An intuitive solution to the problem of anti-causal interference components in MF-DFSE is to cancel them by means of tentative decision feedback. This results in bias-compensated MF-DFSE (BC-MF-DFSE) receivers which are described and analyzed in

Chapter 5. With reliable tentative decisions, the bias can be compensated effectively. As a result, the performance is no longer dominated by untreated interference components but rather by the excellent error distance. Tentative decisions can be obtained by using a decision device which delivers hard or soft decisions based on just the current input sample or by using a multistage configuration. Linear and non-linear minimum mean square error estimates of the symbols are considered as soft decisions. We obtain approximate upper bounds on the error probability for the various BC-MF-DFSE receiver configurations and describe a generating function technique to evaluate the bounds. Using several simulation and analytical examples, we find that a MF-DFSE receiver with soft bias compensation (SBC-MF-DFSE) provides a significant gain over MF-DFSE for most channels of interest without much added complexity. The receiver is particularly suitable for multiuser detection in DS-CDMA systems and performs quite well in near-far conditions.

Chapter 6 deals with soft-output algorithms. The optimum soft-output algorithm (OSA) of Li *et al.* [28] has complexity which grows exponentially with the channel memory and linearly with the decision lag. The algorithm operates on discrete-time statistics containing white noise. The algorithm of Hayes *et al.* [23] operates on the standard matched filter statistics but has complexity which is exponential in the decision lag. The optimum soft-output multiuser estimation algorithm of Verdú [42] requires a backward-forward recursion, due to which it has high latency. We derive an optimum soft-output algorithm with a forward-only-recursion which operates on the standard matched filter statistics. The algorithm has complexity similar to the OSA of Li *et al.*. We derive a reduced-complexity sub-optimal version of this algorithm which requires add-compare-select operations mostly. We also derive a reduced-state alternative to the OSA algorithm. The algorithm is obtained by modifying the algorithm of Lee *et al.* [25] which fails to generate reliable soft information. The complexity of the various algorithms is tabulated. The error-rate performance of the various algorithms is compared via simulation of a DS-CDMA system with convolutional coding and interleaving.

The thesis is organized as follows. In Chapter 2, we describe the system models for a single-user system with ISI and a multiuser DS-CDMA system. We describe optimum equalization and joint equalization/multiuser detection techniques for time-varying transmission media. In Chapter 3, we develop a new fractional MLSE receiver for systems with excess signal bandwidth and discuss its merits compared to other receivers. Chapter 4 deals

with analysis, classification and comparison of reduced trellis and tree search algorithms. In Chapter 5, we describe bias-compensation for matched-filter type receivers and compare the performance of the various receivers via simulation and approximate bounds which are obtained in this chapter. In Chapter 6, we derive novel soft-output algorithms and compare their performance via simulation. Conclusions are drawn and future work is discussed in Chapter 7.

CHAPTER 2

Optimum equalization and multiuser detection

2.1 Introduction

Maximum-likelihood sequence estimation (MLSE) is an optimum detection technique for signals corrupted with intersymbol interference (ISI) and additive white Gaussian noise (AWGN). The technique minimizes the probability of sequence error for *a priori* equiprobable sequences. Forney [13] provided the first MLSE formulation by noting the application of the Viterbi algorithm to equalization over a known time-dispersive, linear and time-invariant channel. Forney's formulation employs a filter matched to the overall channel impulse response (the standard matched filter) followed by a discrete-time noise-whitening filter[1] to produce discrete-time sufficient statistics which are processed by the Viterbi algorithm. Ungerboeck [40] later derived an alternative MLSE formulation which consists of just the standard matched filter and the Viterbi algorithm with a modified metric. The latter formulation was extended for the case of known time-varying channels by Bottomley *et al.* [6]. Verdú [43] derived an optimum multiuser detector for direct-sequence code-division multiple-access (DS-CDMA) channels with AWGN. The detector finds the joint maximum likelihood sequence of symbols for all users transmitted asynchronously over a common channel. Verdu's multiuser receiver is really an extension of Ungerboeck's MLSE formulation to joint detection of multiuser signals.

In this chapter, we describe optimum receivers for single-user equalization and joint equalization/multiuser detection for DS-CDMA systems in a known time-varying environment. This chapter sets up the system models and notation which is followed throughout

[1]The cascade of the two filters is referred to as the whitened matched filter.

the thesis. The chapter is organized as follows. In Section 2.2, we present the model for a single-user system with ISI. In Section 2.3, we describe the functionality of an MLSE receiver. In Section 2.4, we re-derive the Ungerboeck-Bottomley formulation for time-varying channels. In Section 2.5, we describe the model for a multi-user DS-CDMA system. In Section 2.6, we obtain an optimum receiver for joint equalization/multiuser detection as an extension of the Ungerboeck-Bottomley formulation.

2.2 System model

Consider the transmission of linearly-modulated digital data over a linear, time-dispersive medium. The system model consists of a transmitter, a linear time-varying transmission medium and a receiver. The baseband transmitted signal is modeled as

$$s_t(t) = \sum_{n=0}^{N-1} a_n d(t - nT) \tag{2.1}$$

where $d(t)$ is the impulse response of the transmit filter and $\{a_n\}_{n=0}^{N-1}$ is a finite sequence of complex symbols (taken from a finite alphabet $\mathcal{A}$). The radio signal transmitted propagates through the medium to reach the receiver where it is converted to a complex-valued, baseband signal $y(t)$, given by

$$\begin{aligned} y(t) &= g(\tau; t) * s_t(t) + w(t) \\ &= \int g(t - \lambda; t) s_t(\lambda) d\lambda + w(t) \end{aligned} \tag{2.2}$$

where $g(\tau; t)$ is the output of the transmission medium at time t when an impulse is applied at time $t - \tau$ and $w(t)$ is a complex white Gaussian noise process with power spectral density N_0. Substituting (2.1) in (2.2), we get

$$y(t) = \sum_{n=0}^{N-1} a_n h(t - nT; t) + w(t) \tag{2.3}$$

where $h(\tau; t)$ models the overall response of the transmit filter and the transmission medium and is given by

$$h(\tau; t) = \int g(\tau - \lambda; t) d(\lambda) d\lambda. \tag{2.4}$$

The received signal $y(t)$ is collected over a finite time interval, denoted I, which is much larger than $[0, (N-1)T]$. The response $h(\tau; t)$ is assumed to be square integrable over the

interval I, i.e.

$$\int_{-\infty}^{\infty} |h(\tau;t)|^2 d\tau < \infty \text{ for } t \in I. \tag{2.5}$$

2.3 Maximum likelihood sequence estimation

A maximum likelihood sequence estimation (MLSE) receiver finds the hypothetical sequence of symbols $\{\alpha_n\}$ ($\alpha_n \in \mathcal{A}$) that maximizes the likelihood of the received signal $y(t)$ given that $\{\alpha_n\}$ was transmitted. Assuming equiprobable symbols, an MLSE receiver maximizes the log-likelihood function derived from the *a posteriori* distribution of the received signal. Ignoring constant scaling factors and additive terms, the log-likelihood function reduces to

$$J_H = -\int_{t\in I} |y(t) - y_H(t)|^2 \, dt = -\int_{t\in I} \left| y(t) - \sum_{n=0}^{N-1} \alpha_n h(t - nT; t) \right|^2 dt, \tag{2.6}$$

where H is the hypothesis corresponding to the sequence $\{\alpha_n\}$. It is assumed that $y(t)$ is band-limited in the receiver front end, using a bandwidth larger than the signal bandwidth, so that the integral in (2.6) is well defined.

2.4 The Ungerboeck-Bottomley formulation

In this section, we re-derive an MLSE formulation following the development of Bottomley *et al.* [6]. The receiver is an extension of Ungerboeck's MLSE formulation [40] to time-varying channels.

The log-likelihood function J_H can be expanded as

$$J_H = A + B_H + C_H, \tag{2.7}$$

where

$$A = -\int_{t\in I} |y(t)|^2 dt, \tag{2.8}$$

$$B_H = \int_{t\in I} 2\mathrm{Re}\left\{ \sum_{n=0}^{N-1} \alpha_n^* h^*(t - nT; t) y(t) \right\} dt, \tag{2.9}$$

$$C_H = -\int_{t\in I} \sum_{n=0}^{N-1} \sum_{k=0}^{N-1} \alpha_n^* \alpha_k h^*(t - nT; t) h(t - kT; t) dt. \tag{2.10}$$

Since term A is independent of the sequence hypothesis, an MLSE receiver chooses the sequence hypothesis that maximizes the metric

$$\Lambda_H = B_H + C_H. \tag{2.11}$$

Terms B_H and C_H can be written as

$$B_H = \sum_{n=0}^{N-1} 2\mathrm{Re}\left\{\alpha_n^* z(n)\right\}, \tag{2.12}$$

$$C_H = -\sum_{n=0}^{N-1}\sum_{k=0}^{N-1} \alpha_n^* \alpha_k s(n-k;n), \tag{2.13}$$

where $\{z(n)\}_{n=0}^{N-1}$ is the sequence of symbol-spaced samples obtained at the output of a receive filter matched to the channel impulse response $h(\tau;t)$, as

$$z(n) = h^*(-\tau; t-\tau) * y(t)|_{t=nT} = \int_{t\in I} h^*(t-nT;t)y(t)dt \tag{2.14}$$

and the s parameter is the sampled channel autocorrelation function, given by

$$s(l;n) = \int_{t\in I} h^*(t-nT;t)h(t-(n-l)T;t)dt \tag{2.15}$$

where $n \in \{0,1,\ldots,N-1\}$ and $l \in \{0,\pm 1,\ldots,\pm(N-1)\}$. Noting that $s^*(k-n;k) = s(n-k;n)$ and using the following identity for multi-dimensional summation

$$\sum_{n=i}^{f}\sum_{k=i}^{f} x(n,k) = \sum_{n=i}^{f}\left[x(n,n) + \sum_{k=i}^{n-1}\left(x(n,k)+x(k,n)\right)\right], \tag{2.16}$$

the term C_H can be expanded as

$$C_H = -\sum_{n=0}^{N-1}\left[\alpha_n^*\alpha_n s(0;n) - \sum_{k=0}^{n-1} 2\mathrm{Re}\{\alpha_n^*\alpha_k s(n-k;n)\}\right]. \tag{2.17}$$

Substituting (2.12) and (2.17) into (2.11) and letting L be the smallest integer such that $s(l;n) = 0$ for $|l| > L$, we get the metric as

$$\Lambda_H = \sum_{n=0}^{N-1} \Gamma_n(\alpha_n, \sigma_n) \tag{2.18}$$

where σ_n represents the subsequence hypothesis $\sigma_n : \alpha_{n-1}, \alpha_{n-2}, \ldots, \alpha_{n-L}$ and $\Gamma_n(\alpha_n, \sigma_n)$ is the branch metric, given by

$$\Gamma_n(\alpha_n, \sigma_n) = \mathrm{Re}\left\{\alpha_n^*\left[2z(n) - s(0;n)\alpha_n - 2\sum_{l=1}^{L} s(l;n)\alpha_{n-l}\right]\right\}. \tag{2.19}$$

The receiver can be implemented as shown in Fig. 2.1. The front-end filter in the receiver is matched to the overall channel response $h(\tau;t)$. The Viterbi algorithm in Fig. 2.1 finds the sequence $\{\alpha_n\}$ that maximizes the metric of (2.18). It does so by computing recursively the accumulated metric defined as

$$\mathcal{M}_n(\sigma_n) \triangleq \max_{\alpha_1,\alpha_2,\ldots,\alpha_{n-L-1}} \sum_{i=0}^{n-1} \Gamma_n(\alpha_i,\sigma_i) \tag{2.20}$$

for all subsequence hypotheses (or states) σ_n. The recursion follows from (2.19) and (2.20) as

$$\mathcal{M}_n(\sigma_{n+1}) = \max_{\alpha_{n-L}} [\mathcal{M}_n(\sigma_n) + \Gamma_n(\alpha_n,\sigma_n)]. \tag{2.21}$$

The number of states in the Viterbi algorithm is $|\mathcal{A}|^L$, where $|\mathcal{A}|$ is the size of the input alphabet and L is the overall channel memory in symbols (assumed finite). The output of the Viterbi algorithm is the estimated sequence $\{\hat{a}_n\}$.

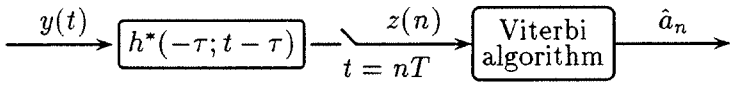

Figure 2.1: Ungerboeck-Bottomley receiver

2.5 Multiuser DS-CDMA system model

Consider a linear, time-dispersive channel shared by K users who transmit independent unsynchronized data streams by linearly modulating assigned signal waveforms. The system model consists of K transmitters, K independent time-varying and dispersive transmission media and one receiver. The baseband signal transmitted by user k is modeled as

$$s_{t,k}(t) = \sum_{m=0}^{N'-1} a_k(m) d_k(t - mT) \tag{2.22}$$

where $\{a_k(m)\}_{m=0}^{N'-1}$ is a finite sequence of complex symbols taken from a finite alphabet $\mathcal{A}$ (common to all users $k = 1,\ldots,K$). The filter $d_k(t)$ models the transmit filter for user k which, in general, includes a pulse-shaping filter common to all users and a signature waveform (spreading code) uniquely assigned to each user which may be pseudo-randomly

time-varying over the duration of several symbols (long code). The radio signal transmitted by each user propagates through a dispersive transmission medium to reach the receiver. The receiver sees the sum of the K signals in AWGN. The received signal is converted to a complex-valued, baseband signal $y(t)$, given by

$$y(t) = \sum_{k=1}^{K} g_k(\tau; t) * s_{t,k}(t - \tau_k) + w(t) \tag{2.23}$$

where $g_k(\tau; t)$ is the output of the transmission medium for user k at time t when an impulse is applied at time $t-\tau$, τ_k is the relative delay for user k and $w(t)$ is a complex white Gaussian noise process with power spectral density N_0. Substituting (2.22) into (2.23), we get

$$y(t) = \sum_{m=0}^{N'-1} \sum_{k=1}^{K} a_k(m) h_k(t - mT; t) + w(t) \tag{2.24}$$

where $h_k(\tau; t)$ models the overall response of the transmit filter and the transmission medium for user k and is given by

$$h_k(\tau; t) = \int g_k(\tau - \lambda; t) d_k(\lambda - \tau_k) d\lambda. \tag{2.25}$$

The above model accurately represents the uplink (mobile station to base station) of a DS-CDMA cell. The model can be simplified for the downlink (base station to mobile station) by considering synchronized user transmission over a single transmission medium.

From the viewpoint of joint multiuser detection/equalization, the multiuser system model of (2.24) can be represented equivalently in a single-user form as

$$y(t) = \sum_{n=0}^{N-1} a_{\kappa(n)}(\eta(n)) h_{\kappa(n)}(t - \eta(n)T; t) + w(t) \tag{2.26}$$

where $\kappa(n)$ and $\eta(n)$ represent the user index and the time index respectively and are given by

$$\kappa(n) = (n \bmod K) + 1 \tag{2.27}$$

$$\eta(n) = \left\lfloor \frac{n}{K} \right\rfloor \tag{2.28}$$

and $N = N'K$ is the length of the combined data stream of all users $\{a_{\kappa(n)}(\eta(n))\}_{n=0}^{N-1}$ which is ordered in increasing user and time indices assuming $\tau_k < \tau_{k+1}$ $\forall k$, without loss of generality . Henceforth, we will use the notation $\{a_n\}_{n=0}^{N-1}$ for the combined data sequence of all users for brevity.

Note that the above model has the same form as the single-user model of Section 2.2. This allows us to provide a unified treatment for problems of single-user equalization and multiuser detection. Throughout this thesis, we will consider receivers for single-user equalization which also find applications in multiuser detection. A special mention will be made where different considerations apply.

2.6 Joint equalization/multiuser detection

Noting the similarity between the multiuser system model of (2.26) and the single-user model of (2.3), it can be seen that a receiver that performs joint equalization and multiuser detection for DS-CDMA systems has the form of the Ungerboeck-Bottomley receiver of Section 2.4. The receiver is shown in Fig. 2.2. It consists of a bank of filters each of which is matched to the overall channel impulse response of a user. The sequence of joint statistics obtained at the output of the bank of filters is given by

$$z(n) = h^*_{\kappa(n)}(-\tau; t-\tau) * y(t)\Big|_{t=\eta(n)T} = \int_{t\in I} h^*_{\kappa(n)}(t-\eta(n)T; t)y(t)dt. \tag{2.29}$$

The receiver processes the joint sequence of matched filter statistics using the Viterbi algorithm which hypothesizes the symbols of all users jointly using the recursion of (2.21), where the branch metric is given by (2.19). The sampled channel autocorrelation function in this case is given by

$$s(l;n) = \int_{t\in I} h^*_{\kappa(n)}(t-\eta(n)T; t)h_{\kappa(n-l)}(t-\eta(n-l)T; t)dt. \tag{2.30}$$

The receiver is a generalization of Verdu's optimum multiuser detector [43] to linearly dispersive and time-varying transmission media. Note that the number of states in the Viterbi algorithm is $|\mathcal{A}|^L$, where the memory L is defined as the smallest integer such that $s(l;n)$ (given by (2.30)) equals zero for $|l| > L$. For non-dispersive media, $L = K-1$, while for dispersive (frequency-selective) media, $L > K-1$.

For the case of non-dispersive and time-invariant AWGN channels, a baseband asynchronous DS-CDMA system, with symbol-length (short) spreading codes and rectangular transmit pulses, is generally specified in terms of a code partial-correlation matrix polynomial known as the channel spectrum $S(D)$, given by

$$S(D) = S_1^T D^{-1} + S_0 + S_1 D \tag{2.31}$$

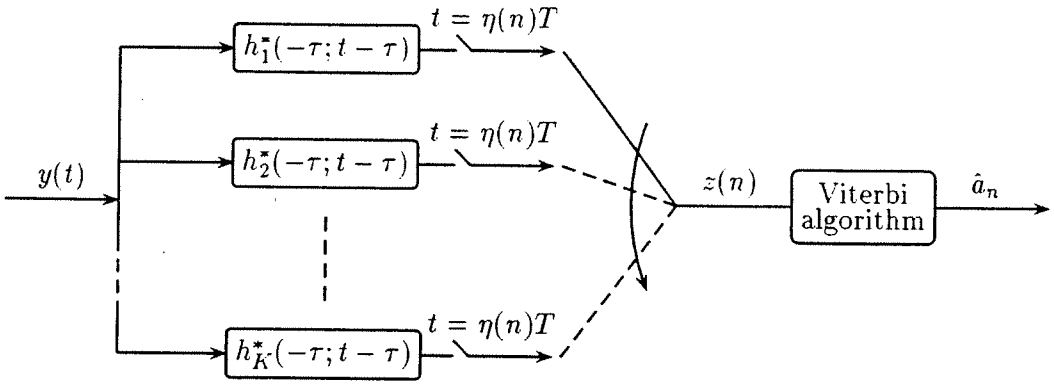

Figure 2.2: Multiuser receiver

where S_0 is a $K \times K$ Hermitian matrix and S_1 is a $K \times K$ upper-triangular matrix, assuming that the users are ordered in increasing delay. The element $S_0(i,j)$ of the matrix S_0 is the partial correlation of the code of user i with the code of user j for the current symbol period, i.e.

$$S_0(i,j) = \int d_i^*(t-\tau_i) d_j(t-\tau_j) dt. \tag{2.32}$$

The element $S_1(i,j)$ of the matrix S_1 is the partial correlation of the code of user i with the code of user j for the past symbol period, given by

$$S_1(i,j) = \int d_i^*(t-\tau_i) d_j(t-\tau_j+T) dt. \tag{2.33}$$

In this case, the normalized sampled channel correlations $\bar{s}(l;n) = s(l;n)/s(0;n)$ are given by

$$\bar{s}(l;n) = \begin{cases} S_1(\kappa(n), \kappa(n)-l+K) & \kappa(n)-l < 1 \\ S_0(\kappa(n), \kappa(n)-l) & 1 \le \kappa(n)-l \le K \\ S_1(\kappa(n)-l-K, \kappa(n)) & \kappa(n)-l > K \end{cases}. \tag{2.34}$$

The memory of the multiuser channel is $K-1$ and there is no ISI.

CHAPTER 3

Fractionally-spaced MLSE receivers

3.1 Introduction

In wireless communication systems, the channel is generally considered as comprising a time-invariant transmit (pulse-shaping) filter followed by a time-varying transmission medium. Forney and Ungerboeck's maximum-likelihood sequence estimation (MLSE) receivers [13,40] employ an analog front-end filter which is matched to the overall channel impulse response. If the transmission medium is time-varying or unknown at the receiver, the front-end filter has to be adaptive. This is not desirable for implementation purposes. Ungerboeck also described an adaptive receiver in [40] which uses a discrete-time transversal filter at the front end to synthesize matched filter characteristics. The receiver, however, does not take advantage of the fact that the transmit filter is generally known at the receiver and this information can be exploited to improve channel estimation.

Many wireless radio systems transmit signals with a bandwidth more than the data rate. Narrowband TDMA systems based on the IS-54/IS-136 and PDC standards employ 35% and 50% excess bandwidth, respectively. In the presence of excess signal bandwidth, fractional sampling is effective due to its insensitivity to the sampler timing phase [34]. Some authors [30,33] have considered using an analog front-end filter which is matched to the transmit filter response (transmit matched filter) followed by a fractional sampler. They, however, assume that the noise affecting the sampled statistics is white. The branch metric of the Viterbi algorithm ignores the correlation in the noise samples. As a result the performance improvement is marginal.

Hamied *et al.* [22] derived an MLSE receiver for systems that employ at most 100%

excess bandwidth. Their receiver employs a transmit matched filter followed by a fractional sampler and a fixed noise-whitening filter. The sequence of statistics thus obtained has white noise. However, we note that practical pulse-shaping filters like the square-root raised cosine filter have nulls in the Nyquist spectrum, due to which the noise-whitening filter has a long slowly-damped delay response. Any practical length truncation of the filter leads to severe distortion.

Following the development in [6], we derive an Ungerboeck-type receiver which does not need noise-whitening. The branch metric of the Viterbi algorithm accounts for the correlation in the noise samples affecting the fractionally sampled statistic obtained at the output of a transmit matched filter. An adaptive algorithm exploits the knowledge of the pulse-shaping filter and adapts just the fractionally-spaced medium response coefficients. However, the branch metric for the receiver depends on future medium response coefficients up to the span of the medium response. The prediction (adaptation) of these future coefficients using decision feedback would result in excess estimation error and thus degrade performance. We derive an alternative formulation for the branch metric which depends on causal medium response coefficients only. Thus, only one step prediction is needed to adapt the medium response coefficients. The receiver is suitable for systems with excess signal bandwidth and rapidly time-varying channels.

The chapter is organized as follows. In Section 3.2, we describe the channel model for a single-user system with excess signal bandwidth. A fractional Ungerboeck-type receiver is then derived in Section 3.3. In Section 3.4, we discuss the receiver of Hamied *et al.*. A new fractional MLSE receiver that does not need noise-whitening and minimizes channel prediction is described in Section 3.5.

3.2 Channel model

Consider the single-user system model of Section 2.2. If the baseband transmitted signal $s_t(t)$ has bandwidth $W \leq \nu/2T$, where ν is an integer, then an arbitrary medium response $g(\tau;t)$ can be modeled as a fractionally-spaced tapped delay line [41, pp. 488]

$$g(\tau;t) = \sum_j c(jT/\nu;t)\delta(\tau - jT/\nu) \tag{3.1}$$

where

$$c(jT/\nu;t) = c(j;t) = \int g(\tau;t)\mathrm{sinc}\left(\frac{\tau - jT/\nu}{T/\nu}\right) d\tau. \tag{3.2}$$

Assuming that the medium response can be well-approximated by L_c+1 fractionally-spaced taps (i.e. $c(j;t) = 0$ for $j > L_c$), the overall channel impulse response can be written as

$$h(\tau;t) = g(\tau;t) * d(\tau) = \sum_{j=0}^{L_c} c(j;t)d(\tau - jT/\nu). \tag{3.3}$$

Typically, $\frac{1}{2} < WT < 1$ for full-response signaling and $WT < \frac{1}{2}$ for partial-response signaling (continuous phase modulation) used in narrowband mobile communication systems. Symbol-spaced channel models have been used to develop MLSE receivers [24, 38]. Symbol-spaced MLSE receivers yield close to optimum performance if the excess signal bandwidth (WT in excess of $\frac{1}{2}$) is small. However, the performance of these receivers is highly sensitive to the timing phase [22] in the presence of excess bandwidth. This is due to the inability of a symbol-spaced transversal filter to invert a null in the sampled signal spectrum without excessive noise enhancement [34]. Fractionally-spaced MLSE receivers, on the other hand, are insensitive to the timing phase as aliasing does not occur in the sampled signal spectrum in the case of a fractionally-spaced transversal filter.

3.3 A fractional Ungerboeck-type receiver

Adaptation of channel parameters is usually needed for an MLSE receiver on time-varying channels. Ungerboeck's adaptive receiver [40] consists of a fractionally-spaced transversal filter followed by a symbol-rate sampler and a Viterbi algorithm. The coefficients of the front-end filter and the sampled channel autocorrelation function 's' are adapted using a stochastic steepest descent algorithm. The s parameters are needed to compute the branch metric (2.19) in the Viterbi algorithm. Note that the s parameters depend on the transmit filter response and the medium response. Since the transmit filter response is known at the receiver, channel estimation can be improved by adapting the medium response coefficients directly instead of adapting the s parameters. The formulation of Section 2.4 can be modified for this purpose as shown in [6] for the case of symbol-spaced channel models.

Substituting (3.3) in (2.14) and (2.15), and assuming that the medium response coeffi-

cients $c(j;t)$ are fixed (time-invariant) over the span of the transmit filter response[1] $d(t)$, we get

$$z(n) \approx \sum_{j=0}^{L_c} c^* \left(j; n + \frac{j}{\nu}\right) Y \left(n + \frac{j}{\nu}\right), \tag{3.4}$$

$$s(l;n) \approx \sum_{j=0}^{L_c} \sum_{k=0}^{L_c} c^* \left(j; n + \frac{j}{\nu}\right) c \left(k; n - l + \frac{k}{\nu}\right) \phi(l\nu + j - k), \tag{3.5}$$

where the discrete-time medium response coefficients are defined as $c(j;i) = c(jT;iT)$ for values of i in multiples of T/ν and $\{Y(\cdot)\}$ is the sequence of fractionally-spaced samples obtained at the output of a receive filter matched to the transmit filter response $d(t)$, as

$$Y \left(n + \frac{j}{\nu}\right) = \int_{t \in I} d^* \left(t - \left(n + \frac{j}{\nu}\right) T\right) y(t) dt \tag{3.6}$$

and $\phi(i)$ is the fractionally-sampled autocorrelation function of the transmit filter, given by

$$\phi(i) = \int_{t \in I} d^*(t) d \left(t + \frac{iT}{\nu}\right) dt. \tag{3.7}$$

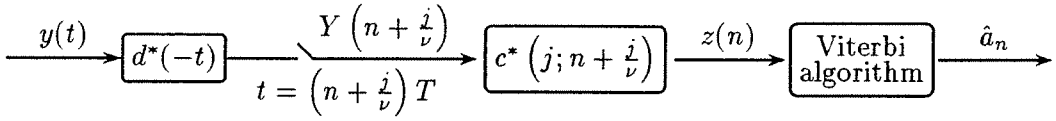

Figure 3.1: A fractional Ungerboeck-type receiver.

The receiver is shown in Fig. 3.1. It has a front-end filter matched to the transmit filter response $d(t)$, followed by a fractional-rate sampler. The fractionally-sampled statistic is filtered by an adaptive discrete-time filter and fed to a Viterbi algorithm. The Viterbi algorithm uses the branch metric of (2.19) with the s parameters given by (3.5). Note that the receiver in Fig. 3.1 has a fixed analog front-end filter unlike the receiver of Fig. 2.1, where the front-end filter is adaptive.

Note from (3.4) and (3.5), that the branch metric at time nT given by (2.19), depends on medium response coefficients for times up to $(n+L_c/\nu)T$. Thus, medium response coefficients have to be predicted (for L_c+1 future steps) in the adaptive receiver of Fig. 3.1. The accuracy of prediction decreases in general with the number of steps over which prediction

[1]The assumption makes sense when the time variation in the channel coefficients $c(j;t)$ is slow relative to the span of the transmit filter.

is required. This makes the adaptive receiver of Fig. 3.1 unsuitable for channels with rapid time variation.

3.4 Hamied's fractional MLSE receiver

An alternative receiver is obtained by noting that the statistic given by (3.6) can also be expressed as

$$Y\left(n+\frac{j}{\nu}\right)=\sum_{i=0}^{L_c} c\left(i;n+\frac{j}{\nu}\right)\sum_{l=-L_d}^{L_d}\phi(l)a_{n+\frac{j-i-l}{\nu}}+v\left(n+\frac{j}{\nu}\right) \tag{3.8}$$

where $\{v(\cdot)\}$ is a complex Gaussian noise sequence with autocorrelation

$$\mathrm{E}\left[v\left(n+\frac{j}{\nu}\right)v^*\left(m+\frac{i}{\nu}\right)\right]=N_0\phi((n-m)\nu+j-i), \tag{3.9}$$

$$a_{k/\nu}=\begin{cases} a_i & \text{if } k=i\nu,\ i \text{ is an integer} \\ 0 & \text{otherwise} \end{cases} \tag{3.10}$$

and L_d is the smallest integer such that $\phi(i)=0$ for $|i|>L_d$. Thus, it is assumed that the transmit filter has a finite impulse response. In practice, transmit pulse-shaping filters like the square-root raised cosine (SRRC) filter are truncated to a span of several symbols. Let the D-transform of the transmit filter autocorrelation function $\phi(n)$ (the sampled autocorrelation spectrum) be defined as

$$\Phi(D)=\sum_{n=-L_d}^{L_d}\phi(n)D^n \tag{3.11}$$

where D stands for fractional symbol duration.

Hamied *et al.* [22] obtain an adaptive MLSE receiver by assuming that the statistic $\{Y(\cdot)\}$ obtained at the output of the front-end filter in Fig. 3.1 can be whitened by using a fixed noise-whitening filter. The noise-whitening filter is determined by factoring the sampled autocorrelation spectrum $\Phi(D)$ as

$$\Phi(D)=F'^*(D^{-1})F'(D). \tag{3.12}$$

In case the transmit filter spectrum has no roots on the unit circle, the factor $F'(D)=\sum_{n=0}^{L_d} f'(n)D^n$ is chosen such that all its roots are outside the unit circle. The anti-causal noise-whitening filter is then given by $F'^*(D^{-1}))^{-1}$ which is stable in the sense that its coefficients are square summable.

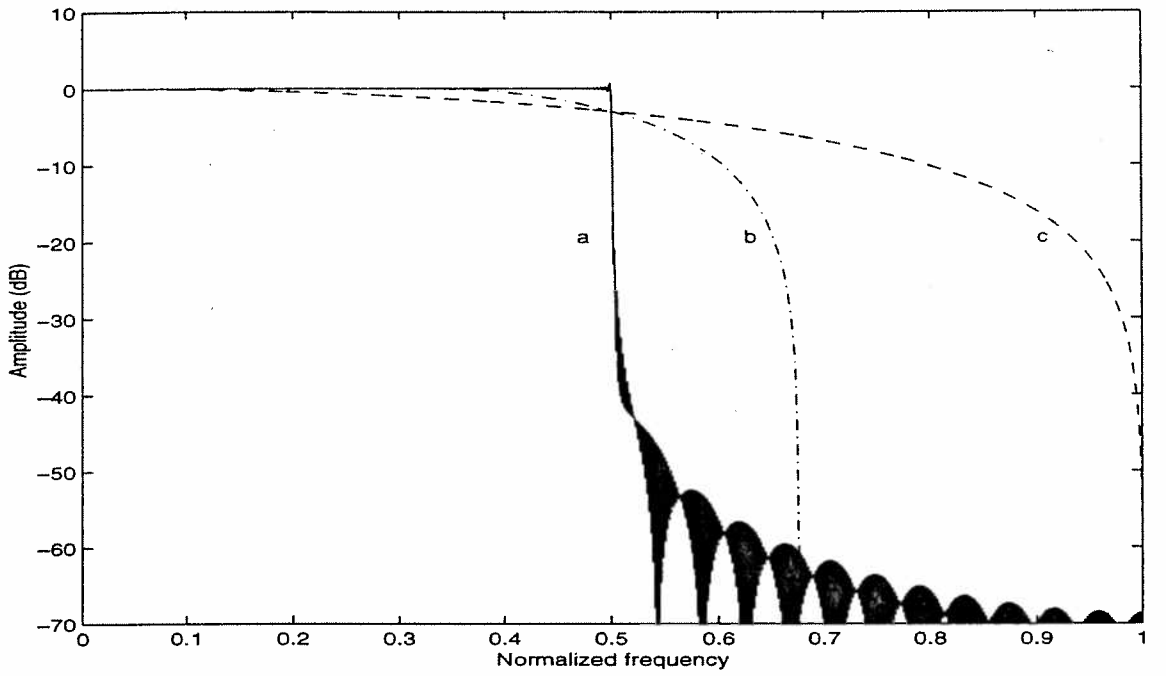

Figure 3.2: Sampled autocorrelation spectra for SRRC pulses truncated to 500 symbols (a) $\beta = 0$, (b) $\beta = 0.35$, (c) $\beta = 1$.

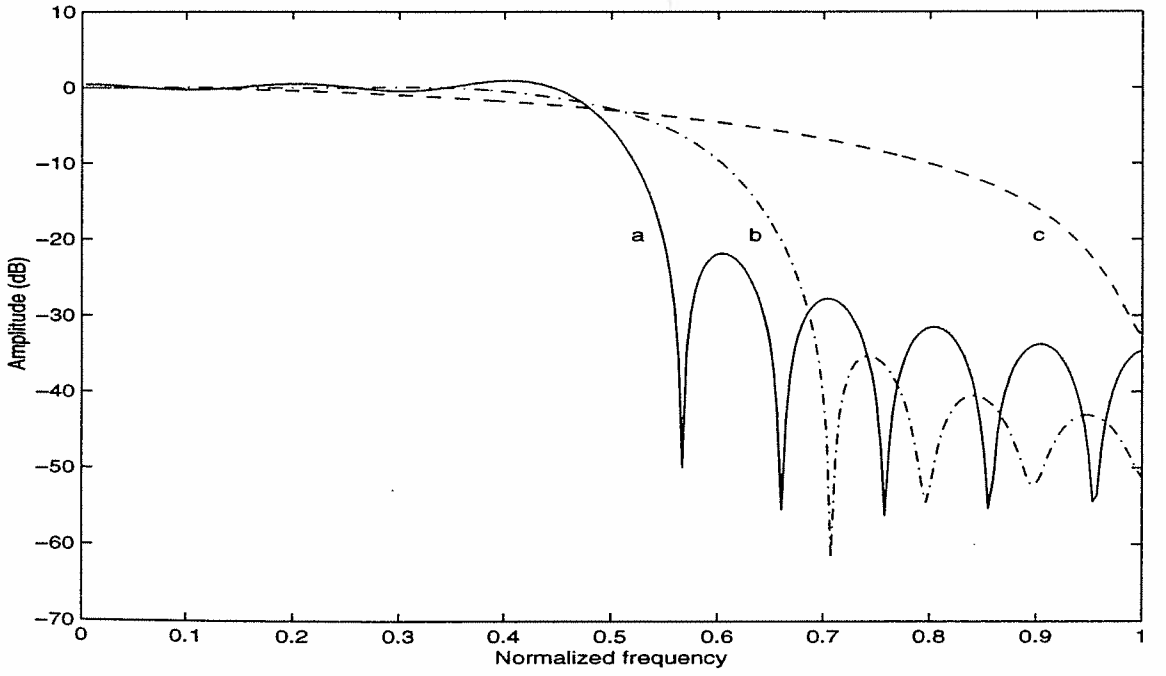

Figure 3.3: Sampled autocorrelation spectra for SRRC pulses truncated to 10 symbols (a) $\beta = 0$, (b) $\beta = 0.35$, (c) $\beta = 1$.

For many practical pulse-shaping filters like the SRRC filter, the sampled autocorrelation spectrum has zeros on the unit circle. This is illustrated in Fig. 3.2 which shows the amplitude of the sampled autocorrelation spectrum for SRRC pulses (truncated to a span of 500 symbols) with various roll-off factors. The spectrum exhibits nulls in the Nyquist bandwidth $1/T$ (corresponding to $\nu = 2$). This is true for all SRRC pulses with roll off factor $\beta \in [0, 1]$. The noise-whitening filter does not exist for these pulses as the nulls in the Nyquist band can not be inverted. Fig. 3.3 shows the sampled autocorrelation spectra for the same SRRC pulses but with a truncation of 10 symbols. Note that the nulls are less severe in this case. Strictly speaking, the noise-whitening filter exists for all practical finite-length transmit pulse-shaping filters. However, due to the presence of zeros near the unit circle, the noise-whitening filter has a long slowly-damped impulse response and any practical length truncation results in severe distortion. Fig. 3.4 shows the effect of truncation of the noise-whitening filter. The squared error resulting from truncation is given by

$$\|\hat{F}'(D) - F'(D)\|^2 \tag{3.13}$$

where $\hat{F}'(D)$ is the whitened channel spectrum obtained from using a truncated noise-whitening filter $\mathcal{W}(D^{-1})$ as $\hat{F}'(D) = \mathcal{W}(D^{-1})\Phi(D)$. Fig. 3.4 shows the squared error for the SRRC pulse of Fig. 3.3 (truncated to 10 symbols) with $\beta = 0.35$ and $\nu = 2$. Note that the squared error exhibits damped oscillations and is significant even with 500 taps of the noise-whitening filter (spanning 250 symbols). The error would increase with the length of the SRRC pulse because the nulls would be deeper as demonstrated in Fig. 3.2.

3.5 A new fractional MLSE receiver

In this section, we derive an alternative fractional MLSE receiver that does not require noise-whitening unlike the receiver of Hamied *et al.* [22]. Moreover, it does not require extra prediction for the medium response coefficients, unlike the Ungerboeck-type receiver of Fig. 3.1.

Substituting (3.4) into (2.12) and making a change of variables gives

$$B_H = \sum_{n=0}^{N-1} \sum_{m=0}^{\nu-1} 2\mathrm{Re}\left\{ \sum_{j=0}^{L_c} \alpha^*_{n+\frac{m-j}{\nu}} c^*\left(j; n+\frac{m}{\nu}\right) Y\left(n+\frac{m}{\nu}\right) \right\}. \tag{3.14}$$

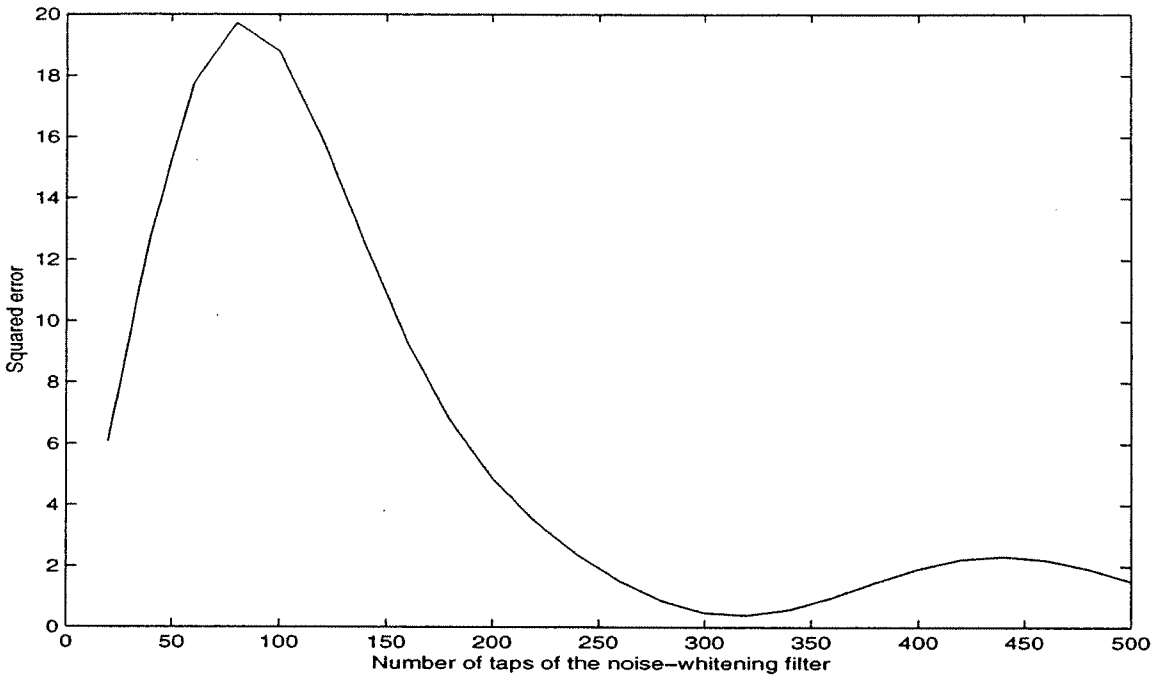

Figure 3.4: Squared error due to truncation of the noise-whitening filter for SRRC pulse truncated to 10 symbols with $\beta = 0.35$.

Substituting (3.5) into (2.13) and making a change of variables gives

$$C_H = -\sum_{n=0}^{(N-1)\nu}\sum_{j=0}^{L_c}\sum_{k=0}^{(N-1)\nu}\sum_{l=0}^{L_c}\alpha^*_{\frac{n-j}{\nu}}\alpha_{\frac{k-l}{\nu}}c^*\left(j;\frac{n}{\nu}\right)c\left(l;\frac{k}{\nu}\right)\phi(n-k). \tag{3.15}$$

Using (2.16), C_H can be written as

$$\begin{aligned} C_H = \; & -\sum_{n=0}^{N-1}\sum_{m=0}^{\nu-1}\sum_{j=0}^{L_c}\mathrm{Re}\left\{c^*\left(j;n+\frac{m}{\nu}\right)\alpha^*_{n+\frac{m-j}{\nu}}\left[\phi(0)\sum_{l=0}^{L_c}c\left(l;n+\frac{m}{\nu}\right)\alpha_{n+\frac{m-l}{\nu}}\right.\right. \\ & \left.\left. + \; 2\sum_{i=1}^{L_d}\phi(i)\sum_{l=0}^{L_c}c\left(l;n+\frac{m-i}{\nu}\right)\alpha_{n+\frac{m-i-l}{\nu}}\right]\right\}. \end{aligned} \tag{3.16}$$

Thus, the metric Λ_H in (2.11) can be written as

$$\Lambda_H = \sum_{n=0}^{N-1}\Gamma'_n(\alpha_n,\sigma_n) \tag{3.17}$$

where $\Gamma'_n(\alpha_n,\sigma_n)$ is the branch metric, given by

$$\begin{aligned} &\Gamma'_n(\alpha_n,\sigma_n) = \\ &\sum_{m=0}^{\nu-1}\sum_{j=0}^{L_c}\mathrm{Re}\left\{c^*\left(j;n+\frac{m}{\nu}\right)\alpha^*_{n+\frac{m-j}{\nu}}\left[2Y\left(n+\frac{m}{\nu}\right)\right.\right. \end{aligned}$$

$$- \phi(0) \sum_{l=0}^{L_c} c\left(l; n + \frac{m}{\nu}\right) \alpha_{n+\frac{m-l}{\nu}} - 2 \sum_{i=1}^{L_d} \phi(i) \sum_{l=0}^{L_c} c\left(l; n + \frac{m-i}{\nu}\right) \alpha_{n+\frac{m-i-l}{\nu}} \Bigg] \Bigg\} \quad (3.18)$$

Again using (2.16) for the term involving $\phi(0)$ in (3.18), the branch metric can alternatively be written as

$$\Gamma'_n(\alpha_n, \sigma_n) =$$
$$\sum_{m=0}^{\nu-1} \sum_{j=0}^{L_c} \mathrm{Re} \Bigg\{ c^*\left(j; n + \frac{m}{\nu}\right) \alpha^*_{n+\frac{m-j}{\nu}} \Bigg[2Y\left(n + \frac{m}{\nu}\right) - \phi(0) \Bigg(c\left(j; n + \frac{m}{\nu}\right) \alpha_{n+\frac{m-j}{\nu}}$$
$$+ 2 \sum_{l=1}^{L_c - j} c\left(j + l; n + \frac{m}{\nu}\right) \alpha_{n+\frac{m-j-l}{\nu}} \Bigg) - 2 \sum_{i=1}^{L_d} \phi(i) \sum_{l=0}^{L_c} c\left(l; n + \frac{m-i}{\nu}\right) \alpha_{n+\frac{m-i-l}{\nu}} \Bigg] \Bigg\} \quad (3.19)$$

The receiver is shown in Fig. 3.5. It employs a fixed front-end filter matched to the transmit filter response. The output of the front-end filter is sampled at the fractional-rate and fed to a Viterbi algorithm. The number of states in the Viterbi algorithm is $|\mathcal{A}|^L$, where $L = \left\lceil \frac{L_c + L_d}{\nu} \right\rceil$ is the overall channel memory in symbols. The Viterbi algorithm processes ν samples of the input statistic every symbol time T. The branch metric given by (3.18) or (3.19) has ν terms corresponding to each sample. Note that an ν step prediction of medium response coefficients is needed to compute the branch metric at each recursion. An alternative approach is to process one sample of the input statistic every T/ν seconds by computing one component (of the ν components) of the branch metric at each recursion followed by an update of the medium response coefficients. An advantage of this method is that the medium response coefficients can be estimated more accurately as only one step prediction is performed at the fractional rate.

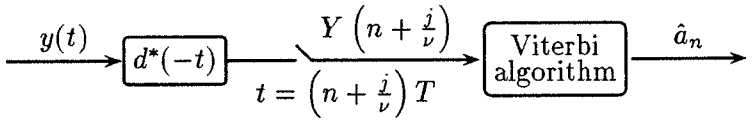

Figure 3.5: A new fractional MLSE receiver

For a symbol-spaced channel model ($\nu = 1$), the branch metric given by (3.19) simplifies to

$$\Gamma'_n(\alpha_n, \sigma_n) =$$

$$\sum_{j=0}^{L_c} \mathrm{Re}\left\{ c^*(j;n)\,a_{n-j}^* \left[2Y(n) - \phi(0)\left(c(j;n)\,a_{n-j} + 2\sum_{l=1}^{L_c-j} c(j+l;n)\,a_{n-j-l} \right) \right.\right.$$
$$\left.\left. - 2\sum_{i=1}^{L_d} \phi(i) \sum_{l=0}^{L_c} c(l;n-i)\,a_{n-i-l} \right] \right\} \tag{3.20}$$

which reduces to the "Partial Ungerboeck" formulation of Bottomley [6] for the case of Nyquist pulse-shaping (i.e. $\phi(n) = \delta(n)$).

3.6 Conclusions

In this chapter, we derived a new MLSE receiver for linearly-dispersive time-varying channels with additive white Gaussian noise. The receiver consists of a fixed analog front-end filter matched to the transmit pulse-shaping filter, a fractional sampler and a Viterbi algorithm. The branch metric of the Viterbi algorithm accounts for the correlation in the noise samples (due to fractional sampling) which is known at the receiver. The branch metric depends on causal fractionally-spaced medium response coefficients which can be adapted using only one step prediction. The receiver is suitable for communication systems with excess signal bandwidth and rapidly time-varying channels.

CHAPTER 4

Reduced Trellis and Tree Search Algorithms

4.1 Introduction

Maximum-likelihood sequence estimation (MLSE) [6, 13, 40, 43] is an optimum detection technique for channels with memory and additive noise. As the complexity of the various MLSE algorithms is exponential in the channel memory, several low-complexity suboptimal methods have been proposed. One method is to ignore the tail of the delay response or to select a subset of states in the Viterbi algorithm for reduced state detection [14, 45]. The residual interference that remains limits the performance of these methods even at modest intersymbol interference (ISI) levels [32]. Another approach is to pre-cancel the tail of the delay response using a linear or a decision feedback equalizer (DFE). The DFE approach [26, 49] suffers from severe error propagation on channels where the tail contains a significant fraction of the total energy in the channel while the linear pre-filtering approach [12, 35] enhances noise.

Decision feedback sequence estimation (DFSE) [7, 8, 10, 11, 17, 19, 20, 39, 50] and the M-algorithm [2, 48, 51] are two well-known reduced-complexity alternatives to MLSE. These algorithms find applications in equalization of ISI [7, 8, 10, 17, 19, 20, 39, 50], detection of partial response signals, trellis-coded modulation [8, 10, 11] and multiuser detection [17, 19, 20, 48, 51]. DFSE is a trellis-based method where the complexity is controlled by reducing the memory of the trellis in the Viterbi algorithm. On the other hand, the M-algorithm is a tree-based method where the complexity is reduced by pruning the tree (representing sequence hypotheses) to maintain a given number of branches at each step. Both schemes feed back conditional decisions taken from survivor paths to cancel the tail of the delay

response. This manner of decision feedback has been shown to alleviate the problem of error propagation that arises in the conventional DFE approach.

DFSE and M-algorithm receivers were originally proposed and thoroughly investigated for discrete-time statistics containing white noise for which case they have been thoroughly investigated [2, 8, 10, 39, 48]. However, receivers that operate on matched filter statistics have also been proposed for various applications [7, 17, 48, 50, 51]. The main advantage of these receivers is that they do not require noise-whitening. Computing the noise-whitening filter involves channel inversion and/or factorization operations which may not be feasible for time-varying, cyclo-stationary or bidirectional channels, or for channels with deep spectral nulls. Applications that particularly involve such channels include multiuser detection for direct-sequence code-division multiple-access (DS-CDMA) systems [19], bidirectional equalization for the global system for mobile communications (GSM) system [50] and fractional equalization for narrowband systems with excess signal bandwidth. An investigation of the DFSE and M-algorithm receivers with matched filter statistics is given in [20] and [48] respectively. It has been noted that the receive filter has a significant influence on the bit-error performance of these receivers.

In this chapter, we consider DFSE and M-algorithm receivers operating on the output of a general transversal processing filter which follows a front-end matched filter. We provide two different formulations of the branch metric — one for the case of standard matched filtering (front-end filter matched to the overall channel response) and the other for the case of transmit matched filtering (front-end filter matched to the transmit filter response). The latter formulation is desirable for fractional equalization in the presence of excess signal bandwidth. We conduct a first event error analysis of the various receivers which indicates that error events in certain receivers depend on the transmitted sequence. The error-rate performance of such receivers is affected, and generally dominated, by untreated interference components which we call *bias*. Bias occurs in a DFSE or M-algorithm receiver due to a mismatch between the processing filter and the branch metric. This leads to the classification of the various receivers as biased and unbiased, where the notion of "unbiasedness" means that error events are independent of the transmitted sequence given the error sequence.

We find that there exist only two processing filters for each type of matched filtering (i.e. standard and transmit) that result in unbiased receivers, namely the filter that whitens

(or partially decorrelates) the effect of the matched filter and the filter that zero-forces (or completely decorrelates) the effect of the matched filter. The whitening filter DFSE (WF-DFSE) and whitening filter M-algorithm (WF-MA) receivers with a standard matched filter are the well-known receivers described in [2, 8, 10, 39, 48]. The zero-forcing DFSE (ZF-DFSE) receiver with a standard matched filter was derived in [37]. The class of biased receivers includes matched filter DFSE (MF-DFSE) and matched filter M-algorithm (MF-MA) receivers where the matched filter statistic is fed directly into the reduced trellis or tree search algorithm without further processing. The MF-DFSE(S)[1] receiver was proposed in [7,50]. The MF-MA(S) receiver was proposed in [51] for multiuser detection.

We find the probability $\Pr(\varepsilon)$ of the occurrence of a given first event error ε for the various DFSE receivers. The probability $\Pr(\varepsilon)$ in the case of unbiased DFSE receivers is completely characterized by the error distance $\delta(\varepsilon)$ of the receiver. We use a broader definition for the error distance (than given in [13]) that includes the effect of noise enhancement. In the case of BPSK modulation, the probability $\Pr(\varepsilon)$ for an unbiased DFSE receiver is equal to the error probability of a memoryless system with signal amplitude equal to $\frac{1}{2}\delta(\varepsilon)$. We show that the error distance is maximized by the MF-DFSE(S) receiver. However, the error performance of the MF-DFSE(S) receiver is dominated by untreated interference components (bias) for most channels of interest and is therefore not very good. Among unbiased DFSE receivers, the error distance is maximized by the WF-DFSE receivers for each type of matched filtering. We also show that the error distance of truncated memory MLSE receivers that employ pre-filtering to reduce memory [12,35], is lower than the error distance of WF-DFSE. Thus, WF-DFSE receivers have the best error performance among these unbiased trellis-based receivers, not considering the effects of error propagation.

We obtain approximate upper bounds on the symbol error probability of the various DFSE receivers assuming absence of error propagation. We show that these bounds can be evaluated using a generating function method similar to MLSE, clearing the misconception that a generating function method is not applicable to DFSE receivers due to the use of decision feedback [39].

The chapter is organized as follows. The system model is given in Section 4.2. MLSE receivers that consist of a front-end matched filter followed by a general transversal processing filter are described in Section 4.3. The corresponding DFSE and M-algorithm receivers

[1]Where 'S' stands for standard matched filtering.

are described in Sections 4.4 and 4.5, respectively. In Section 4.6, we conduct a first event error analysis of the various receivers. Sections 4.7 and 4.8 deal with unbiased and biased receivers, respectively. In Section 4.9, we discuss truncated memory MLSE receivers that employs pre-filtering to reduce memory. In Section 4.10, we derive bounds on the symbol error probability of the various trellis-based receivers and in Section 4.11, we compare the error distance of the various receivers. In Section 4.12, we show how the bounds can be evaluated using an error state diagram. We compare the error-rate performance of the various receivers in Section 4.13 for a symbol-sampled system and a fractionally sampled system via simulation and analysis for some example channels.

4.2 System model

In this chapter, we assume the same system model as in Section 2.2 except with a time-invariant transmission medium. Thus, the baseband received signal is given by

$$y(t) = \sum_{n=0}^{N-1} a_n h(t - nT) + w(t) \tag{4.1}$$

where $h(t)$ represents the overall response of a transmit filter $d(t)$ and a time-invariant transmission medium, which is modeled as a tapped delay line with L_c complex-valued symbol-spaced tap coefficients $c(i)$,

$$h(t) = \sum_{i=0}^{L_c} c(i) d(t - iT). \tag{4.2}$$

4.3 A generalized MLSE receiver

Maximum likelihood sequence estimation (MLSE) is an optimal detection algorithm that minimizes the probability of sequence error for *a priori* equiprobable sequences. In this section, we describe an MLSE receiver with a general transversal processing filter. The processing filter has no influence on MLSE performance as we will see in the next section. However, the expressions developed in this section will be useful when we consider the effect of the processing filter on reduced trellis and tree search algorithms.

It is well-known [6, 13, 40] that the sequence of symbol-spaced samples $\{z(n)\}_{n=0}^{N-1}$ obtained at the output of a receive filter matched to the overall channel impulse response $h(t)$ forms a set of sufficient statistics for detecting the transmitted sequence $\{a_n\}_{n=0}^{N-1}$ given the

received signal $y(t)$. The matched-filter statistic $z(n)$ is given by

$$z(n) = h^*(-t) * y(t)|_{t=nT} = \int h^*(t - nT)y(t)dt \tag{4.3}$$

$$= \sum_i s(i)a_{n-i} + u_n. \tag{4.4}$$

In vector notation, the sequence of matched-filter statistics can be written as

$$\underline{z} = S\underline{a} + \underline{u} \tag{4.5}$$

where $\underline{a} = [a_0, a_1, \ldots, a_{N-1}]^T$, $\underline{z} = [z(0), z(1), \ldots, z(N-1)]^T$, $\underline{u} = [u(0), u(1), \ldots, u(N-1)]^T$, and S is an $N \times N$ Hermitian Toeplitz[2] matrix known as the channel spectrum. The (i,j)-th element of S is given by

$$s(i,j) = s(i-j) = \int h^*(t)h(t + (i-j)T)dt. \tag{4.6}$$

The elements $s(i)$ are samples of the autocorrelation function of the overall channel response which is assumed to have finite span. The smallest integer L such that $s(i) = 0$ for $|i| > L$ is known as the channel memory. We assume that the channel memory L is much smaller than the length N of the transmitted sequence. The matrix S is thus banded. The vector $\underline{u}$ is a discrete Gaussian noise vector with elements

$$u(n) = \int_{t \in I} h^*(t - nT)w(t)dt \tag{4.7}$$

and autocorrelation $\mathrm{E}[\underline{u}^H\underline{u}] = N_0 S$.

Consider a transversal processing filter P which processes the output of the matched filter. The output of the processing filter, which is an $N \times N$ matrix, is given by

$$\underline{x} = P\underline{z} = P(S\underline{a} + \underline{u}). \tag{4.8}$$

From (4.5), it follows that $\underline{x} = [x(0), x(1), \ldots, x(N-1)]^T$ is a Gaussian random vector with mean $PS\underline{a}$ and autocovariance $N_0 PSP^H$, given the information sequence $\underline{a}$. Assume that the inverse processing filter P^{-1} exists. Then, it is possible to recover the original sequence $\underline{z}$ from the filtered sequence $\underline{x}$. Thus, the sequence $\underline{x}$ forms a set of sufficient statistics for detecting the transmitted sequence $\underline{a}$ given the received signal $y(t)$.

Consider the receiver shown in Fig. 4.1. The receiver finds the hypothetical sequence of symbols $\{\alpha_n\}$ ($\alpha_n \in \mathcal{A}$) that maximizes the likelihood of the received signal $y(t)$ given

[2] i.e. the elements of S satisfy $s(i,j) = s(i-j)$.

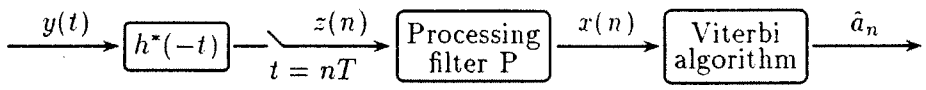

Figure 4.1: A generalized MLSE receiver

that $\{\alpha_n\}$ was transmitted. Assuming equiprobable symbols, the receiver maximizes the log-likelihood function derived from the *a posteriori* distribution of the received signal. Ignoring constant scaling factors and additive terms, the log-likelihood function reduces to

$$J_H = -(\underline{x} - PS\underline{\alpha})^H (PSP^H)^{-1} (\underline{x} - PS\underline{\alpha}) \tag{4.9}$$

where the superscript H stands for Hermitian transpose and the subscript H corresponds to the hypothesized sequence $\underline{\alpha}$. Neglecting terms common to all hypotheses, the metric to be maximized by the Viterbi algorithm can be written as

$$\Lambda_H = 2\mathrm{Re}\{\underline{\alpha}^H P^{-1} \underline{x}\} - \underline{\alpha}^H S \underline{\alpha}. \tag{4.10}$$

Assume that the matrix S is positive definite. Then, it can be decomposed into its unique Cholesky factors as

$$S = \tilde{F}^H \tilde{F} \tag{4.11}$$

where $\tilde{F}$ is an $N \times N$ invertible lower-triangular matrix. For $N \gg L$, the matrix $\tilde{F}$ is near Toeplitz[3]. Also note that

$$S = F_+^H F_+ \tag{4.12}$$

where F_+ is an $(N + L) \times N$ matrix with elements

$$f(i,j) = \begin{cases} f(i-j) & 0 \le i - j \le L \\ 0 & \text{otherwise} \end{cases} \tag{4.13}$$

obtained from the inverse z-transform of the minimum-phase Cholesky factor $F(z)$ of the z-transform of $\{s(i)\}$. Then, the metric in (4.10) can be written as

$$\Lambda_H = 2\mathrm{Re}\{\underline{\alpha}^H P^{-1} \underline{x}\} - \|F_+ \underline{\alpha}\|^2. \tag{4.14}$$

[3]The matrix has constant elements along each diagonal except the elements in some bottom rows.

The metric can be approximated as

$$\Lambda_H \approx 2\mathrm{Re}\{\underline{\alpha}^H P^{-1}\underline{x}\} - \|F\underline{\alpha}\|^2 \tag{4.15}$$

where F is an $N \times N$ lower-triangular Toeplitz matrix with elements given by (4.13). The approximation in (4.15) is a result of premature trellis termination in the Viterbi algorithm at the tail of the transmitted sequence. We adopt the approximate expression for the total metric (4.15) rather than (4.14) for simplicity of notation and analysis. In order to be consistent then, we let $S = F^H F$ throughout the rest of the chapter, without loss of generality.

The two expressions for the total metric (4.10) and (4.15) lead to two different additive decompositions (branch metrics). In order to obtain a general expression for the branch metric, we write the channel spectrum as

$$S = RQ \tag{4.16}$$

where R is an $N \times N$ upper-triangular Toeplitz matrix with elements

$$r(i,j) = \begin{cases} r(i-j) & -l_r \le i-j \le 0 \\ 0 & \text{otherwise} \end{cases} \tag{4.17}$$

where l_r is either 0 or L and Q is an $N \times N$ Toeplitz matrix with elements

$$q(i,j) = \begin{cases} q(i-j) & -L+l_r \le i-j \le L \\ 0 & \text{otherwise} \end{cases} \tag{4.18}$$

In (4.10), $R = I$ and $Q = S$ while in (4.15), $R = Q^H = F^H$.

Assume that the inverse processing filter consists of $l_p + l_f + 1$ coefficients ($l_p + 1$ causal and l_f anti-causal). The elements of the $N \times N$ banded Toeplitz matrix P^{-1} are given by

$$p'(i,j) = \begin{cases} p'(i-j) & -l_f \le i-j \le l_p \\ 0 & \text{otherwise} \end{cases} \tag{4.19}$$

This structure for the inverse processing filter encompasses many filters of interest, including the zero-forcing filter and the noise-whitening filter.

Using (4.17), (4.18) and (4.19), the total metric in (4.10) can then be written as

$$\Lambda_H = 2\mathrm{Re}\{\underline{\alpha}^H[(P^{-1})^L\underline{x}]\} + 2\mathrm{Re}\{[\underline{\alpha}^H(P^{-1})^{UD}]\underline{x}\} - [\underline{\alpha}^H R][(Q)^L\underline{\alpha}] - [\underline{\alpha}^H R(Q)^{UD}]\underline{\alpha} \tag{4.20}$$

where the superscripts L, U and D denote the lower-triangular, the upper-triangular and the diagonal part of a matrix, respectively. The above form for the total metric leads to the additive decomposition

$$\Lambda_H = \sum_{n=0}^{N-1} \Gamma(\alpha_n, \sigma_n) \tag{4.21}$$

where $\Gamma(\alpha_n, \sigma_n)$ is the branch metric corresponding to the state $\sigma_n : \alpha_{n-1}, \ldots, \alpha_{n-L_v}$ ($L_v = \max(L, l_f)$) in the trellis of the Viterbi algorithm, given by

$$\begin{aligned}\Gamma(\alpha_n, \sigma_n) &= 2\mathrm{Re}\left\{\alpha_n^* \sum_{l=1}^{l_p} p'(l)x(n-l) + x(n)\sum_{l=0}^{l_f} p'(-l)\alpha_{n-l}^*\right\} \\ &\quad - \left(\sum_{l=0}^{l_r} r(-l)\alpha_{n-l}^*\right)\left(\sum_{l=1}^{L} q(l)\alpha_{n-l}\right) - \alpha_n \sum_{l=0}^{l_r} r(-l) \sum_{k=0}^{L-l_r} q(-k)\alpha_{n-l-k}^* \end{aligned} \tag{4.22}$$

where $\alpha_n = 0$ for $N-1 < n < 0$ and $x(n) = 0$ for $n < 0$. The Viterbi algorithm recursively computes the accumulated metric given by

$$\mathcal{M}(\sigma_{n+1}) = \max_{\alpha_{n-L_v}} [\mathcal{M}(\sigma_n) + \Gamma(\alpha_n, \sigma_n)]. \tag{4.23}$$

for all subsequence hypotheses (or states) σ_n. The number of states in the Viterbi algorithm is $|\mathcal{A}|^{L_v}$ (note that the memory of the Viterbi algorithm L_v may be greater than the channel memory L). The output of the Viterbi algorithm is the estimated sequence $\{\hat{a}_n\}$.

Figure 4.2: An alternative MLSE receiver

An alternative MLSE receiver is shown in Fig. 4.2. It differs from the receiver of Fig. 4.1 in that it has a front-end filter which is matched to just the transmit filter response $d(t)$ instead of the overall channel response $h(t)$. The transmit filter matched-filter statistic $z'(n)$ is given by

$$\begin{aligned} z'(n) &= d^*(-t) * y(t)|_{t=nT} = \int d^*(t-nT)y(t)dt \\ &= \sum_{l=-L_d}^{L_d}\sum_{i=0}^{L_c} c(i)\phi(n, n-l)a_{n-l-i} + u'(n) \end{aligned} \tag{4.24}$$

which can be written in vector notation as

$$\underline{z}' = \Phi C \underline{a} + \underline{u}' \tag{4.25}$$

where $\underline{z}' = [z'(0), z'(1), \ldots, z'(N-1)]^T$, $\underline{u}' = [u'(0), u'(1), \ldots, u'(N-1)]^T$. The matrix C is a lower-triangular Toeplitz matrix with elements

$$c(i,j) = \begin{cases} c(i-j) & 0 \le i-j \le L_c \\ 0 & \text{otherwise} \end{cases} \tag{4.26}$$

and the matrix Φ is a Hermitian Toeplitz matrix with elements which are samples of the transmit filter autocorrelation function

$$\phi(i,j) = \phi(i-j) = \int d^*(t) d(t + (i-j)T) dt. \tag{4.27}$$

Let $\phi(i) = 0$ for $|i| > L_d$. The overall channel memory is then $L = L_c + L_d$. The vector $\underline{u}'$ is a Gaussian random vector with mean zero and autocorrelation $\mathrm{E}[\underline{u}'^H \underline{u}'] = N_0 \Phi$. Note that the statistic $\underline{z}$ can be obtained from the statistic $\underline{z}'$ as $\underline{z} = C^H \underline{z}'$. The sequence $\underline{z}'$, thus, forms a set of sufficient statistics for detecting the transmitted sequence given $y(t)$. The statistic $\underline{x}'$ input to the Viterbi algorithm is given by

$$\underline{x}' = P\underline{z}' = P(\Phi C \underline{a} + \underline{u}'). \tag{4.28}$$

The log-likelihood function in this case is given by

$$J'_H = -(\underline{x}' - P\Phi C \underline{\alpha})^H (P \Phi P^H)^{-1} (\underline{x}' - P\Phi C \underline{\alpha}) \tag{4.29}$$

which yields the likelihood metric to be maximized by the Viterbi algorithm in Fig. 4.2, as

$$\Lambda'_H = 2\mathrm{Re}\{\underline{\alpha}^H C^H P^{-1} \underline{x}'\} - \underline{\alpha}^H C^H \Phi C \underline{\alpha}. \tag{4.30}$$

Again two different additive decompositions of the above metric are possible corresponding to the two decompositions of the matrix Φ, i.e.

$$\Phi = R'Q' \tag{4.31}$$

where the elements of R' are given by

$$r'(i,j) = \begin{cases} r'(i-j) & -l_{r'} \le i-j \le 0 \\ 0 & \text{otherwise} \end{cases} \tag{4.32}$$

where $l_{r'}$ is either 0 or L_d and the elements of Q' are given by

$$q'(i,j) = \begin{cases} q'(i-j) & -L_d + l_{r'} \leq i-j \leq L_d \\ 0 & \text{otherwise} \end{cases} . \tag{4.33}$$

In one case $R' = I$, $Q' = \Phi$ and in the other case $R' = Q'^H = F'^H$. The matrix F' is a lower-triangular Toeplitz matrix with elements $f'(i)$ given by the inverse z-transform of the minimum-phase Cholesky factor $F'(z)$ of the z-transform of $\{\phi(i)\}$. Then, (4.30) can be written as

$$\Lambda'_H = \sum_{n=0}^{N-1} \Gamma'(\alpha_n, \sigma_n) = 2\mathrm{Re}\{\underline{\alpha}^H C^H P^{-1} \underline{x}'\} - \underline{\alpha}^H C^H R' Q' C \underline{\alpha} \tag{4.34}$$

where the branch metric $\Gamma'(\alpha_n, \sigma_n)$ is given by

$$\begin{aligned} \Gamma'(\alpha_n, \sigma_n) \;=\; & 2\mathrm{Re}\left\{ \left(\sum_{l=0}^{L_c} c^*(l) \alpha^*_{n-l} \right) \left(\sum_{l=1}^{l_p} p'(l) x'(n-l) \right) + x'(n) \sum_{l=0}^{L_c} c^*(l) \sum_{k=0}^{l_f} p'(-k) \alpha^*_{n-l-k} \right\} \\ & - \left(\sum_{l=0}^{L_c} c^*(l) \sum_{k=0}^{l_{r'}} r'(-k) \alpha^*_{n-l-k} \right) \left(\sum_{l=0}^{L_c} c(l) \sum_{k=1}^{L_d} q'(k) \alpha_{n-l-k} \right) \\ & - \left(\sum_{l=0}^{L_c} c^*(l) \sum_{k=0}^{l_{r'}} r'(-k) \sum_{m=0}^{L_d - l_{r'}} q'(-m) \alpha^*_{n-l-k-m} \right) \left(\sum_{l=0}^{L_c} c(l) \alpha_{n-l} \right) . \end{aligned} \tag{4.35}$$

The memory of the Viterbi algorithm in this case is $L'_v = \max(L, L_c + l_f)$. Note that the receiver of Fig. 4.2 can be easily extended for the case of a fractionally-spaced medium response model. In this case, the output of the transmit matched filter in Fig. 4.2 is sampled at a multiple of the symbol rate (say ν/T). The memory of the Viterbi algorithm is $\lceil L'_v/\nu \rceil$ and the branch metric is modified by replacing α_n in (4.35) by π_n, given by

$$\pi_n = \begin{cases} \alpha_{n/\nu} & n/\nu \text{ integer} \\ 0 & \text{otherwise} \end{cases} . \tag{4.36}$$

4.4 Decision Feedback Sequence Estimation

Decision feedback sequence estimation (DFSE) is a reduced complexity alternative to maximum likelihood sequence estimation which provides an adjustable performance/complexity tradeoff. Proposed by Duel-Hallen *et al.* [7,8][4] and Eyuboglu *et al.* [10], the scheme employs a reduced trellis search algorithm to search through a subset of sequence hypotheses searched by the full-blown Viterbi algorithm. The complexity is controlled by a parameter

[4]The algorithm is referred to as Delayed Decision Feedback Sequence Estimation in [7,8]

called the memory order J, which is chosen arbitrarily smaller than the memory of the Viterbi algorithm. The trellis in the reduced trellis search algorithm then comprises $|\mathcal{A}|^J$ states corresponding to the J most recent symbol hypotheses. Survivor paths or sequences are chosen in the reduced trellis search algorithm on the basis of the same cost function as in MLSE (i.e. the accumulated likelihood metric). A transition in the reduced trellis specifies the $J+1$ most recent hypothesized symbols. The remaining $L-J$ symbols needed to compute the branch metric are obtained from decisions taken from the survivor history (past decisions) of the path.

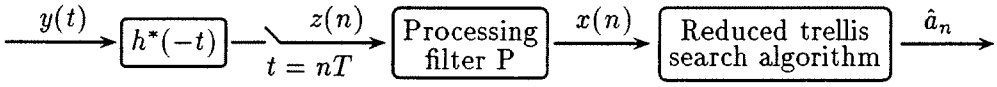

Figure 4.3: A generalized DFSE receiver

The DFSE algorithms proposed by Duel-Hallen *et al.* operate on matched-filter and whitened statistics obtained from conventional matched filtering and whitened matched filtering respectively. Here we generalize the DFSE algorithm to operate with a general transversal processing filter. The receiver is shown in Fig. 4.3. The reduced trellis search algorithm has memory order J chosen such that $0 \leq J \leq L_v$. It employs the recursion:

$$\mathcal{M}(\beta_{n+1}) = \max_{\alpha_{n-J}} [\mathcal{M}(\beta_n) + \Gamma(\alpha_n, \beta_n)] \tag{4.37}$$

where $\beta_n : \alpha_{n-1}, \alpha_{n-2}, \ldots, \alpha_{n-J}$ represents states in the reduced trellis at time n, $\mathcal{M}(\beta_n)$ is the accumulated metric of the survivor path associated with state β_n and $\Gamma(\alpha_n, \beta_n)$ is the corresponding branch metric given by

$$\begin{aligned}\Gamma(\alpha_n, \beta_n) &= 2\mathrm{Re}\left\{\alpha_n^* \sum_{l=1}^{l_p} p'(l)x(n-l) + x(n)\sum_{l=0}^{l_f} p'(-l)\eta_{n-l}^*\right\} \\ &- \left(\sum_{l=0}^{l_r} r(-l)\eta_{n-l}^*\right)\left(\sum_{l=1}^{L} q(l)\eta_{n-l}\right) - \alpha_n \sum_{l=0}^{l_r} r(-l) \sum_{k=0}^{L-l_r} q(-k)\eta_{n-l-k}^* \end{aligned} \tag{4.38}$$

where at time n

$$\eta_{n-i} = \begin{cases} \alpha_{n-i} & 0 \leq i \leq J \\ \hat{\alpha}_{n-i}(\beta_n) & J+1 \leq i \leq L_v \end{cases} . \tag{4.39}$$

In (4.39), $\{\hat{\alpha}_i(\beta_n)\}$ are tentative conditional decisions on symbols more than J samples in the past obtained from the history of the survivor path associated with state β_n, as

$$\hat{\alpha}_{n-J}(\beta_n) = \arg\max_{\alpha_{n-J}} [\mathcal{M}(\beta_n) + \Gamma(\alpha_n, \beta_n)]. \tag{4.40}$$

The reduced trellis branch metric $\Gamma(\alpha_n, \beta_n)$ of (4.38) corresponds to the full trellis branch metric $\Gamma(\alpha_n, \sigma_n)$ given by (4.22). Note that the (whitened matched filter) DFSE algorithm of [8] is obtained by substituting $P^{-1} = R = Q^H = F^H$ and the DFSE algorithm with the standard matched filter, proposed in [7], is obtained by substituting $P^{-1} = R = I$, $Q = S$. In the first case, the whitened channel F with coefficients $\{f(n)\}$ is minimum-phase.

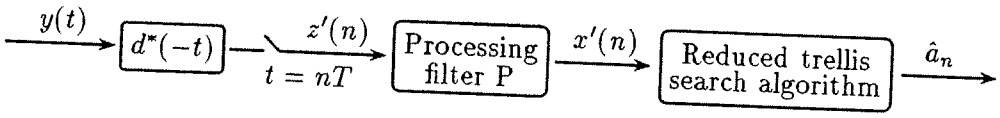

Figure 4.4: An alternative DFSE receiver

An alternative DFSE receiver shown in Fig. 4.4 corresponds to the MLSE receiver of Fig. 4.2, in that the front-end filter is matched to the transmit filter response. It follows the recursion:

$$\mathcal{M}'(\beta_{n+1}) = \max_{\alpha_{n-J}} [\mathcal{M}'(\beta_n) + \Gamma'(\alpha_n, \beta_n)] \tag{4.41}$$

where the memory order is chosen in the range $0 \le J \le L'_v$ and the reduced trellis branch metric $\Gamma'(\alpha_n, \beta_n)$ is obtained by replacing α_{n-i} in (4.35) by

$$\eta'_{n-i} = \begin{cases} \alpha_{n-i} & 0 \le i \le J \\ \hat{\alpha}'_{n-i}(\beta_n) & J+1 \le i \le L'_v \end{cases} \tag{4.42}$$

where $\{\hat{\alpha}'_i(\beta_n)\}$ are tentative conditional decisions obtained as

$$\hat{\alpha}'_{n-J}(\beta_n) = \arg\max_{\alpha_{n-J}} [\mathcal{M}'(\beta_n) + \Gamma'(\alpha_n, \beta_n)]. \tag{4.43}$$

The branch metric is given by

$$\Gamma'(\alpha_n, \sigma_n) = 2\mathrm{Re}\left\{ \left(\sum_{l=0}^{L_c} c^*(l) \eta'^*_{n-i} \right) \left(\sum_{l=1}^{l_p} p'(l) x'(n-l) \right) + x'(n) \sum_{l=0}^{L_c} c^*(l) \sum_{k=0}^{l_f} p'(-k) \eta'^*_{n-l-k} \right\}$$

$$- \left(\sum_{l=0}^{L_c} c^*(l) \sum_{k=0}^{l_{r'}} r'(-k) \eta'^*_{n-l-k} \right) \left(\sum_{l=0}^{L_c} c(l) \sum_{k=1}^{L_d} q'(k) \eta'_{n-l-k} \right)$$
$$- \left(\sum_{l=0}^{L_c} c^*(l) \sum_{k=0}^{l_{r'}} r'(-k) \sum_{m=0}^{L_d - l_{r'}} q'(-m) \eta'^*_{n-l-k-m} \right) \left(\sum_{l=0}^{L_c} c(l) \eta'_{n-l} \right). \quad (4.44)$$

With $P = R' = Q' = I$, we get the case of Nyquist pulse-shaping[5] at the transmitter and transmit-filter matched-filtering at the receiver. This results in the DFSE receiver of [8] where the statistic is white without any linear processing and the channel C with coefficients $\{c(n)\}$ may have any phase (minimum, mixed, or maximum phase). With $P^{-1} = R' = Q'^H = F'^H$, the whitened channel $F'C$ with coefficients $\{f'(n) * c(n)\}$ has mixed phase in general. With $P^{-1} = R' = I$, $Q' = \Phi$, we get the DFSE receiver corresponding to the new fractional MLSE formulation of Section 3.5.

4.5 M-Algorithm

The M-algorithm (MA) [2] is well-known as another reduced complexity alternative to MLSE. The scheme was originally proposed to operate on white (or whitened) statistics. However, it has also been used with the standard matched filter (see for example [48,51]). The M-algorithm is essentially a reduced tree search algorithm. At each step, M survivor paths (hypothesized sequences) are extended to $M\mathcal{A}$ paths, of which the M paths with the best accumulated likelihood metric are retained and the rest are discarded.

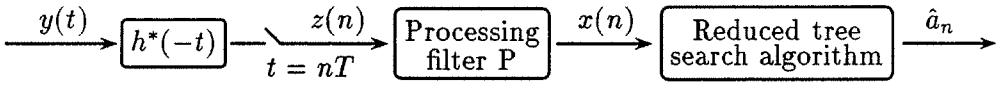

Figure 4.5: A generalized M-algorithm receiver

In this section, we extend the M-algorithm to operate with a general transversal processing filter. The receiver is shown in Fig. 4.5. Let $\underline{\alpha}_n(j) = (\alpha_0, \alpha_1, \ldots, \alpha_{n-1})$ be one of the M survivor paths ($j = 1, \ldots, M$) at time n. At time $n+1$, the reduced tree search algorithm extends each survivor into $\mathcal{A}$ paths $\underline{\alpha}_{n+1} = (\underline{\alpha}_n(j), \alpha_n)$ and computes their accumulated

[5] Using transmit pulses that satisfy the Nyquist criterion for ISI free transmission.

likelihood metric using

$$\mathcal{M}(\underline{\alpha}_{n+1}) = \mathcal{M}(\underline{\alpha}_n(j)) + \Gamma(\alpha_n, \sigma_n(j)) \tag{4.45}$$

where the branch metric $\Gamma(\alpha_n, \sigma_n(j))$ which depends on the last L_v hypothetical symbols $\sigma_n(j)$ in the survivor path $\underline{\alpha}_n(j)$, is given by (4.22). The M paths with the highest accumulated metric are then selected.

An alternative M-algorithm receiver has a front-end filter matched to the transmit filter response and uses the branch metric of the MLSE receiver of Fig. 4.2, given by (4.35).

4.6 First Event Error Analysis

In this section, we examine the first event error (FEE) probability of the generalized DFSE receiver of Section 4.4 (Fig. 4.3) and the generalized M-algorithm receiver of Section 4.5 (Fig. 4.5). We say that a *first event error* is made in the reduced trellis or tree search algorithm (at time j) if the correct path is abandoned for the first time in favor of a competitor path or paths that diverge from the correct path at time j. Note that our definition of a first event error is different from the definition given in [29], in that we consider the start time of an error event as the time of its occurrence as opposed to the end time as in [29]. We assume that the channel is stationary. Thus, a first event error is independent of the start time and time 0 can be chosen as the start time without loss of generality.

4.6.1 Trellis Search Algorithms

Consider the generalized DFSE receiver of Fig. 4.3. Let $\{a_n\}$ be the sequence of symbols transmitted and $\{b_n\}$ $(b_n : a_{n-1}, a_{n-2}, \ldots, a_{n-J})$ be the sequence of states in the path of $\{a_n\}$ in the reduced trellis of the DFSE receiver (with memory order J). Let $\{\bar{a}_n\}$ be a hypothetical sequence of symbols and $\{\bar{b}_n\}$ be the corresponding sequence of states in the reduced trellis that diverges from the correct sequence of states at time unit 0 and re-merges with it at a later time (say k), i.e.

$$\bar{b}_n = b_n \text{ for } n = 0, k \text{ and } \bar{b}_n \neq b_n \text{ for } 0 < n < k. \tag{4.46}$$

A first event error occurs at time 0 if the reduced trellis search algorithm picks $\{\bar{a}_n\}$ as the survivor sequence over $\{a_n\}$. It follows from (4.37) that the event occurs if the metric

accumulated on the incorrect path is greater than the metric accumulated on the correct path i.e.

$$\sum_{n=0}^{k-1} \Gamma(\bar{a}_n, \bar{b}_n) > \sum_{n=0}^{k-1} \Gamma(a_n, b_n) \tag{4.47}$$

where $\{\Gamma(a_n, b_n)\}$ and $\{\Gamma(\bar{a}_n, \bar{b}_n)\}$ are branch metrics corresponding to the paths $\{a_n\}$ and $\{\bar{a}_n\}$ respectively, computed using (4.38). Note that the conditional decisions $\{\hat{a}_{n-l}(b_n)\}$ and $\{\hat{a}_{n-l}(\bar{b}_n)\}$ which are fed back to compute the branch metrics, are taken from the paths corresponding to the sequences of states $\{b_n\}$ and $\{\bar{b}_n\}$ respectively. Thus, $\hat{a}_{n-l}(b_n) = a_{n-l}$ and $\hat{a}_{n-l}(\bar{b}_n) = \bar{a}_{n-l}$ and (4.47) can be written in matrix notation as

$$2\mathrm{Re}\{\underline{\bar{a}}_k^H (P^{-1})_k \underline{x}_k\} - \underline{\bar{a}}_k^H R_k Q_k \underline{\bar{a}}_k > 2\mathrm{Re}\{\underline{a}_k^H (P^{-1})_k \underline{x}_k\} - \underline{a}_k^H R_k Q_k \underline{a}_k \tag{4.48}$$

where $\underline{a}_k = [a_0, a_1, \ldots, a_{k-1}]^T$, $\underline{\bar{a}}_k = [\bar{a}_0, \bar{a}_1, \ldots, \bar{a}_{k-1}]^T$ and $\underline{x}_k = [x(0), x(1), \ldots, x(k-1)]^T$. The matrices $(P^{-1})_k$, R_k and Q_k are principal submatrices[6] of dimension k of the matrices P^{-1}, R and Q respectively given by (4.16), (4.17), (4.18) and (4.19). Defining $\underline{e}_k = \underline{\bar{a}}_k - \underline{a}_k$ as the error sequence and noting that $R_k Q_k = Q_k^H R_k^H$, (4.48) can also be expressed as

$$2\mathrm{Re}\{\underline{e}_k^H (P^{-1})_k \underline{x}_k\} > \underline{e}_k^H R_k Q_k \underline{e}_k + 2\mathrm{Re}\{\underline{e}_k^H R_k Q_k \underline{a}_k\}. \tag{4.49}$$

From (4.8), it follows that

$$\underline{x}_k = P_{k\times N}(S\underline{a} + \underline{u}) \tag{4.50}$$

where $P_{k\times N}$ is the $k \times N$ matrix comprising the top k rows of the matrix P. Using (4.50), (4.49) can be written as

$$2\mathrm{Re}\{\underline{e}_k^H (P^{-1})_k P_{k\times N} \underline{u}\} > \underline{e}_k^H R_k Q_k \underline{e}_k + 2\mathrm{Re}\{\underline{e}_k^H R_k Q_k \underline{a}_k\} - 2\mathrm{Re}\{\underline{e}_k^H (P^{-1})_k P_{k\times N} S\underline{a}\} \tag{4.51}$$

which is the condition for the error event ε : $\underline{a}_k$ is eliminated in favor of $\underline{a}_k + \underline{e}_k$ (with $\underline{a}_k$ and $\underline{e}_k$ given, i.e. non-random). The error event ε is associated with the error sequence $\underline{e}_k$. The length of the error event is $k - J$ symbols, not counting the last J components of $\underline{e}_k$ which must be zero as $\bar{b}_k = b_k$ according to (4.46).

MLSE

In the case of maximum likelihood sequence estimation, the memory order is $J = L_v$ (Viterbi algorithm). Thus, we have $e_{k-i} = 0$ for $i = 1, 2, \ldots, L_v$. Using the fact that $R_k Q_k$

[6]The principal submatrix of dimension k of a square matrix A (with dimension $\geq k$) is obtained by erasing all but the first k rows and columns of A.

is a square banded matrix with $L \leq L_v$ elements in the right band[7], we get

$$\underline{e}_k^H R_k Q_k \underline{e}_k = \underline{e}_{k-L_v}^H S_{k-L_v} \underline{e}_{k-L_v} \tag{4.52}$$

$$\underline{e}_k^H R_k Q_k \underline{a}_k = \underline{e}_{k-L_v}^H S_{k-L_v \times k} \underline{a}_k \tag{4.53}$$

where $\underline{e}_{k-L_v} = [e_0, e_1, \ldots, e_{k-L_v-1}]^T$ and $S_{k-L_v \times k}$ is a $(k - L_v) \times k$ matrix comprising the top $k - L_v$ rows of S_k. Since $(P^{-1})_k$ is a banded matrix with $l_f \leq L_v$ elements in the right band), the top $k - L_v$ rows of $(P^{-1})_k P_{k \times N}$ are given by $[I_{k-L_v} | O_{k-L_v \times N+L_v-k}]$ and we have

$$\underline{e}_k^H (P^{-1})_k P_{k \times N} S \underline{a} = \underline{e}_{k-L_v}^H S_{k-L_v \times k} \underline{a}_k \tag{4.54}$$

Combining (4.52), (4.53) and (4.54) with (4.51), we see that the error event ε occurs in an MLSE receiver if

$$2\mathrm{Re}\{\underline{e}_{k-L_v}^H \underline{u}_{k-L_v}\} > \underline{e}_{k-L_v}^H S_{k-L_v} \underline{e}_{k-L_v}. \tag{4.55}$$

Given the error sequence $\underline{e}_k$, the left hand side of (4.55) is a Gaussian random variable with mean 0 and variance $4N_0 \underline{e}_{k-L_v}^H S_{k-L_v} \underline{e}_{k-L_v}$. Thus, the probability of the error event ε is given by

$$\Pr(\varepsilon) = \mathrm{Q}\left(\frac{1}{2}\sqrt{\frac{\underline{e}_{k-L_v}^H S_{k-L_v} \underline{e}_{k-L_v}}{N_0}}\right) \tag{4.56}$$

It follows from (4.46) and (4.56) that the first event error probability can be over-bounded using a union bound, as

$$P_{FEE} \leq \sum_{\underline{e} \in E} p_{\underline{e}} \mathrm{Q}\left(\frac{\delta(\underline{e})}{2\sqrt{N_0}}\right) \tag{4.57}$$

where E is the set of all error sequences $\underline{e} = e_0, e_1, \ldots, e_{l-1}$ (such that $l > 0$, $e_{l-1} \neq 0$) with less than J consecutive zeros in the midst of the sequence, $p_{\underline{e}}$ is the *a priori* probability of the error sequence $\underline{e}$ and $\delta(\underline{e})$ is known as the distance of the error sequence $\underline{e}$ and is given by

$$\delta(\underline{e}) = \sqrt{\underline{e}^H S_l \underline{e}} = \sqrt{\sum_{i=0}^{l-1} \sum_{j=0}^{l-1} e_i^* s(i-j) e_j}. \tag{4.58}$$

Notice that the first event error probability given by (4.57) is independent of the processing filter P and the form of the branch metric used. It is the same as obtained by Forney [13] and Ungerboeck [40] for MLSE receivers with specific processing filter and branch metric combinations. Our result validates the fact that the Viterbi algorithm does in fact yield

[7]The elements on the right hand side of (but not including) the diagonal.

maximum likelihood sequence estimates regardless of the form of the processing filter as long as the inverse processing filter P^{-1} exists and the trellis is expanded by $l_f - L$ symbols if the number of anti-causal taps l_f of P^{-1} is greater than the channel memory L.

DFSE

For a memory order $J < L$, the first term on the right hand side of (4.51) depends on the error sequence $\underline{e}_k$ only, while the other two terms depend, in addition, on the transmitted sequence $\underline{a}$. These terms do not cancel for a general transversal processing filter P and thus represent "raw or untreated" interference. The error performance of a DFSE receiver thus depends on the processing filter unlike the case of an MLSE receiver. Moreover, the error performance also depends on the branch metric formulation employed by the reduced trellis-search algorithm. This can be seen by noting that the two branch metric formulations: $R_k = Q_k^H = F_k^H$ and $R_k = I_k$, $Q_k = S_k$ result in different error distance and interference terms as $F_k^H F_k \neq S_k$. Note that the asymptotic equivalence of the matrices S and $F^H F$ (for N large) assumed in Section 4.3 does not apply here, as error events are generally short, i.e. $k \ll N$.

In view of the above discussion, it is desirable to have a processing filter plus branch metric combination which eliminates the problem of untreated interference and maximizes the error distance. We devise the notion of "unbiasedness" to describe such DFSE receivers whose error performance is not affected by untreated interference (or bias). Let E' be the set of all error sequences in the set E with J zeros appendid at the tail.

Definition 4.6.1 *A DFSE receiver is termed "unbiased" if each error event ε (corresponding to an error sequence in E') is conditionally independent of the transmitted sequence $\underline{a}$ given the error sequence $\underline{e}_k$, for any memory order $0 \leq J < L_v$.*

It can be expected that an unbiased DFSE receiver would have good error performance for any memory order. On the other hand, a biased DFSE receiver would be affected by untreated interference components and could thus exhibit an error floor. In order to obtain an unbiased DFSE receiver, one must find a processing filter that causes the cancelation of the interference terms in (4.51) for any memory order. It follows that such a processing filter P must satisfy the condition:

$$(P^{-1})_k P_{k\times N} S = R_k Q_k [I_k | O_{k\times N-k}] \quad \forall\, 1 \leq k < N \tag{4.59}$$

or equivalently (noting that $R_k Q_k = Q_k^H R_k^H$ for the cases in hand):

$$(P^{-1})_k P_{k\times N} = Q_k^H (Q^{-H})_{k\times N} \quad \forall\, 1 \le k < N \tag{4.60}$$

where the matrix $(Q^{-H})_{k\times N}$ comprises the top k rows of the matrix Q^{-H}.

It follows from (4.51) and (4.59) that the probability of the error event ε for an unbiased DFSE receiver is given by

$$\Pr(\varepsilon) = \mathrm{Q}\left(\frac{\underline{e}_k^H R_k Q_k \underline{e}_k}{2\sqrt{N_0 \underline{e}_k^H R_k Q_k (S^{-1})_k R_k Q_k \underline{e}_k}}\right). \tag{4.61}$$

The first event error probability for an unbiased DFSE receiver can then be overbounded as

$$P_{FEE} \le \sum_{\underline{e}\in E'} p_{\underline{e}} \mathrm{Q}\left(\frac{\delta(\underline{e})}{2\sqrt{N_0}}\right) \tag{4.62}$$

where $\delta(\underline{e})$ is the distance of the error sequence $\underline{e}$ defined, in general, as

$$\delta(\underline{e}) \triangleq \frac{\underline{e}^H R_k Q_k \underline{e}}{\sqrt{\underline{e}^H R_k Q_k (S^{-1})_k R_k Q_k \underline{e}}} \tag{4.63}$$

where the subscript k denotes the length of the composite error sequence $\underline{e}$. Note that the above definition of the error distance includes the effect of noise enhancement (the term in the denominator of (4.63)).

A first event error analysis of the alternative DFSE receiver of Fig. 4.4 is similar to the analysis presented above and is given in Appendix A.

4.6.2 Tree Search Algorithms

Consider the generalized M-algorithm receiver of Fig. 4.5. Let $\{a_n\}$ be the sequence of symbols transmitted. Let $\underline{a}_k(i)$ ($i \in \{0, 1, \ldots, M\mathcal{A} - 1\}$) be the $M\mathcal{A}$ paths extended at a time unit $k > \log_{\mathcal{A}} M$, including the correct path $\underline{a}_k(0) = \underline{a}_k$. A first event error occurs at time 0 in the M-algorithm receiver if the tree search algorithm eliminates the path $\underline{a}_k$. It follows from (4.45) that the error event occurs if the metric accumulated on the correct path is less than the metric accumulated on at least M of the other extended paths, i.e.

$$\mathcal{M}(\underline{a}_k) < \mathcal{M}(\underline{a}_k(i)) \tag{4.64}$$

for at least M values of $i \in \mathcal{I} = \{1, 2, \ldots, M\mathcal{A} - 1\}\}$. Let $\{\sigma_n(i)\}_{n=0}^{k-1}$ be the sequence of states[8] in the path of $\underline{a}_k(i)$. Then, using (4.45), (4.64) can be written as

$$\sum_{n=0}^{k-1} \Gamma(a_n(i), \sigma_n(i)) > \sum_{n=0}^{k-1} \Gamma(a_n, \sigma_n(0)). \tag{4.65}$$

Defining $\underline{e}_k(i) = \underline{a}_k(i) - \underline{a}_k$ as an error sequence and following the development of (4.51), we get equivalently

$$\begin{aligned} 2\mathrm{Re}\{\underline{e}_k(i)^H (P^{-1})_k P_{k\times N} \underline{u}\} \;>\; & \underline{e}_k(i)^H R_k Q_k \underline{e}_k(i) + 2\mathrm{Re}\{\underline{e}_k(i)^H R_k Q_k \underline{a}_k\} \\ & -2\mathrm{Re}\{\underline{e}_k(i)^H (P^{-1})_k P_{k\times N} S \underline{a}\} \end{aligned} \tag{4.66}$$

for at least M values of $i \in \mathcal{I}$. This is the condition for the error event ε' : $\underline{a}_k$ is eliminated in favor of M of the extended paths $\underline{a}_k + \underline{e}_k(i)$ (with $\underline{a}_k$ and $\underline{e}_k(i)$ given, $i \in \mathcal{I}$).

Notice that like the case of the DFSE receiver, the error performance of the generalized M-algorithm receiver depends on the processing filter and is, in general, affected by untreated interference components. Thus, the concept of "unbiasedness" also applies to M-algorithm receivers. Specifically, we define a class of unbiased M-algorithm receivers as follows

Definition 4.6.2 *An M-algorithm receiver is termed "unbiased" if each error event ε' (for each depth k) is conditionally independent of the transmitted sequence $\underline{a}$ given the error sequences $\underline{e}_k(i)$ $(i \in \mathcal{I})$.*

Clearly the processing filter P of an unbiased M-algorithm receiver must satisfy (4.60) as in the case of unbiased DFSE receivers. The probability of the error event ε' for an unbiased M-algorithm receiver is, thus, given by

$$\Pr(\varepsilon') = \Pr\left(X(\underline{e}_k(i)) > \underline{e}_k(i)^H R_k Q_k \underline{e}_k(i), \quad \text{for } M \text{ values of } i \in \mathcal{I}\right) \tag{4.67}$$

where $X(\underline{e}_k(i))$ are jointly Gaussian random variables with mean zero and covariance $\mathrm{E}[X(\underline{e}_k(i))X^*(\underline{e}_k(j))] = 4N_0 \underline{e}_k(i)^H R_k Q_k (S^{-1})_k R_k Q_k \underline{e}_k(j)$.

4.7 Unbiased receivers

In Appendix B, we show that the processing filters that satisfy the unbiasedness conditions of (4.60) and (A.4) (corresponding to the case where the front-end filter is matched

[8]The notion of state in a tree search algorithm is as defined in Section 4.5.

to the overall channel response and where it is matched to the transmit filter response respectively) are unique (within a scaling factor) and are given by

$$P = Q^{-H} \tag{4.68}$$

and

$$P = Q'^{-H} \tag{4.69}$$

respectively. In the first case, the processing filter P that results in an unbiased receiver when used with a reduced trellis or tree search algorithm with branch metric formulation $R = Q^H = F^H$, is the noise-whitening filter F^{-H}, while for the formulation $R = I$ and $Q = S$, it is the zero-forcing filter S^{-1}. In the second case, the processing filter in the case of branch metric formulation $R' = Q'^H = F'^H$, is the appropriate noise-whitening filter F'^{-H}, while for the formulation $R' = I$ and $Q' = \Phi$, it is the appropriate zero-forcing filter Φ^{-1}. Note that the processing filters in both cases correspond to the autocorrelation spectrum of the front-end filter in the receiver. The processed statistics given by

$$\underline{x} = R^H \underline{a} + Q^{-H} \underline{u} \tag{4.70}$$

in the first case, and

$$\underline{x}' = R'^H C \underline{a} + Q'^{-H} \underline{u}' \tag{4.71}$$

in the second case, depend on the past transmitted symbols only and not on any future transmitted symbols. Thus, the statistics fed to a reduced trellis or tree search algorithm must have causal dependence only, for unbiased operation. Note that it is also necessary to match a given processing filter with the proper branch metric of the reduced trellis or tree search algorithm in order to achieve unbiasedness.

We considered two additive decompositions of the likelihood metric in each case of the front-end filter, which led to two different unbiased receivers. The two branch metric formulations correspond to the two decompositions of the front-end filter autocorrelation matrix (S or Φ)- one actually being no decomposition and the other being the unique Cholesky decomposition. Note that there is no other decomposition of a positive definite and banded matrix of the form RQ (or equivalently $R^H Q^H$), where the matrix R is upper-triangular and both matrices R and Q are banded. The matrix R is constrained to be upper-triangular to get a causal form for the additive metric. Both R and Q are constrained

to be banded in order for the branch metric to have finite complexity. Thus, our treatment of unbiased receivers is complete in this sense.

In the case of an infinite length transmitted sequence, the processing filters described above have infinite impulse responses. In practice, these filters can be implemented by truncating the impulse response at a sufficient length. However, this leads to some bias (untreated interference) in the receiver. Thus, there is no truly unbiased DFSE or M-algorithm receiver for an infinite length transmitted sequence. An exception to this is the case of Nyquist pulse-shaping at the transmitter and transmit-filter matched-filtering at the receiver. No processing filter is required in this case for unbiased operation.

4.7.1 Receivers with a noise-whitening filter

One type of unbiased DFSE and M-algorithm receivers have a noise-whitening filter. Henceforth, they will be referred to as whitening filter DFSE (WF-DFSE) and whitening filter M-algorithm (WF-MA) receivers. For the case where the front-end filter is matched to the overall channel response with autocorrelation spectrum S (standard matched filtering), the noise-whitening filter is given by F^{-H}. The branch metric for the WF-DFSE(S) and WF-MA(S) receivers[9] is obtained by replacing $P^{-1} = R = Q^H = F^H$ in (4.38) and (4.22) respectively. An upper bound on the first event error probability of the WF-DFSE(S) receiver is given by (4.62), with the error distance obtained by substituting $R_k = Q_k^H = F_k^H$ in (4.63) and noting that

$$(S^{-1})_k = (F^{-1}F^{-H})_k = (F^{-1})_k(F^{-H})_k = (F_k)^{-1}(F_k)^{-H} \tag{4.72}$$

where the second and third equalities follow from the following identity.

If X and Y are $N \times N$ matrices and Y is upper-triangular (or X is lower-triangular), then

$$(XY)_k = X_k Y_k \tag{4.73}$$

where $(XY)_k$ is the principal submatrix of dimension $k < N$ of the matrix XY.

The error distance is then given by

$$\delta(\underline{e}) = \|F_k \underline{e}\| \tag{4.74}$$

For the case where the front-end filter is matched to the transmit filter response with autocorrelation spectrum Φ (transmit matched filtering), the noise-whitening filter is given

[9]Where 'S' stands for standard matched filtering.

by F'^{-H}. The branch metric is obtained by replacing $P^{-1} = R' = Q'^H = F'^H$ in (4.44) and (4.35) respectively for the WF-DFSE(T)[10] and WF-MA(T) receivers. The error distance for the WF-DFSE(T) receiver follows from (A.6) as

$$\delta(\underline{e}) = \|F'_k C_k \underline{e}\|. \tag{4.75}$$

Note that the two expressions for the error distance of WF-DFSE receivers (4.74) and (4.75) differ from each other due to the different phase characteristic of the whitened channel in each case. In the first case, the whitened channel $\{f(n)\}$ has minimum-phase while in the second case, the whitened channel $\{f'(n) * c(n)\}$ has mixed phase, in general. We will see later that the error distance and hence the error probability is superior in the case of the minimum-phase channel. Note that the first event error probability expressions derived here are equivalent to the expression obtained in [8].

4.7.2 Receivers with a zero-forcing filter

The other type of unbiased DFSE and M-algorithm receivers consist of a zero-forcing filter. Henceforth, they will be referred to as zero-forcing filter DFSE (ZF-DFSE) and zero-forcing filter M-algorithm (ZF-MA) receivers. For the case of standard matched filtering, the zero-forcing filter is given by S^{-1}. The branch metric for the ZF-DFSE(S) and ZF-MA(S) receivers is obtained by replacing $P^{-1} = Q = S$, $R = I$ in (4.38) and (4.22) respectively. Substituting these values in (4.63) gives the error distance for the ZF-DFSE(S) receiver as

$$\delta(\underline{e}) = \frac{\underline{e}^H S_k \underline{e}}{\sqrt{\underline{e}^H S_k (S^{-1})_k S_k \underline{e}}}. \tag{4.76}$$

For the case of transmit matched filtering, the zero-forcing filter is given by Φ^{-1}. The branch metric is obtained by replacing $P^{-1} = Q' = \Phi$, $R' = I$ in (4.44) and (4.35), respectively for the ZF-DFSE(T) and ZF-MA(T) receivers. The error distance for the ZF-DFSE(T) receiver follows from (A.6) as

$$\delta(\underline{e}) = \frac{\underline{e}^H C_k^H \Phi_k C_k \underline{e}}{\sqrt{\underline{e}^H C_k^H \Phi_k (\Phi^{-1})_k \Phi_k C_k \underline{e}}}. \tag{4.77}$$

Note that the zero-forcing filter Φ^{-1} in the latter case does not null out inter-symbol interference entirely. It decorrelates only the part due to the autocorrelation of the front-end filter response while the part which is due to the dispersion caused by the medium response $\{c(n)\}$ is left untouched.

[10] Where 'T' stands for transmit matched filtering.

4.8 Biased receivers

Several biased receivers are possible. One example is a DFSE receiver considered in [37]. It comprises a front-end filter matched to the overall channel response followed by the noise-whitening filter $P = F^{-H}$. The reduced trellis search algorithm uses the branch metric formulation $R = I$, $Q = S$. To see that the receiver is biased, note that $F_k^H F_k \neq S_k$ ($k \ll N$). It follows from (4.51) that the error event ε depends on the transmitted sequence $\underline{a}$ through $(S_k - F_k^H F_k)\underline{a}_k$.

Note that a transversal processing filter adds complexity to a receiver. The computation of a noise-whitening or zero-forcing filter requires channel inversion and factorization operations. Moreover, the filter has to track the variation in the channel if the channel is time-varying. One solution to this problem is to omit the processing filter and pass the output of the matched filter directly to the trellis or tree search algorithm, resulting in a class of receivers which we refer to as matched filter receivers. Matched filter receivers, however, are biased. In other words, their error performance is limited by untreated interference components. Some useful matched filter receivers are described in the following sections.

4.8.1 Matched filter receivers

An important type of matched filter DFSE (MF-DFSE) and matched filter M-algorithm (MF-MA) receivers have a front-end filter matched to the overall channel response followed by a reduced trellis or tree search algorithm with branch metric obtained by replacing $P^{-1} = R = I$, $Q = S$ in (4.38) and (4.22) respectively. The MF-DFSE receiver of this type was proposed in [7,50]. The MF-MA receiver of this type was considered in [48,51]. An upper bound on the first event error probability of the MF-DFSE(S) receiver was derived in [19,20]. Using $P^{-1} = R = I$, $Q = S$ in (4.51), note that the error event ε occurs in the MF-DFSE(S) receiver if

$$2\mathrm{Re}\{\underline{e}_k^H \underline{u}_k\} > \underline{e}_k^H S_k \underline{e}_k - 2\mathrm{Re}\{\underline{\xi}^H \dot{S}_{L-J}^H \dot{\underline{a}}_k\} \tag{4.78}$$

where $\dot{\underline{a}}_k = [a_k, \ldots, a_{k+L-J-1}]^T$, $\underline{\xi}$ is the tail of the error sequence $\underline{e}_k$ comprising the last $L - J$ non-zero components of $\underline{e}_k$, given by[11]

$$\underline{\xi} = [e_{k-L}, \ldots, e_{k-J-1}]^T \tag{4.79}$$

[11] In (4.79), $e_i = 0$ for $i < 0$.

and $\dot{S}$ is an $L \times L$ matrix given by

$$\dot{S} = \begin{bmatrix} s(L) & \cdots & s(2) & s(1) \\ 0 & \ddots & & \vdots \\ \vdots & \ddots & s(L) & s(L-1) \\ 0 & \cdots & 0 & s(L) \end{bmatrix}. \tag{4.80}$$

It then follows that the first event error probability can be upperbounded using the union bound as

$$P_{FEE} \leq \sum_{\underline{e} \in E'} p_{\underline{e}} \mathrm{E}_{\underline{a}} \left[\mathrm{Q} \left(\frac{\delta(\underline{e}) - \gamma(\underline{e}, \underline{a})}{2\sqrt{N_0}} \right) \right] \tag{4.81}$$

where $\delta(\underline{e})$ is the error distance given by

$$\delta(\underline{e}) = \sqrt{\underline{e}^H S_k \underline{e}} \tag{4.82}$$

and $\gamma(\underline{e}, \underline{a})$ is the untreated interference given by

$$\gamma(\underline{e}, \underline{a}) = 2\mathrm{Re}\{\underline{\xi}^H \dot{S}_{L-J}^H \dot{\underline{a}}_k\}/\delta(\underline{e}). \tag{4.83}$$

McLane investigated truncated-state Viterbi detectors (TSVD) with standard matched filters in [32]. The difference between the TSVD algorithm of [32] and the MF-DFSE algorithm is that the MF-DFSE algorithm uses conditional tentative decisions to cancel the tail of the channel response while the TSVD algorithm simply ignores it. The error bounds obtained by McLane indicate the presence of untreated interference. However, the untreated interference in his bounds arises due to ignoring the tail of the channel response in the TSVD algorithm. Such an interference term does not appear in the bounds for DFSE as it is canceled by means of tentative conditional decisions in the DFSE algorithm. The untreated interference component that appears in the DFSE bound of (4.81) is, however, absent in McLane's bounds. The cause of this latter untreated interference component can be intuitively explained as follows. The matched filter statistics at the input of a reduced trellis search algorithm depend on L past and L future transmitted symbols (cf. (4.5)). The reduced trellis search algorithm (with memory order J) selects survivor paths extending up to time n on the basis of the metric accumulated up to time $n + J$. This premature elimination of candidate paths does not account for the interference arising from the $L - J$ future transmitted symbols. Clearly, this type of untreated interference affects both the

DFSE and TSVD algorithms. Hence, the bounds in [32] should be corrected to include this interference component.

A second type of matched filter receivers is obtained in the case where the front-end filter is matched to the transmit filer response. The reduced trellis and tree search algorithms of MF-DFSE(T) and MF-MA(T) receivers employ the branch metric given by (4.44) and (4.35) respectively with $P^{-1} = R' = I$, $Q' = \Phi$. Substituting these values in (A.2), we see that an upper bound on the first event error probability of the MF-DFSE(T) receiver is given by (4.81), where the error distance $\delta(\underline{e})$ is given by

$$\delta(\underline{e}) = \underline{e}^H C_k^H \Phi_k C_k \underline{e} \tag{4.84}$$

and the untreated interference $\gamma(\underline{e}, \underline{a})$ is given by

$$\gamma(\underline{e}, \underline{a}) = 2\mathrm{Re}\{\underline{\xi}^H (\ddot{C}_{L_d \times L-J})^H \ddot{\Phi} \ddot{C} \underline{\ddot{a}}_k\}/\delta(\underline{e}) \tag{4.85}$$

where $\underline{\ddot{a}}_k = [a_{k-L_c}, \ldots, a_k, \ldots, a_{k+L_d-1}]^T$ and $\ddot{C}$ and $\ddot{\Phi}$ are $L_d \times L$ and $L_d \times L_d$ matrices respectively, given by

$$\ddot{C} = \begin{bmatrix} c(L_c) & \cdots & c(1) & c(0) & 0 & \cdots & 0 \\ 0 & \ddots & & & \ddots & \ddots & \vdots \\ \vdots & \ddots & \ddots & & & \ddots & 0 \\ 0 & \cdots & 0 & c(L_c) & \cdots & c(1) & c(0) \end{bmatrix}, \tag{4.86}$$

$$\ddot{\Phi} = \begin{bmatrix} \phi(-L_d) & \cdots & \phi(-2) & \phi(-1) \\ 0 & \ddots & & \vdots \\ \vdots & \ddots & \phi(-L_d) & \phi(-L_d+1) \\ 0 & \cdots & 0 & \phi(-L_d) \end{bmatrix}. \tag{4.87}$$

The matrix $\ddot{C}_{L_d \times L-J}$ comprises the first $L - J$ columns of the matrix $\ddot{C}$. In the case of fractional sampling, the MF-DFSE(T) receiver corresponds to the fractional MLSE receiver of Section 3.5.

Note that for a given error sequence $\underline{e}$, the untreated interference $\gamma(\underline{e}, \underline{a})$ in (4.81) has zero mean in the case of i.i.d. transmitted symbols. The interference, thus, increases or decreases the error distance of the MF-DFSE receivers with equal probability. Due to the convexity of the Q(·) function, the error performance is, however, dominated by the

destructive effect of the untreated interference and is, thus, rather poor. Without giving an expression for the error probability of the MF-MA receivers, it can be noted that the MF-MA receivers also suffer from untreated interference.

4.9 Truncated memory MLSE receivers

Linear pre-filtering was proposed in [12,35] as a means to truncate the memory of the Viterbi algorithm in an MLSE receiver. In [12], the overall response of the channel/pre-filter combination is forced to a truncated and causal desired impulse response (DIR) of acceptably short span (say J symbols). Pre-filtering colors the noise in the output statistic. However, the Viterbi algorithm is used on the pre-filtered statistic as if the noise were white. An important difference between this approach and our generalized DFSE approach is that the receive filter in the case of DFSE is not specifically designed for a memory order. This allows one to vary the memory order of the trellis search algorithm without changing the receive filter. In the following, we look at the error performance of the pre-filtering method.

Let $\underline{x}$ be the statistic obtained after matched filtering/noise-whitening, i.e.

$$\underline{x} = F\underline{a} + \underline{w} \tag{4.88}$$

where $\underline{w}$ is a white Gaussian noise sequence with covariance $\mathrm{E}[\underline{w}\underline{w}^H] = N_0 I$. Let G be an $N \times N$ lower-triangular banded Toeplitz matrix (with band width $J < L$) representing the DIR and H be the corresponding pre-filter matrix, given by $HF = G$. The statistic at the output of the pre-filter is given by

$$\underline{x}^p = G\underline{a} + \underline{w}^p \tag{4.89}$$

where $\underline{w}^p = H\underline{w}$ is the filtered noise.

Consider a path $\{\bar{a}_n\}$ in a truncated memory MLSE (TM-MLSE) receiver that diverges from the correct path $\{a_n\}$ at time 0 and remerges with it at a later time k. A first event error occurs at time 0 if $\{\bar{a}_n\}$ is picked as a survivor path. The error event occurs if the metric accumulated on the incorrect path is greater than the metric on the correct path, i.e.

$$-\|\underline{x}_k^p - G_k\underline{\bar{a}}_k\|^2 > -\|\underline{x}_k^p - G_k\underline{a}_k\|^2. \tag{4.90}$$

Using (4.89), we get

$$2\mathrm{Re}\{\underline{e}_k^H G_k^H \underline{w}_k^p\} > \|G_k\underline{e}_k\|^2 \tag{4.91}$$

where $\underline{\epsilon}_k = \underline{\tilde{a}}_k - \underline{a}_k$ is the error sequence. Note that H is a lower-triangular matrix. Therefore, $\mathrm{E}[\underline{w}_k^p \underline{w}_k^{pH}] = N_0 H_k H_k^H$ and the probability of the error event ε: the sequence $\underline{a}_k$ is eliminated in favor of the sequence $\underline{a}_k + \underline{e}_k$, is given by

$$\Pr(\varepsilon) = \mathrm{Q}\left(\frac{\delta(\underline{e})}{2\sqrt{N_0}}\right) \tag{4.92}$$

where $\delta(\underline{e})$ is the distance of the error sequence $\underline{e}$ (we drop the subscript k), given by

$$\delta(\underline{e}) = \frac{\|G_k \underline{e}\|^2}{\sqrt{\underline{e}^H G_k^H H_k H_k^H G_k \underline{e}}}. \tag{4.93}$$

4.10 Symbol error probability

Consider a path in the reduced-state trellis of a DFSE receiver that diverges from the correct path at time n_1 and remerges with it at a later time n_2. Due to feedback incorporated in the reduced trellis search algorithm, the event that the correct path is eliminated in favor of the incorrect path (an error event) depends on previous error events. The effect of the error propagation is, however, small in DFSE receivers as compared to simple decision feedback equalizers (DFE). This is because the decisions fed back in DFSE are conditioned on the state of the reduced trellis unlike the decisions in DFE. Moreover, the effect of error propagation is small at medium to high signal-to-noise ratio (SNR). This was shown to be the case for WF-DFSE receivers in [8,9]. Assuming no error propagation (i.e. a separation of more than $L - J$ correct decisions between error events), the probability that an error event occurs in a DFSE receiver can be upperbounded by the first event error probability [29]. The symbol error probability for unbiased DFSE receivers can then be upperbounded as [8,13]

$$P_s \leq \sum_{\underline{e} \in E'} \mathrm{w}(\underline{e}) p_{\underline{e}} \mathrm{Q}\left(\frac{\delta(\underline{e})}{2\sqrt{N_0}}\right) \tag{4.94}$$

where $\mathrm{w}(\underline{e})$ is the number of symbol errors entailed by the error sequence $\underline{e}$, $\delta(\underline{e})$ is the distance of the error sequence and $p_{\underline{e}}$ is the probability that a transmitted sequence can have $\underline{e}$ as an error sequence. For i.i.d. transmitted sequences and input alphabet $\mathcal{A} = \{\pm 1, \pm 3, \ldots, \pm(|\mathcal{A}| - 1)\}$ (for $|\mathcal{A}|$ even), we have

$$p_{\underline{e}} = \prod_{n=0}^{k-1-J} \frac{|\mathcal{A}| - \frac{1}{2}|e_n|}{|\mathcal{A}|} \tag{4.95}$$

which reduces to

$$p_{\underline{e}} = 2^{-\mathrm{w}(\underline{e})} \tag{4.96}$$

in the case of BPSK modulation. The error distance $\delta(\underline{e})$ is given by (4.74) and (4.75) for WF-DFSE receivers with the standard and transmit matched filters, respectively. The error distance for ZF-DFSE receivers given by (4.76) and (4.77), depends on the location and length of the error event. This is because the correlation in the noise samples given by S^{-1} varies over the length of the data sequence. However, note that the noise correlation is constant in the middle of a long sequence (i.e. S^{-1} is nearly Toeplitz except at the edges for $N \gg L$). In Appendix C, we obtain expressions for the error distance that assume the noise correlation to be constant. The error distance in the case of standard and transmit matched filtering is given by (C.5) and (C.6) respectively. The symbol error probability bound of (4.94) also holds for the truncated memory MLSE receiver of Section 4.9 with the error distance given by (4.93). In this case, it is a strict upper bound as there is no decision feedback and thus no error propagation.

For moderate SNRs, the upper bound given by (4.94) is dominated by the term

$$\mathrm{Q}\left(\frac{\delta_{min}}{2\sqrt{N_0}}\right) \sum_{\underline{e} \in E'_{min}} \mathrm{w}(\underline{e}) p_{\underline{e}} \tag{4.97}$$

where E'_{min} is the set of error sequences in E' that achieve the minimum distance (known as minimum distance sequences)

$$\delta_{min} = \min_{\underline{e} \in E'} \delta(\underline{e}). \tag{4.98}$$

The symbol error probability for MF-DFSE receivers can similarly be upperbounded as

$$P_s \leq \sum_{\underline{e} \in E'} \mathrm{w}(\underline{e}) p_{\underline{e}} \mathrm{E}_{\underline{a}} \left[\mathrm{Q}\left(\frac{\delta(\underline{e}) - \gamma(\underline{e}, \underline{a})}{2\sqrt{N_0}} \right) \right] \tag{4.99}$$

where the error distance $\delta(\underline{e})$ and the untreated interference $\gamma(\underline{e}, \underline{a})$ are given by (4.82) and (4.83) for the case of standard matched filtering and (4.84) and (4.85) for the case of transmit matched filtering respectively. Due to the presence of untreated interference, the upper bound in (4.99) is not dominated by the minimum distance error sequences only, unlike the bound for unbiased DFSE receivers. Higher distance error sequences should also be considered with worst case interference.

4.11 Error distance

The various DFSE receivers derived in the previous sections can be compared on the basis of their error distance. In the case of an unbiased DFSE receiver, the minimum error

distance squared per noise spectral density can be considered as its effective SNR [8]. For a given channel and memory order, the distance of a given error sequence depends on the type of the DFSE receiver. Specifically, it depends on the receive filter and the branch metric. In this section, we compare the error distance for various receivers.

Let $\underline{e} = [e_0, e_1, \ldots, e_{k-1-J}, 0, \ldots, 0]^T$ be an error sequence of length k belonging to the set E'_J (the set E' of allowable error sequences for a DFSE receiver with memory order $J < L$). Let $\underline{e}_+ = [\underline{e}^T, 0, \ldots, 0]^T$ (length $l = k + L - J$). Then, $\underline{e}_+ \in E'_L$, the set of allowable error sequences for an MLSE receiver. The distance of this sequence in the case of an MLSE receiver is given by

$$\delta(\underline{e}_+) = \underline{e}_+^H S_l \underline{e}_+ = \underline{e}^H S_k \underline{e} \tag{4.100}$$

which is equal to the distance of the corresponding error sequence in the case of a MF-DFSE receiver with the standard matched filter. Let E''_J be the set of all error sequences in E'_J appended by $L-J$ zeros ($L > J$). Note that $E''_J \subset E'_L$, i.e. the upper bounds given by (4.94) and (4.99) for DFSE receivers are determined using only a subset of the error sequences considered for an MLSE receiver[12]. Thus, if the untreated interference in the case of MF-DFSE(S) could be removed ideally with the aid of a genie, the upper bound for the receiver would be lower than MLSE. In fact, the error rate performance of the genie-aided receiver is generally better than MLSE in moderate SNRs where error propagation is negligible. For the other DFSE receivers, we will show that the error distance is smaller, in general, compared to the MF-DFSE(S) receiver (or an MLSE receiver).

4.11.1 WF-DFSE

Consider the case of WF-DFSE(S) receiver. Note that

$$\underline{e}_+^H S_l \underline{e}_+ = \underline{e}_N^H S \underline{e}_N = \|F \underline{e}_N\|^2 = \|F_l \underline{e}_+\|^2 = \|F_k \underline{e}\|^2 + \|\dot{\Psi} \underline{\xi}\|^2 \tag{4.101}$$

[12]The error sequences excluded have more than $J-1$ consecutive zeros in the midst and hence cause a reduced trellis encoder with memory J to flush.

where $\underline{e}_N = [\underline{e}_+^T 0 \ldots . 0]^T$ (length N), $\underline{\xi}$ is given by (4.79) and $\dot{\Psi}$ is an $L-J \times L-J$ matrix given by

$$\dot{\Psi} = \begin{bmatrix} f(L) & \cdots & \cdots & f(J+1) \\ 0 & \ddots & & \vdots \\ \vdots & \ddots & f(L) & f(L-1) \\ 0 & \cdots & 0 & f(L) \end{bmatrix}. \tag{4.102}$$

The matrix $\dot{\Psi}$ is illustrated in Fig. 4.6. The distance of a given error sequence is thus

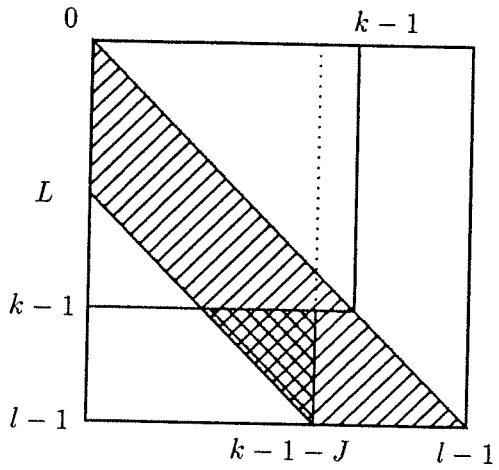

Figure 4.6: Illustration of $\dot{\Psi}$ within F_l.

smaller for WF-DFSE(S) as compared to MF-DFSE(S). The loss in squared distance is given by

$$\|\dot{\Psi}\underline{\xi}\|^2. \tag{4.103}$$

Now consider the case of the WF-DFSE(T) receiver. Let

$$v(i,j) = \begin{cases} v(i-j) & 0 \le i-j \le L \\ 0 & \text{otherwise} \end{cases} \tag{4.104}$$

be the coefficients of the lower-triangular Toepltiz matrix $V = F'C$. Then, similar to (4.101), we can write

$$\underline{e}_+^H S_l \underline{e}_+ = \|F_l' C_l \underline{e}_+\|^2 = \|F_k' C_k \underline{e}\|^2 + \|\ddot{\Psi}\underline{\xi}\|^2 \tag{4.105}$$

where $\ddot{\Psi}$ is an $L-J \times L-J$ matrix given by

$$\ddot{\Psi} = \begin{bmatrix} v(L) & \cdots & \cdots & v(J+1) \\ 0 & \ddots & & \vdots \\ \vdots & \ddots & v(L) & v(L-1) \\ 0 & \cdots & 0 & v(L) \end{bmatrix}. \tag{4.106}$$

The loss in squared distance in this case is given by

$$\|\ddot{\Psi}\underline{\xi}\|^2. \tag{4.107}$$

Note that the matrix F of the whitened channel coefficients $\{f(n)\}$ (in the case of standard matched filtering), is invertible since $F(z)$, the z-transform of $\{f(n)\}$, is minimum-phase (has all roots inside the unit circle). Similarly, $F'(z)$, the z-transform of $\{f'(n)\}$, is minimum-phase. However, the z-transform $C(z)$ of the medium response coefficients $\{c(n)\}$ may be non-minimum phase. Therefore, $V(z) = F'(z)C(z)$, the z-transform of the coefficients of the whitened channel $\{v(n)\}$ (in the case of transmit matched filtering), is mixed-phase in general. The whitened channels in the two cases have the same magnitude response, as

$$F^*(z^{-1})F(z) = V^*(z^{-1})V(z) = S(z) \tag{4.108}$$

where $S(z)$ is the z-transform of the sampled channel autocorrelation function $\{s(n)\}$. Note that channels with identical magnitude response but different phase responses have different energy distribution among tap coefficients. The minimum-phase channel has most of its energy contained in the leading tap coefficients, while the maximum-phase channel (with all roots outside the unit circle) has most of its energy contained in the lagging tap coefficients. As a result, the coefficients of the matrix $\dot{\Psi}$ (belonging to the minimum-phase channel F) have smaller magnitude, in general, than the coefficients of the matrix $\ddot{\Psi}$. Thus, the loss in squared distance compared to MLSE in the case of standard and transmit matched filtering given by (4.103) and (4.107) respectively is smaller in the first case.

4.11.2 ZF-DFSE

Next, consider ZF-DFSE receivers. In Appendix C, we show that the error distance for the case of ZF-DFSE(S) can be written as

$$\frac{\underline{e}^H S_k \underline{e}}{\sqrt{\underline{e}^H S_k (S^{-1})_k S_k \underline{e}}} = \frac{\underline{e}^H S_k \underline{e}}{\sqrt{\underline{e}^H S_k \underline{e} + \underline{\xi}^H \dot{S}_{L-J}^H (S_{22}^I)_L \dot{S}_{L-J} \underline{\xi}}} \tag{4.109}$$

where $(S_{22}^I)_L$ is a submatrix of the matrix S^{-1} and is thus positive definite. Note that the second term in the denominator of the RHS of (4.109) is greater than zero as the matrix $\dot{S}$ is full rank (since $s(-L) \neq 0$). Thus, the error distance for ZF-DFSE(S) is less than MF-DFSE(S). Similarly, it can be shown that the error distance for ZF-DFSE(T) is smaller than that for MF-DFSE(T).

4.11.3 Optimum unbiased DFSE receivers

In this section, we show that WF-DFSE receivers are optimum in the sense that they minimize the first event error probability of unbiased DFSE receivers. Equivalently, we show that WF-DFSE receivers maximize the distance of a given error sequence in the class of DFSE receivers that satisfy the unbiasedness condition, i.e.

$$\frac{\underline{e}^H R_k Q_k \underline{e}}{\sqrt{\underline{e}^H R_k Q_k (S^{-1})_k R_k Q_k \underline{e}}} \leq \|F_k \underline{e}\| \tag{4.110}$$

with equality only if $Q_k = F_k$, where $(R, Q) = (I, S)$ or (F^H, F) and

$$\frac{\underline{e}^H C_k^H R_k' Q_k' C_k \underline{e}}{\sqrt{\underline{e}^H C_k^H R_k' Q_k' (\Phi^{-1})_k R_k' Q_k' C_k \underline{e}}} \leq \|F_k' C_k \underline{e}\| \tag{4.111}$$

with equality only if $Q_k' = F_k'$, where $(R', Q') = (I, \Phi)$ or (F'^H, F').

To prove Proposition (4.110), we note that

$$\begin{aligned} \underline{e}^H R_k Q_k \underline{e} &= \underline{e}^H (F_k)^H (F_k)^{-H} R_k Q_k \underline{e} \\ &\leq \|\dot{F}_k \underline{e}\| \|(F_k)^{-H} R_k Q_k \underline{e}\| \\ &= \|F_k \underline{e}\| \sqrt{\underline{e}^H Q_k^H R_k^H (S^{-1})_k R_k Q_k \underline{e}} \end{aligned} \tag{4.112}$$

where the inequality in (4.112) is the Schwartz inequality which becomes an equality only if $R_k = Q_k^H = F_k^H$. The last equality in (4.112) follows from (4.72). Proposition (4.111) can be shown similarly.

Comparing the error distance of the WF-DFSE receiver with the truncated memory MLSE receiver of Section 4.9 (with the same memory order), we note that

$$\begin{aligned} \underline{e}^H G_k^H G_k \underline{e} &= \underline{e}^H G_k^H H_k F_k \underline{e} \\ &\leq \|H_k^H G_k \underline{e}\| \|F_k \underline{e}\| \end{aligned} \tag{4.113}$$

where $G_k = (HF)_k = H_k F_k$ follows from (4.73) as H is a lower-triangular matrix and we again use the Schwartz inequality. Thus, we get

$$\frac{\|G_k \underline{e}\|^2}{\sqrt{\underline{e}^H G_k^H H_k H_k^H G_k \underline{e}}} \leq \|F_k \underline{e}\|. \tag{4.114}$$

In conclusion, we see that the distance of a given error sequence for a DFSE receiver depends on the type of filtering and the branch metric. The distance for the MF-DFSE(S) receiver is the same as in the case of an MLSE receiver. For the unbiased DFSE receivers – WF-DFSE and ZF-DFSE, the distance is smaller. This is due to the fact that the standard matched filter collects all the energy of the pulse transmitted at a given time in the corresponding output sample (in other words, it maximizes the output SNR, given by $|s(0)|^2/N_0$). The noise-whitening filter spreads out the signal energy into $L+1$ output samples in the process of whitening noise ($\sum_{i=0}^{L} |f(i)|^2 = |s(0)|^2$). The linear zero-forcing filter decorrelates all interfering signal components but enhances (and correlates) noise in the process. The reduced trellis-search algorithms that follow these filters recover part of the signal energy (or SNR) that is spread out but are unable to recover all of it. Thus, WF-DFSE and ZF-DFSE suffer from a loss of the effective SNR, while MF-DFSE(S) does not. Of course, the drawback with MF-DFSE is that the reduced trellis search algorithm is unable to resolve some anticausal interfering signal components. This problem is alleviated in BC-MF-DFSE where the untreated components are canceled using tentative decisions. If reliable tentative decisions can be obtained, the BC-MF-DFSE receiver presents an advantage over the unbiased DFSE receivers in terms of SNR.

The noise-whitening filter removes only the anti-causal signal components which is necessary for unbiasedness. The causal signal components forming the tail of the channel response are equalized using decision feedback which does not enhance noise. The zero-forcing filter on the other hand performs complete signal decorrelation. This leads to noise enhancement and a further loss of the error distance. Similarly, the use of pre-filtering to remove some of the causal signal components in a truncated memory MLSE receiver enhances noise. Thus, WF-DFSE has greater error distance than ZF-DFSE and truncated memory MLSE receivers with pre-filtering. Practically, error propagation slightly degrades DFSE performance at moderate SNRs. Error propagation, however, does not occur in a truncated memory MLSE receiver with pre-filtering as there is no decision feedback.

4.12 Bound evaluation

In this section, we describe a generating function method to evaluate the symbol error probability bounds given in Section 4.10 for unbiased DFSE receivers. Note that a generating function method has never been considered for the well-known WF-DFSE receiver. In [10] and [8], the minimum distance was used to approximate the symbol error probability. However, the approximation may not be very good depending on the system, even at high SNRs [39]. In [39], a stack algorithm was proposed to obtain a chosen number of the largest terms in the union upper bound of (4.94). It was stated in [39] that a generating function method can not be applied to the case of DFSE because unlike MLSE, branch distances in DFSE can not be uniquely determined from pairs of error states due to decision feedback incorporated in the branch metric calculation. We note that the problem with the approach in [39] is that the branch distance depends on $L+1$ error symbols (where L is the channel memory) while the states in the error state diagram of [39] represent $J+1$ error symbols (where $J < L$ is the memory order of DFSE). In the following, we show how an error state diagram used to obtain error distances in MLSE, can be modified in the case of DFSE.

An error state diagram (ESD) in the case of DFSE enumerates the distance $\delta(\underline{e})$, the number of symbol errors $\mathrm{w}(\underline{e})$ and the *a priori* probability $p(\underline{e})$ of all error sequences $\underline{e}$ in the set of allowable sequences E'. Each path through the ESD corresponds to an error sequence in E'. For WF-DFSE, ZF-DFSE and MF-DFSE, the branch distance (defined later for each case) depends on $L+1$ error symbols identified uniquely by a pair of error states, where an error state is defined as the value of L consecutive error symbols: $\{e_{j-L}, e_{j-L+1}, \ldots, e_{j-1}\}$. Since, an error symbol can take on any of $2|\mathcal{A}|-1$ values (including zero), the diagram has $(2|\mathcal{A}|-1)^L$ error states or nodes, as in MLSE [46]. The nodes are connected to each other through branches. Since an error sequence in the set E' can have no more than $J-1$ consecutive zeros in the middle of the sequence, the nodes and branches that correspond to J or more consecutive zeros in the middle of the error path are expurgated. The modified error state diagram is shown in Fig. 4.7 for the case of a binary symbol alphabet, channel memory $L=3$ and memory order $J=1$. The error states or nodes are ternary L-tuples that take values in $\{0,+2,-2\}$. The pairs of error states that are negative of each other have been combined, as in [46]. This is because the branch distances for such error states are identical, as we will see later. Note that with $L=3$, there should be $(3^3-1)/2=13$

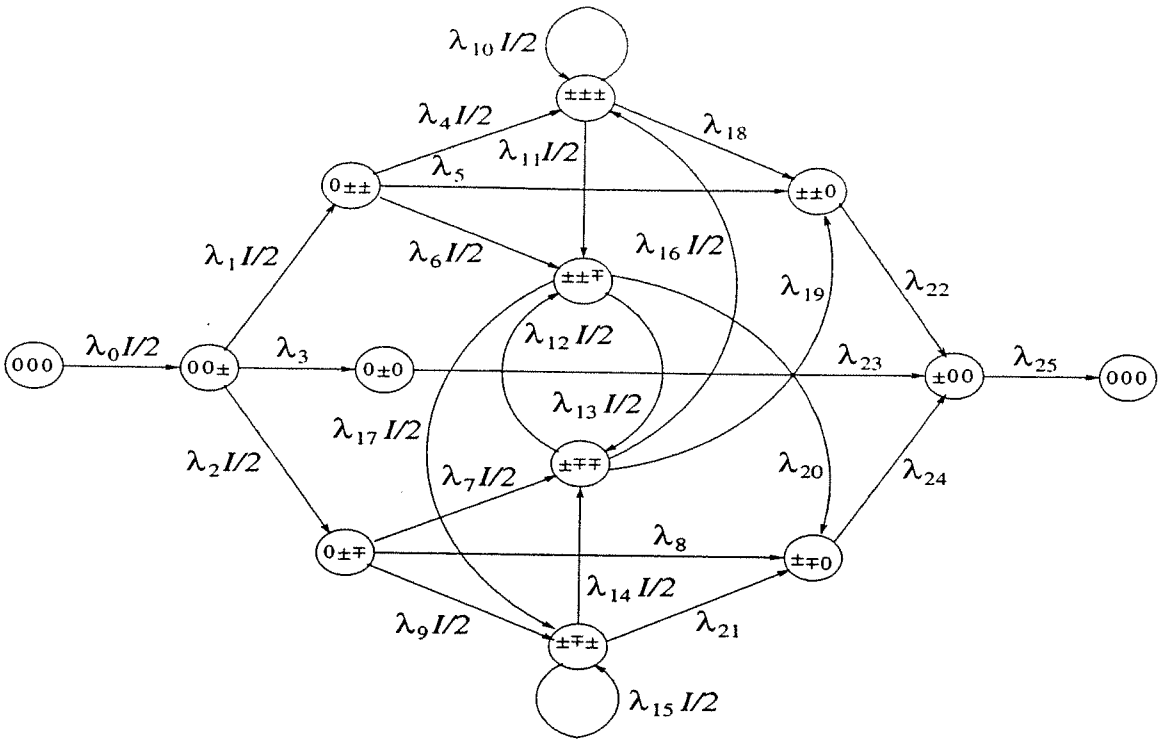

Figure 4.7: Error state diagram for DFSE ($L = 3, J = 1$).

non-zero error state pairs in the ESD. However, the nodes $\pm 0 \pm$ and $\pm 0 \mp$ do not appear in the ESD of Fig. 4.7. Moreover, the nodes 0 ± 0, $\pm \pm 0$, $\pm \mp 0$ and ± 00 have only one outgoing branch each. This is because the nodes and branches that correspond to a zero in the middle of the error path, have been eliminated because with $J = 1$, an allowable error sequences can not have any zeros in the middle of the sequence. The branches are labeled with the branch distance parameter λ and the number of symbol errors entailed by the transition as the exponent of dummy variable I. A factor of $1/2$ is used to account for the *a-priori* probability of error if the transition involves an error.

For the case of WF-DFSE, the error distance (squared) $\delta^2(\underline{e})$ is given by

$$\delta^2(\underline{e}) = \sum_{j=0}^{k-1+L-J} b_j \tag{4.115}$$

where k is the length of the error sequence $\underline{e} = \{e_0, e_1, \ldots, e_{k-1}\} \in E'_J$ and b_j is the branch

Table 4.1: Branch distance parameters for WF-DFSE ($L = 3, J = 1$)

$\lambda_0 = D^{4f(0)^2}$	$\lambda_1 = D^{4[f(0)+f(1)]^2}$
$\lambda_2 = D^{4[f(0)-f(1)]^2}$	$\lambda_3 = D^{4f(1)^2}$
$\lambda_4 = D^{4[f(0)+f(1)+f(2)]^2}$	$\lambda_5 = D^{4[f(1)+f(2)]^2}$
$\lambda_6 = D^{4[f(0)-f(1)-f(2)]^2}$	$\lambda_7 = D^{4[f(0)+f(1)-f(2)]^2}$
$\lambda_8 = D^{4[f(1)-f(2)]^2}$	$\lambda_9 = D^{4[f(0)-f(1)+f(2)]^2}$
$\lambda_{10} = D^{4[f(0)+f(1)+f(2)+f(3)]^2}$	$\lambda_{11} = D^{4[f(0)-f(1)-f(2)-f(3)]^2}$
$\lambda_{12} = D^{4[f(0)-f(1)-f(2)+f(3)]^2}$	$\lambda_{13} = D^{4[f(0)+f(1)-f(2)-f(3)]^2}$
$\lambda_{14} = D^{4[f(0)+f(1)-f(2)+f(3)]^2}$	$\lambda_{15} = D^{4[f(0)-f(1)+f(2)-f(3)]^2}$
$\lambda_{16} = D^{4[f(0)+f(1)+f(2)-f(3)]^2}$	$\lambda_{17} = D^{4[f(0)-f(1)+f(2)+f(3)]^2}$
$\lambda_{18} = D^{4[f(1)+f(2)+f(3)]^2}$	$\lambda_{19} = D^{4[f(1)+f(2)-f(3)]^2}$
$\lambda_{20} = D^{4[f(1)-f(2)-f(3)]^2}$	$\lambda_{21} = D^{4[f(1)-f(2)+f(3)]^2}$
$\lambda_{22} = \lambda_{23} = \lambda_{24} = \lambda_{25} = 1$	

distance given by[13]

$$b_j = \begin{cases} \left(\sum_{i=0}^{L} f(i) e_{j-i} \right)^2 & j = 0, 1, \ldots, k-1 \\ 0 & \text{otherwise} \end{cases} \tag{4.116}$$

Note that the segment of an error path $\underline{e}$ between the node $\{e_{k-L}, \ldots, e_{k-1-J}, 0, \ldots, 0\}$ ($e_{k-1-J} \neq 0$) and the all-zeros node corresponds to the tail of the error sequence $\underline{\xi}$. Note from (4.116) that the branches within this segment of an error path (which we refer to as tail branches) have distance zero. This is in accordance with (4.101) and (4.105), where the loss in squared distance (compared to MLSE) as given by $\|\dot{\Psi}\underline{\xi}\|^2$ and $\|\ddot{\Psi}\underline{\xi}\|^2$, respectively, occurs on the tail branches.

Table 4.1 lists the branch distance parameters λ_i for Fig. 4.7 for the case of WF-DFSE (also see footnote 13). The branch distance appears as the exponent of a dummy variable D. Let $T(D, I)$ be the generating function for the error paths for WF-DFSE, found by solving the state equations in the ESD of Fig. 4.7 simultaneously. The generating function

[13] In the case of transmit matched filtering, $f(i)$ should be replaced by $v(i)$.

can be expanded in a series as

$$\frac{\partial}{\partial I}T(D,I)\Big|_{I=1} = \sum_l N_l D^{\delta^2(l)} \tag{4.117}$$

where N_l is the number of error path pairs (negative of each other) with distance $\delta(l)$, per the number of symbol errors and the number of the corresponding input sequences. Then, the symbol error probability bound of (4.94) for WF-DFSE can be computed as[14]

$$P_s \leq \sum_l 2N_l D^{\delta^2(l)}\Big|_{D^x=\mathrm{Q}\left(\sqrt{x/2N_0}\right)}. \tag{4.118}$$

In the case of ZF-DFSE(S), the squared error distance is given by $\delta^2(\underline{e}) = b_n^2/b_d$, where

$$b_n = \sum_{j=0}^{k-1+L-J} b_{n,j} \tag{4.119}$$

is the numerator distance and

$$b_d = \sum_{j=0}^{k-1+L-J} b_{d,j} \tag{4.120}$$

is the denominator distance, and $b_{n,j}$ and $b_{d,j}$ are the corresponding branch distances which follow from (C.5) as

$$b_{n,j} = \mathrm{Re}\left\{e_j^*\left(s(0)e_j + 2\sum_{i=1}^{L} s(i)e_{j-i}\right)\right\} \tag{4.121}$$

$$b_{d,j} = \begin{cases} b_{n,j} & j = 0,1,\ldots,k-1 \\ \underline{\xi}^H \dot{S}_{L-J}^H S'_{L-J} \dot{S}_{L-J}\underline{\xi} & j = k \\ 0 & \text{otherwise} \end{cases} \tag{4.122}$$

Note that the numerator and denominator branch distances differ only at the tail branches according to (C.5).

Table 4.2 lists the branch distance parameters λ_i for Fig. 4.7 in the case of ZF-DFSE(S). Dummy variables D_1 and D_2 are used to enumerate the numerator distance and the denominator distance, respectively. Let $T(D_1, D_2, I)$ be the generating function for the error paths in this case, which can be expanded in a series as

$$\frac{\partial}{\partial I}T(D_1,D_2,I)\Big|_{I=1} = \sum_l M_l D_1^{b_n(l)} D_2^{b_d(l)}. \tag{4.123}$$

where M_l is the number of error path pairs with numerator distance $b_n(l)$ and denominator distance $b_d(l)$, per the number of symbol errors and the number of the corresponding input

[14] Note that for real symbol alphabet, the noise is real with power spectral density $N_0/2$.

Table 4.2: Branch distance parameters for ZF-DFSE(S) ($L = 3, J = 1$)

$\lambda_i = D_1^{4\lambda_{1,i}} D_2^{4\lambda_{2,i}}$	
$\lambda_{1,0} = s(0)$	$\lambda_{1,1} = s(0) + 2s(1)$
$\lambda_{1,2} = s(0) - 2s(1)$	$\lambda_{1,4} = s(0) + 2s(1) + 2s(2)$
$\lambda_{1,6} = s(0) - 2s(1) - 2s(2)$	$\lambda_{1,7} = s(0) + 2s(1) - 2s(2)$
$\lambda_{1,9} = s(0) - 2s(1) + 2s(2)$	$\lambda_{1,10} = s(0) + 2s(1) + 2s(2) + 2s(3)$
$\lambda_{1,11} = s(0) - 2s(1) - 2s(2) - 2s(3)$	$\lambda_{1,12} = s(0) - 2s(1) - 2s(2) + 2s(3)$
$\lambda_{1,13} = s(0) + 2s(1) - 2s(2) - 2s(3)$	$\lambda_{1,14} = s(0) + 2s(1) - 2s(2) + 2s(3)$
$\lambda_{1,15} = s(0) - 2s(1) + 2s(2) - 2s(3)$	$\lambda_{1,16} = s(0) + 2s(1) + 2s(2) - 2s(3)$
$\lambda_{1,17} = s(0) - 2s(1) + 2s(2) + 2s(3)$	$\lambda_{1,3} = \lambda_{1,5} = \lambda_{1,8} = \lambda_{1,18-25} = 0$
$\lambda_{2,i} = \lambda_{1,i}$ for $i = 0, 1, \ldots, 21, 25$	
$\lambda_{2,22} = (s(2) + s(3))[s'(0)(s(2) + s(3)) + 2s'(1)s(3)] + s'(0)s(3)^2$	
$\lambda_{2,23} = s(2)[s'(0)s(2) + 2s'(1)s(3)] + s'(0)s(3)^2$	
$\lambda_{2,24} = (s(2) - s(3))[s'(0)(s(2) - s(3)) + 2s'(1)s(3)] + s'(0)s(3)^2$	

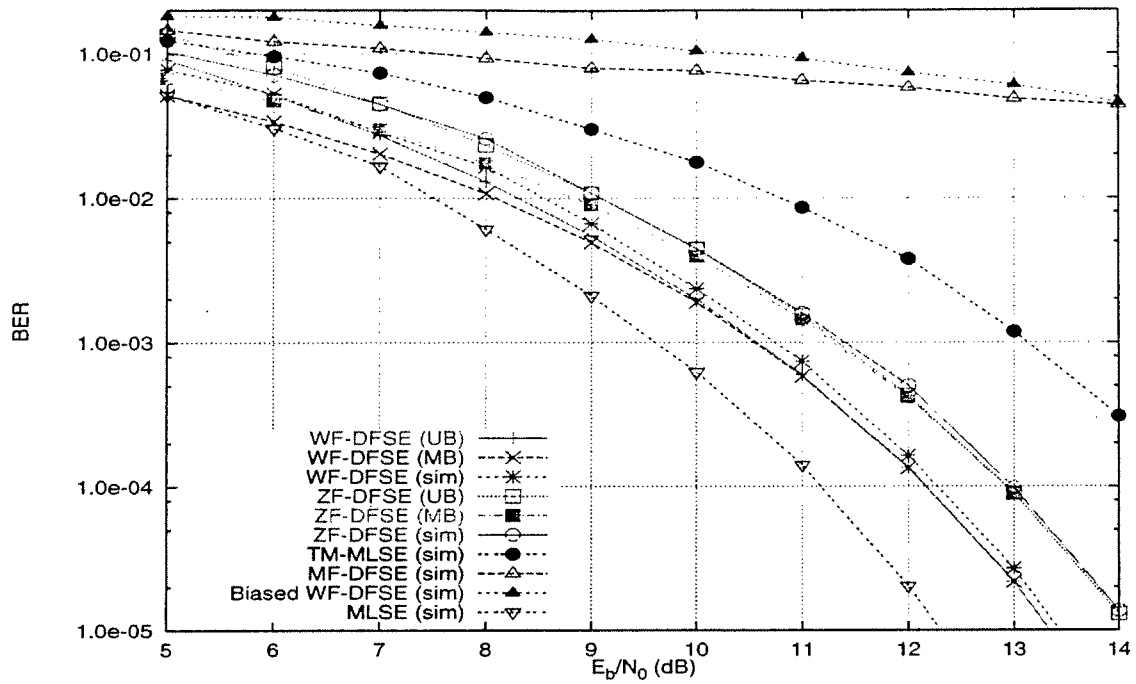

Figure 4.8: BER performance of various receivers in Example 1.

sequences. Then, the symbol error probability bound of (4.94) for ZF-DFSE(S) can be computed as

$$P_s \leq \sum_l 2M_l D_1^{b_n(l)} D_2^{b_d(l)} \Big|_{D_1^x D_2^y = \mathrm{Q}\left(\sqrt{x^2/2N_0 y}\right)} . \tag{4.124}$$

A similar approach can be applied to evaluate the symbol error probability bound for ZF-DFSE(T). A generating function method for MF-DFSE(S) was described in [20].

4.13 Performance results

In this section, we compare the performance of the various receivers described in this chapter via simulation and analysis. We consider BPSK modulation and single-user static time-dispersive AWGN channels. We consider the cases of a symbol-spaced channel model (symbol-rate sampling) and a half symbol-spaced channel model (fractional sampling). The receiver is assumed to have perfect estimates of the symbol timing and the impulse response of the channel. Each simulation was run for a count of 600 errors.

The first example is taken from [39]. The overall channel response is given by symbol-

spaced tap coefficients[15] $f = (0.6335, 0.5456, 0.4479, 0.3167)$. The channel has memory $L = 3$ and is minimum-phase. Nyquist pulse-shaping is assumed. Fig. 4.8 shows the bit-error rate (BER) performance of various receivers for the channel in Example 1 with standard matched filtering. The memory order for the DFSE receivers is set to $J = 1$. With memory order one, the minimum distance in the DFSE receivers is achieved by the error sequences $\pm(2, -2, 0)$. For the MF-DFSE, WF-DFSE and ZF-DFSE receivers, the minimum distance as given by (4.82), (4.74) and (C.5) respectively, equals 0.7322, 0.6470 and 0.5936 respectively[16]. The minimum distance loss for WF-DFSE as compared to MLSE is about 1 dB while that for ZF-DFSE, it is 1.8 dB. Fig. 4.8 shows the upper bound (UB) on the symbol error probability given by (4.94) and the minimum distance bound (MB) given by (4.97) for WF-DFSE and ZF-DFSE. Note that the bounds were obtained assuming absence of error propagation. The simulated BER is marginally higher than the upper bound for both receivers. In the simulations, final decisions were obtained at a lag of 30 symbols. The minimum distance bound converges to the upper bound at high SNR as minimum distance sequences dominate the performance.

Also shown in Fig. 4.8 is the simulated performance of an optimum two-tap TM-MLSE receiver with desired impulse response $(0.7071, 0.7071)$ taken from [12]. Note that the WF-DFSE receiver performs better than the ZF-DFSE and TM-MLSE receivers at all SNRs as discussed in Section 4.11.3. Although the zero-forcing filter in the case of ZF-DFSE, performs more signal decorrelation (which results in noise enhancement) than the prefilter of TM-MLSE, ZF-DFSE performs better than TM-MLSE in this example. This is because, unlike the case of TM-MLSE, the trellis search algorithm in the case of ZF-DFSE takes into account the correlation in the noise samples and is thus able to recover some of the lost signal energy.

The MF-DFSE receiver achieves the maximum error distance equal to that of the MLSE receiver. However, it performs quite poorly due to the presence of untreated interference components. Also shown in Fig. 4.8 is a biased WF-DFSE receiver with the configuration $P^{-1} = F^H, Q = S, R = I$, considered in [37]. Again the effect of untreated interference is evident. The untreated interference arises due to a mismatch between the processing filter and the branch metric as discussed in Section 4.8.

[15] Normalized so that $\sum_{i=0}^{L} |f(i)|^2 = 1$.

[16] After dividing by two.

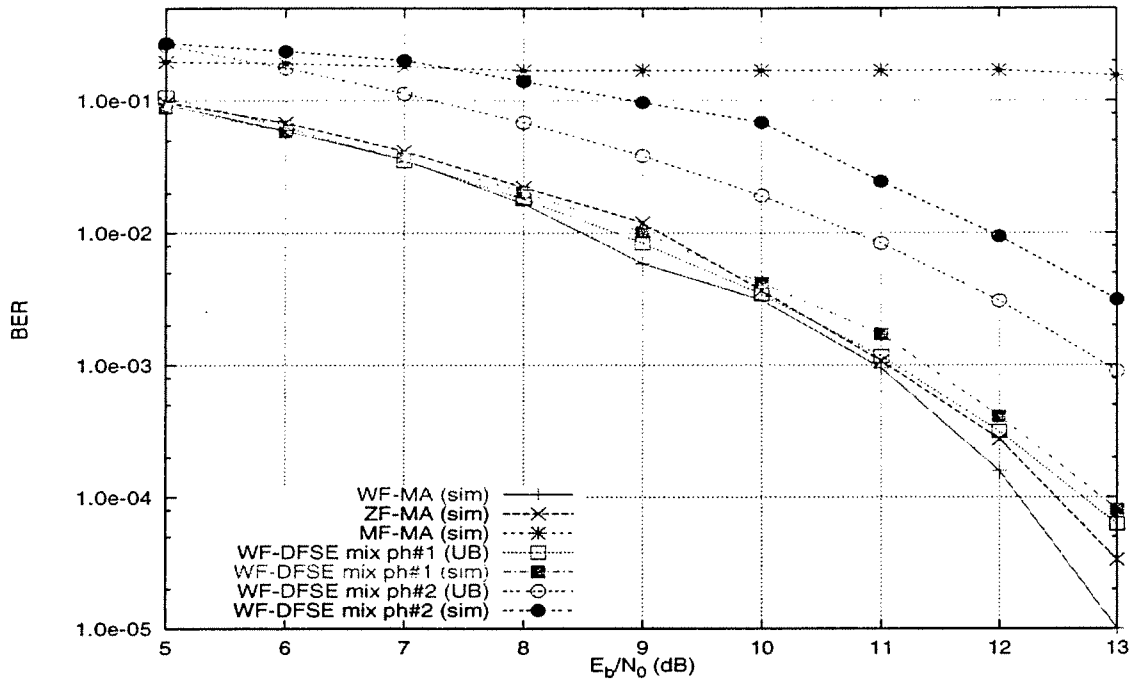

Figure 4.9: BER performance of various receivers in Example 1.

Fig. 4.9 shows the simulated BER performance of the WF-MA, ZF-MA and MF-MA receivers for the channel in Example 1. The number of paths in the M-algorithm receivers is set to $M = 2$. The WF-MA receiver obtains the best performance. The MF-MA receiver exhibits a (high) error floor like the MF-DFSE and the biased WF-DFSE receivers, all of which belong to the class of biased receivers. Fig. 4.9 also shows the BER performance of WF-DFSE(T) receivers on mixed-phase channels with symbol-spaced medium responses $c = (0.4930, 0.6745, 0.3693, 0.4070)$ (#1) and $c = (0.4070, 0.3693, 0.6745, 0.4930)$ (#2). The channels have the same magnitude response as the channel in Example 1, which is minimum-phase. Note that the performance deteriorates as the channel phase increases. The deterioration in performance is due to two factors: the increase in the distance loss with the channel phase as discussed in Section 4.11 and the increase in error propagation. The latter effect is not captured in the upper bound, so the bound diverges as error propagation becomes significant. The loss in the minimum distance for mixed phase channels 1 and 2 as compared to MLSE is 1.6 dB and 3.1 dB as given by (4.103) and (4.107) respectively.

For our second example, the medium response is given by half-symbol spaced tap coefficients $c = (0.6335, 0.5456, 0.4479, 0.3167)$ (same as the minimum-phase channel of Ex-

ample 1 but with fractional spacing). The medium response memory is $L_c = 3$. We consider two different transmit filters specified by the sampled autocorrelation function $o = (0.045, 0.0, 0.4053, 1.0, 0.4053, 0.0, 0.045)$ (T1) and $\phi = (0.33, 0.33, 0.33, 1.0, 0.33, 0.33, 0.33)$ (T2). The first one is a Nyquist-1 pulse (truncated to seven half-symbol samples) taken from [4, (5.5)] while the second one is arbitrarily chosen. The transmit filter memory is $L_d = 3$. The overall channel memory is thus $L = (L_c + L_d)/2 = 3$. The memory order is chosen as $J = 1$ for the DFSE receivers.

Fig. 4.10 shows the BER performance of various receivers for the two transmit filters (T1 and T2) with transmit matched filtering. In the case of T1, the WF-DFSE receiver achieves close to MLSE performance while the performance of MF-DFSE is less than a dB worse. ZF-DFSE is not shown for the case of T1 as its BER is very close to WF-DFSE at all SNRs. Note that the zero-forcing filter in ZF-DFSE(T) decorrelates only the transmit filter response, unlike ZF-DFSE(S) where the zero-forcing filter decorrelates the overall channel response. For the case of T2, we show upper bounds for WF-DFSE and ZF-DFSE which are marginally lower than the simulated results due to error propagation. Note that WF-DFSE performs better than ZF-DFSE at all SNRs as in Example 1. MF-DFSE in the case of T2 is much worse than MLSE as the sampled correlations in the case of T2 are more severe than T1.

4.14 Conclusions

We have presented a unified analysis of DFSE and M-algorithm receivers for channels with finite memory that examines the role of the receive filter and the branch metric. The analysis indicates that the error performance of certain receivers (called biased receivers) is affected by untreated interference components (bias) which arise due to a mismatch between the receive filter and the branch metric. We have shown that an unbiased receiver consists of a front-end filter (matched to the overall channel response or the transmit filter response) followed by the appropriate noise-whitening or zero-forcing filter and a reduced trellis or tree search algorithm. We have shown that the DFSE receivers with the noise-whitening filter (and the proper branch metric) are optimum among unbiased DFSE and truncated memory MLSE receivers (with pre-filtering) in the sense that they maximize the error distance. We have obtained novel receiver structures which employ transmit matched filtering and are

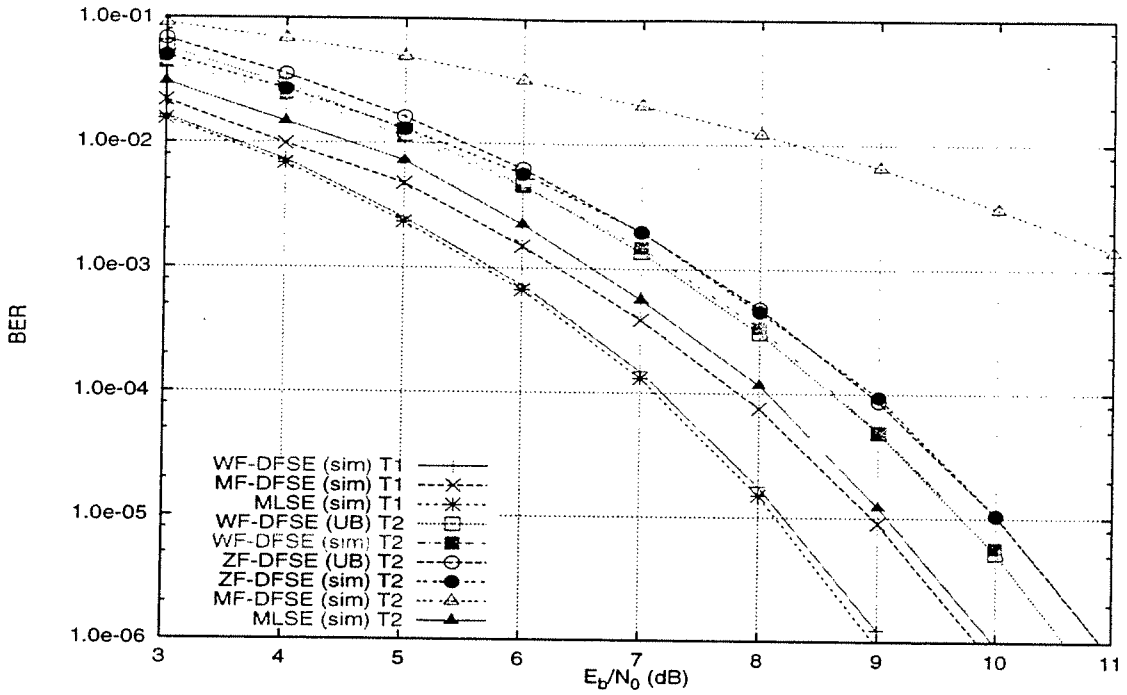

Figure 4.10: BER performance of various receivers in Example 2.

thus suitable for adaptive channel estimation in the presence of excess signal bandwidth. We have obtained upper bounds on the symbol error probability of the various DFSE receivers and described a generating function approach to evaluate the bounds. Simulation and analytical results were presented for the various receivers using a symbol-spaced channel model and a fractionally-spaced channel model. The bounds were found to be tight in each case.

CHAPTER 5

Bias-compensated matched-filter receivers

5.1 Introduction

In Chapter 4, we considered decision feedback sequence estimation (DFSE) and M-algorithm (MA) receivers that operate on matched filter statistics (MF-DFSE and MF-MA). These receivers are simple in that they do not require an additional processing filter like a noise-whitening or zero-forcing filter. Such a filter generally involves channel inversion and/or factorization operations which are not feasible in the case of time-varying, cyclo-stationary and bidirectional channels, as well as channels with deep spectral nulls. Applications that particularly involve such channels include multiuser detection for DS-CDMA systems, bidirectional equalization for the GSM system and fractional equalization for narrowband systems with excess signal bandwidth.

We showed in Chapter 4 that for each case of matched filtering – front-end filter matched to the overall channel response (standard) or transmit filter response (transmit), the MF-DFSE receivers have greater error distance than the corresponding whitening filter DFSE and zero-forcing filter DFSE receivers. In fact, the MF-DFSE receiver with the standard matched filter (MF-DFSE(S)) achieves the same error distance as an MLSE receiver. However, the high error distance of MF-DFSE receivers does not translate into good error-rate performance. This is because the MF-DFSE and MF-MA receivers belong to the class of biased receivers whose error-rate performance is affected by untreated interference components (bias). The bias, in fact, dominates the error-rate performance of these receivers as we saw in simulation examples given in Chapter 4.

The interference components that constitute the bias for the various matched filter

receivers were identified in Chapter 4 using an event error analysis. It was found that the interference arises due to a few anti-causal transmitted symbols. Thus, an intuitive solution to the problem of bias is to cancel it by means of tentative decision feedback. With reliable tentative decisions, the bias can be compensated effectively. As a result, the error-rate performance is no longer dominated by untreated interference components and is improved significantly for most channels of interest. A bias-compensated MF-DFSE (BC-MF-DFSE) receiver was proposed in [20][1] for the case of standard matched filtering. In this chapter, we describe this receiver and obtain a similar receiver for the case of transmit matched filtering. We also discuss an extension of this approach to the case of M-algorithm.

Tentative decisions needed for bias compensation can be obtained by employing a conventional symbol-by-symbol decision device. In a multistage scheme, the decisions obtained in the first stage can also be used to cancel bias in the next stage. On channels with severe intersymbol interference (ISI) or multiple-access interference (MAI), it is not possible to obtain reliable decisions by means of symbol-by-symbol detection. However, by using a minimum mean square error (MMSE) estimator (an optimal symbol-by-symbol soft decision), one can always reduce the mean square error after bias compensation no matter how severe the interference. In practice, we find that a MF-DFSE receiver with soft bias compensation (SBC-MF-DFSE) provides a significant gain over MF-DFSE for most channels of interest without much added complexity.

We analyze the performance of the MF-DFSE receiver for the case of standard matched filtering without and with bias compensation using hard as well as soft tentative decisions. In the case of hard tentative decisions, we obtain approximate semi-analytic upper bounds on the error probability by assuming independence between the main and tentative decision errors. In the case of soft linear tentative decisions, we apply a Chebyshev type technique to upper-bound the error probability in the presence of residual interference. We outline a generating function method to evaluate union bounds on the error probability of the various receivers. The bounds are relatively simple to compute when the memory order of the DFSE receiver and the channel memory is small. For channels with large memory, we use monte carlo simulations to compare the performance of the various receivers.

The chapter is organized as follows. In Sections 5.2 and 5.3, we describe the BC-MF-DFSE receiver for the case of standard (S) and transmit (T) matched filtering respectively.

[1]The algorithm is referred to as modified unwhitened DFSE (MUDFSE) in [20].

In Section 5.4, we briefly discuss bias compensation for matched-filter M-algorithm. In Section 5.5, we analyze the BC-MF-DFSE(S) receiver. In Section 5.6, we describe bias compensation using soft decisions and obtain various estimators. We analyze the SBC-MF-DFSE algorithm with linear soft decisions in Section 5.7. Simple Chebyshev type bounds for MF-DFSE and SBC-MF-DFSE are described in Section 5.8. In Section 5.9, we describe a generating function approach to evaluate the various bounds. The performance of the various receivers is compared via simulation and analysis in Section 5.10, where we give examples of equalization for ISI channels and multiuser detection for DS-CDMA channels.

5.2 The BC-MF-DFSE(S) receiver

The receiver consists of a front-end filter, which is matched to the overall channel impulse response, followed by a reduced trellis search algorithm. The trellis search algorithm computes path metrics as in MF-DFSE(S) i.e. using (4.37) and (4.38) with the formulation $P^{-1} = R = I$, $Q = S$. Conditional decisions are made (and the corresponding survivor paths are chosen) using the modified rule:

$$\hat{\alpha}_{n-J}(\beta_n) = \arg\max_{\alpha_{n-J}} [\mathcal{M}(\beta_n) + \Gamma(\alpha_n, \beta_n) - \text{bias}(\beta_n)], \tag{5.1}$$

where $\mathcal{M}(\beta_n)$ and $\Gamma(\alpha_n, \beta_n)$ are the accumulated metric and the branch metric of MF-DFSE(S) respectively and the bias term is given by

$$\text{bias}(\beta_n) = 2\text{Re}\left\{\underline{\mu}_n^H \dot{S}_{L-J}^H \underline{\tilde{a}}_{n+1}\right\} \tag{5.2}$$

where $\underline{\mu}_n = [\hat{\alpha}_{n-L+1}(\beta_n), \ldots, \hat{\alpha}_{n-J-1}(\beta_n), \alpha_{n-J}]^T$ are the $L-J$ most recent symbols in the survivor path associated with state β_n, $\dot{S}_{L-J}$ is the principal submatrix of dimension $L-J$ of the matrix $\dot{S}$ given by (4.80) and $\underline{\tilde{a}}_{n+1} = [\tilde{a}_{n+1}, \ldots, \tilde{a}_{n+L-J}]^T$ are tentative decisions on $L-J$ future symbols obtained using conventional matched filter detection. In the case of antipodal transmitted symbols, the tentative decisions are obtained as

$$\tilde{a}_n = \text{sign}(z_n). \tag{5.3}$$

The algorithm is delayed by $L-J$ symbols as the statistic up to time $n+L-J$ is needed in the nth step to obtain tentative decisions. Note that the bias term follows from the expression for the untreated interference given by (4.83). The bias is used for survivor path selection only and does not contribute to the accumulated path metric. The bias

in (5.2) depends on the symbol α_{n-J} (which is falling out of the state) and the symbols $\alpha_{n-L+1}, \ldots, \alpha_{n-J-1}$ for which conditional decisions, taken from the survivor path history of state β_n, are used. The bias can be simplified to include the leading term only, which depends on α_{n-J}, as follows:

$$\text{bias}(\beta_n) \approx \text{bias}(\alpha_{n-J}) = \text{Re}\left\{2\alpha^*_{n-J} \sum_{i=J+1}^{L} s(-i)\tilde{a}_{n-J+i}\right\}. \tag{5.4}$$

Note that the approximate bias is independent of the state. It does not add significantly to the computational load and storage requirement of the MF-DFSE algorithm which is on the order of $(K-J)|\mathcal{A}|^J$, where K is the decision lag. This reduced-computation form of the algorithm was first proposed in [17].

5.2.1 Multistage BC-MF-DFSE(S)

The above algorithms can be run in a multistage configuration where decisions obtained at the output of the first stage are fed back to compute the bias in the second stage and so on, i.e.

$$(\tilde{a}_n)_1 = \text{sign}(z_n) \text{ and } (\tilde{a}_n)_i = (\tilde{a}_n)_{i-1}, \quad i > 1$$

where $\{(\tilde{a}_n)_i\}$ are decisions obtained from the ith stage at lag K_i ($K_i \gg L$). Note that the decisions $\{(\tilde{a}_n)_1\}$ are likely to be much more reliable than the tentative decisions $\{(\tilde{a}_n)_1\}$. The complexity and delay of an M-stage scheme is given by $\sum_{i=1}^{M}(K_i - J_i)M^{J_i}$ and $\sum_{i=1}^{M} K_i + L - J_1$ respectively.

5.3 The BC-MF-DFSE(T) receiver

A bias-compensated MF-DFSE receiver can also be obtained for the case of transmit matched filtering (BC-MF-DFSE(T)). In this case, the algorithm computes path metrics as in MF-DFSE(T) using (4.41). Conditional decisions are made using the modified rule:

$$\hat{\alpha}'_{n-J}(\beta_n) = \arg\max_{\alpha_{n-J}}[\mathcal{M}'(\beta_n) + \Gamma'(\alpha_n, \beta_n) - \text{bias}'(\beta_n)] \tag{5.5}$$

where $\mathcal{M}'(\beta_n)$ and $\Gamma'(\alpha_n, \beta_n)$ are the accumulated metric and the branch metric of MF-DFSE(T), respectively, and the bias term is given by

$$\text{bias}'(\beta_n) = 2\text{Re}\left\{\underline{\mu}'^H_n (\ddot{C}_{L_d \times L-J})^H \ddot{\Phi} \ddot{C} \underline{\tilde{a}}'_{n+1}\right\} \tag{5.6}$$

where $\underline{\mu}'_n = [\eta'_{n-L+1}, \ldots, \eta'_{n-J-1}, \eta'_{n-J}]^T$ are the $L-J$ most recent symbols in the survivor path associated with state β_n and $\underline{\tilde{a}}'_{n+1} = [\eta'_{n-L_c+1}, \ldots, \eta'_n, \tilde{a}'_{n+1}, \ldots, \tilde{a}'_{n+L_d}]^T$, where $\{\tilde{a}'_n\}$ are tentative decisions obtained as $\tilde{a}'_n = \text{sign}(z'_n)$, in the case of antipodal transmitted symbols. The bias term follows from (4.85).

5.4 Bias compensation for M-algorithm

Note that a bias-compensated MF-MA can also be derived on the same principle as described above for BC-MF-DFSE i.e. using tentative decisions to cancel untreated interference components. The untreated interference in the case of MF-MA (with the standard matched filter) follows from (4.66) as $2\text{Re}\{\underline{\xi}(i)^H \dot{S}^H \underline{\dot{a}}_k\}/\delta(\underline{e}(i))$, where $\underline{\xi}(i) = [e_{k-L}(i), \ldots, e_{k-1}(i)]^T$ is the tail of the error sequence $\underline{e}(i)$ corresponding to the ith contender path and $\underline{\dot{a}}_k = [a_k, \ldots, a_{k+L-1}]^T$. The interference can be canceled by choosing survivor paths in the M-algorithm on the basis of the accumulated metric minus a bias term, computed using tentative decisions. Note that the bias term in this case depends on the last L symbols of the survivor path rather than the last $L-J$, as in the case of BC-MF-DFSE. This is because unlike DFSE, the M-algorithm is a tree search algorithm where contender paths are not constrained to merge. Since contender paths in DFSE always agree on the J most recent symbols, the bias term does not depend on them. However, this is not the case with the M-algorithm. Consequently, bias compensation requires more computation for MF-MA as compared to MF-DFSE. Moreover, as the number of interference components that need to be canceled is more in the case of MF-MA, the residual interference arising from tentative decision errors is more significant in the case of MF-MA. Thus, bias compensation does not look very attractive for MF-MA.

5.5 Analysis of BC-MF-DFSE(S)

Let $\{a_n\}$ be the sequence of symbols transmitted and $\{b_n\}$ be the sequence of states in the path of $\{a_n\}$ in the reduced trellis of the BC-MF-DFSE(S) receiver (with memory order J). Let $\{\bar{a}_n\}$ be a hypothetical sequence of symbols and $\{\bar{b}_n\}$ be the corresponding sequence of states in the reduced trellis that diverges from the correct sequence of states at time unit 0 and re-merges with it at a later time (say k). A first event error occurs at time 0 if the reduced trellis search algorithm picks $\{\bar{a}_n\}$ as the survivor sequence over $\{a_n\}$. It

follows from (5.1) that the error event occurs if

$$\sum_{n=0}^{k-1} \Gamma(\bar{a}_n, \bar{b}_n) - \text{bias}(\bar{b}_{k-1}) > \sum_{n=0}^{k-1} \Gamma(a_n, b_n) - \text{bias}(b_{k-1}) \tag{5.7}$$

where the bias term bias$(\cdot)$ is given by (5.2). Using (4.78) and (5.2), we see that the error event occurs if

$$2\text{Re}\{\underline{e}_k^H \underline{u}_k\} > \underline{e}_k^H S_k \underline{e}_k + 2\text{Re}\{\underline{\xi}^H \dot{S}_{L-J}^H \underline{t}_k\} \tag{5.8}$$

where $\underline{e}_k = \bar{\underline{a}}_k - \underline{a}_k$ is the error sequence with the tail $\xi = (e_{k-L}, \ldots, e_{k-J-1})^H$ and $\underline{t}_k = \bar{\underline{a}}_k - \dot{\underline{a}}_k$ are tentative decision errors in bias cancellation. To simplify analysis, we assume here that tentative decision errors are independent of main decision errors. This is not true in general because noise samples affecting the sampled statistic, obtained at the output of the matched filter, are correlated. However, independence can be assumed if the sampled channel correlations are small. Then, the probability of the error event ε: the sequence $\underline{a}_k$ is eliminated in favor of the sequence $\underline{a}_k + \underline{e}_k$ (for given $\underline{a}_k$ and $\underline{e}_k$), is approximated as

$$\Pr(\varepsilon) \approx \text{E}_{\underline{t}} \left[\text{Q} \left(\frac{\underline{e}_k^H S_k \underline{e}_k + 2\text{Re}\{\underline{\xi}^H \dot{S}_{L-J}^H \underline{t}\}}{2\sqrt{N_0 \underline{e}_k^H S_k \underline{e}_k}} \right) \right] \tag{5.9}$$

where the expectation is taken over all possible values of the tentative decision error vector $\underline{t}$ having $L - J$ components. It follows that the first event error probability of the BC-MF-DFSE(S) receiver can be approximately upper-bounded as

$$P_{FEE} \lesssim \sum_{\underline{e} \in E'} p_{\underline{e}} \text{E}_{\underline{t}} \left[\text{Q} \left(\frac{\delta(\underline{e}) + \gamma(\underline{e}, \underline{t})}{2\sqrt{N_0}} \right) \right] \tag{5.10}$$

where E' is the set of all error sequences $\underline{e} = e_0, e_1, \ldots, e_{l-1}, 0 \ldots, 0$ (of length $l + J$, $l > 0$, $e_{l-1} \neq 0$) with less than J consecutive zeros in the middle of the sequence and the last L components[2] equal to $(\underline{\xi}^T, 0, \ldots, 0)$. The quantity $\delta(\underline{e})$ is the distance of an error sequence $\underline{e} \in E'$ of length k, given by

$$\delta(\underline{e}) = \sqrt{\underline{e}^H S_k \underline{e}}, \tag{5.11}$$

$p_{\underline{e}}$ is the probability that a transmitted sequence can have $\underline{e}$ as an error sequence and $\gamma(\underline{e}, \underline{t})$ is the residual interference arising from tentative decision feedback, given by

$$\gamma(\underline{e}, \underline{t}) = 2\text{Re}\{\underline{\xi}^H \dot{S}_{L-J}^H \underline{t}\} / \delta(\underline{e}). \tag{5.12}$$

[2] $e_i = 0$, for $i < 0$.

The residual interference can be viewed as a normalized projection of the tentative decision error vector $\underline{t}$ onto the main decision error vector $\underline{\epsilon}$ as determined by the sampled channel autocorrelation spectrum S. The symbol error probability can be approximately upper-bounded using the union bound as

$$P_s \tilde{\leq} \sum_{\underline{e} \in E'} \mathrm{w}(\underline{e}) p_{\underline{e}} \mathrm{E}_{\underline{t}} \left[\mathrm{Q} \left(\frac{\delta(\underline{e}) - \gamma(\underline{e}, \underline{t})}{2\sqrt{N_0}} \right) \right] \tag{5.13}$$

where $\mathrm{w}(\underline{e})$ is the number of symbol errors entailed by the error sequence $\underline{e}$. As discussed in Section 4.10, the above bound does not include the effect of error propagation.

In Appendix D, we derive expressions for the probability $\Pr(\varepsilon)$ for a two-stage BC-MF-DFSE receiver, with and without assuming independence between tentative and main decision errors.

5.5.1 Genie-aided MF-DFSE

Assume that perfect information is provided by a genie on the future inputs needed to compute the bias in BC-MF-DFSE i.e. $\underline{t}_k = \underline{0}$ w.p.1. The symbol error probability in this case is given by

$$P_s \leq \sum_{\underline{e} \in E'} \mathrm{w}(\underline{e}) p_{\underline{e}} \mathrm{Q} \left(\frac{\delta(\underline{e})}{2\sqrt{N_0}} \right). \tag{5.14}$$

Note that the above expression for the symbol error probability of genie-aided MF-DFSE (GA-MF-DFSE) is the same as in the case of MLSE. The difference is that the ensemble average is taken over fewer error sequences for GA-MF-DFSE than for MLSE. The set E' does not contain error sequences with more than $J-1$ but less than L consecutive zeros in the middle. However, these sequences are included in the case of MLSE. Thus, the upper-bound on the symbol probability of GA-MF-DFSE given by (5.14) is lower than MLSE. With the memory order J chosen as zero, all error sequences have length $k = 1$ symbol. This implies that the error distance squared is given by $\underline{e}^H S_k \underline{e} = |e|^2 s(0)$. In other words, zero-th order GA-MF-DFSE achieves the performance of the ISI-free channel. This makes sense since we assumed absence of error propagation from previous error events (by limiting ourself to first error events only) which accounts for all past interference in the case of zero memory order. In reality, zero-th order GA-MF-DFSE approaches ISI-free performance asymptotically at high signal-to-noise ratio for channels where the eye is not entirely closed, as error propagation becomes negligible.

5.6 Soft-input BC-MF-DFSE receivers

Instead of using hard tentative decisions to cancel bias in the BC-MF-DFSE receivers, soft tentative decisions can be employed to reduce the mean square error in the bias compensated output. Consider a memoryless AWGN channel, i.e.

$$z_n = \sqrt{E_b} a_n + w_n \tag{5.15}$$

where $\{w_n\}$ is an independent and identically distributed (i.i.d.) Gaussian random process with mean zero and variance σ_w^2 and $a_n \in \{\pm 1\}$. An optimum soft decision $\tilde{a}_n$ that minimizes the mean square error

$$\text{MSE} = \text{E}[(a_n - \tilde{a}_n)^2] \tag{5.16}$$

is given by [15]

$$\tilde{a}_n = \tanh(z_n \sqrt{E_b}/\sigma_w^2). \tag{5.17}$$

5.6.1 Optimum soft decision

Given the standard matched filter statistic z_n (4.4), the (one-shot) minimum mean square error (MMSE) estimator of a_n is given by [27]

$$\tilde{a}_n = \text{E}[a_n | z_n]. \tag{5.18}$$

For a channel with memory as in (4.4), the above estimator does not turn out to be a simple function of the statistic as in (5.17). A simplified estimator can be obtained by invoking the central limit theorem [27] to approximate the sum of the post and pre-cursor interference components as Gaussian. For i.i.d. equiprobable and antipodal symbols a_n, assuming that $\sum_{i \neq 0} s(i) a_{n-i}$ is a Gaussian random variable with mean zero and variance $\sum_{i \neq 0} |s(i)|^2$, the following estimator is obtained[3]

$$\tilde{a}_n = \tanh\left(\frac{z_n}{\frac{N_0}{2} + \frac{1}{s(0)} \sum_{i \neq 0} |s(i)|^2} \right). \tag{5.19}$$

The above estimator replaces the hard decision of (5.3) in a Soft-input BC-MF-DFSE(S) (SBC-MF-DFSE(S)) receiver.

[3]Note that for real symbol alphabet, the noise is real with spectral density $N_0/2$ instead of N_0.

5.6.2 Optimum linear soft decision

Given the statistic z_n (4.4), we determine the (one-shot) linear minimum mean square error (MMSE) estimator of a_n, i.e. we find $\tilde{a}_n$ as a linear function of z_n such that the mean square error given by (5.16) is minimized. Assuming i.i.d., equiprobable antipodal symbols a_n, we get the linear MMSE estimator as

$$\tilde{a}_n = \frac{z_n}{\chi} \tag{5.20}$$

where χ is a normalization factor, given by

$$\chi = \frac{N_0}{2} + \frac{1}{s(0)} \sum_{i=-L}^{L} |s(i)|^2. \tag{5.21}$$

The mean square error of this estimator is given by

$$\text{MSE} = 1 - \frac{s(0)}{\chi} \tag{5.22}$$

which is always less than 1. Thus, the estimator guarantees that the mean square error is reduced at the output of the estimator no matter how severe the interference components.

Note that the MMSE estimator of (5.19) is obtained by using a simplifying assumption, which may not be accurate especially for small channel memory L. However, the linear MMSE estimator of (5.20) is a true optimum estimator.

5.7 Analysis of SBC-MF-DFSE(S)

In this section, we examine the error performance of a SBC-MF-DFSE(S) receiver that employs the linear optimum soft decisions of (5.20) to cancel bias in the case of real antipodal signals. Following the development of (5.8), we see that a first event error, corresponding to the error sequence $\underline{e}_k$, occurs at time 0 in a SBC-MF-DFSE(S) receiver if

$$2\underline{e}_k^T \underline{u}_k > \underline{e}_k^T S_k \underline{e}_k + 2\underline{\xi}^T \dot{S}_{L-J}^T (\underline{\tilde{a}}_k - \underline{\dot{a}}_k) \tag{5.23}$$

where $\underline{\tilde{a}}_k = (\tilde{a}_k, \ldots, \tilde{a}_{k+L-J-1})^T$ are soft tentative decisions given by (5.20). Substituting (4.4) and (5.20) in (5.23), we get

$$2\underline{e}_k^T \underline{u}_k - 2\underline{\xi}^T \dot{S}_{L-J}^T \dot{\underline{u}}_k/\chi > \underline{e}_k^T S_k \underline{e}_k + 2\underline{\xi}^T \dot{S}_{L-J}^T \check{S} \underline{\check{a}}_k/\chi \tag{5.24}$$

where $\underline{\check{a}}_k = (a_{k-L}, a_{k-L+1}, \ldots, a_{k+2L-J-1})^T$, $\underline{\dot{u}}_k = (u_k, \ldots, u_{k+L-J-1})^T$ and $\dot{S}$ is an $(L-J) \times (3L-J)$ matrix given by

$$\dot{S} = \begin{bmatrix} s(L) & \cdots & s(1) & (1-\chi)s(0) & s(-1) & \cdots & s(-L) & 0 & \cdots & 0 \\ 0 & s(L) & \cdots & s(1) & (1-\chi)s(0) & s(-1) & \cdots & s(-L) & \ddots & \vdots \\ \vdots & \ddots & \ddots & & & \ddots & & & \ddots & 0 \\ 0 & \cdots & 0 & s(L) & \cdots & s(1) & (1-\chi)s(0) & s(-1) & \cdots & s(-L) \end{bmatrix}. \tag{5.25}$$

Note that the quantity on the left-hand side of (5.24) is a Gaussian random variable with mean zero and variance given by

$$2N_0 \left(\underline{e}_k^T S_k \underline{e}_k - 2\|\dot{S}_{L-J}\underline{\xi}\|^2/\chi + \underline{\xi}^T \dot{S}_{L-J}^T S_{L-J} \dot{S}_{L-J} \underline{\xi}/\chi^2 \right), \tag{5.26}$$

where we use the fact that the last L components of $\underline{e}_k$ are $(\underline{\xi}^T, 0, \ldots, 0)$. Thus, the probability of the error event ε corresponding to the error sequence $\underline{e}_k$ of length k can be upper-bounded as

$$\Pr(\varepsilon) \leq \mathrm{E}_{\underline{\check{a}}} \left[\mathrm{Q} \left(\frac{\underline{e}_k^T S_k \underline{e}_k + 2\underline{\xi}^T \dot{S}_{L-J}^T \check{S} \underline{\check{a}}/\chi}{\sqrt{2N_0 \left(\underline{e}_k^T S_k \underline{e}_k - 2\|\dot{S}_{L-J}\underline{\xi}\|^2/\chi + \underline{\xi}^T \dot{S}_{L-J}^T S_{L-J} \dot{S}_{L-J} \underline{\xi}/\chi^2 \right)}} \right) \right] \tag{5.27}$$

where the expectation is taken over the $3L-J$ components of $\underline{\check{a}}$ independently of the error sequence $\underline{e}_k$. Since some of the first $L-J$ components of $\underline{\check{a}}$ may be uniquely identified by specifying the error sequence $\underline{e}_k$, the expectation is taken over a slightly broader set than needed to obtain $\Pr(\varepsilon)$. Thus, (5.27) is an upper bound and not an exact expression. The symbol error probability can be upper-bounded using the union bound by assuming absence of error propagation from previous error events, as

$$P_s \leq \sum_{\underline{e} \in E'} \mathrm{w}(\underline{e}) p_{\underline{e}} \mathrm{E}_{\underline{\check{a}}} \left[\mathrm{Q} \left(\frac{\underline{e}^T S_k \underline{e} + 2\underline{\xi}^T \dot{S}_{L-J}^T \check{S} \underline{\check{a}}/\chi}{\sqrt{2N_0 \left(\underline{e}^T S_k \underline{e} - 2\|\dot{S}_{L-J}\underline{\xi}\|^2/\chi + \underline{\xi}^T \dot{S}_{L-J}^T S_{L-J} \dot{S}_{L-J} \underline{\xi}/\chi^2 \right)}} \right) \right]. \tag{5.28}$$

5.8 Simple upper bounds for MF-DFSE and SBC-MF-DFSE

The bounds of (4.99) and (5.28) for MF-DFSE and SBC-MF-DFSE receivers require ensemble averaging over the untreated interference components. In the case of the MF-DFSE(S) receiver, the expectation is taken over $L-J$ interference symbols while in the

case of the SBC-MF-DFSE(S) receiver with linear soft tentative decisions, the expectation is taken over $3L-J$ symbols. The latter is cumbersome to evaluate even for very short channel memory L. Simpler upper bounds can be obtained by extending the results of Glave [16] and Matthews [31] which upper and lower bound the probability of error of a thresholding detector in the presence of ISI. The Glave bound was also applied by Mclane [32] to upper bound the error probability of truncated-state Viterbi detectors. In the following, we apply the Glave bound to the case of MF-DFSE and SBC-MF-DFSE receivers.

Let w be a Gaussian random variable with mean zero and variance σ_w^2 and x be an arbitrary random variable subject to the constraints: $x \in [-I, I]$ almost surely and $\mathrm{E}[x^2] \leq \sigma_x^2$. Glave showed in [16, theorem 3] that the probability $\Pr(|w+x| \geq K)$ can be upper-bounded as

$$\Pr(|w+x| \geq K) \leq \frac{\sigma_x^2}{I^2}\left[\mathrm{Q}\left(\frac{K-I}{\sigma_w}\right)+\mathrm{Q}\left(\frac{K+I}{\sigma_w}\right)\right]+2\left(1-\frac{\sigma_x^2}{I^2}\right)\mathrm{Q}\left(\frac{K}{\sigma_w}\right) \tag{5.29}$$

provided that $K - I \geq \sqrt{3}\sigma_w$. For a system with antipodal signals and symbol-by-symbol detection in the presence of ISI, I can be considered as the peak interference, K as the signal amplitude and $K - I$ as the eye opening.

Now we apply the above result to upper-bound the probability of a particular error event for the MF-DFSE(S) receiver obtained in Section 4.8.1. Given an error sequence $\underline{e} \in E'$ of length k with tail $\underline{\xi}$, the error probability given by

$$\Pr(\varepsilon) = \mathrm{E}_{\underline{a}}\left[\mathrm{Q}\left(\frac{\delta(\underline{e})-\gamma(\underline{e},\underline{a})}{\sqrt{2N_0}}\right)\right], \tag{5.30}$$

for $a_n \in \{\pm 1\}$ (noise spectral density $N_0/2$), where $\gamma(\underline{e},\underline{a})$ is given by (4.83), is upper-bounded as

$$\Pr(\varepsilon) \leq \frac{\sigma_1^2}{2I_1^2}\left[\mathrm{Q}\left(\frac{\delta(\underline{e})-I_1}{\sqrt{2N_0}}\right)+\mathrm{Q}\left(\frac{\delta(\underline{e})+I_1}{\sqrt{2N_0}}\right)\right]+\left(1-\frac{\sigma_1^2}{I_1^2}\right)\mathrm{Q}\left(\frac{\delta(\underline{e})}{\sqrt{2N_0}}\right) \tag{5.31}$$

provided that

$$\delta(\underline{e}) - I_1 \geq \sqrt{6N_0}, \tag{5.32}$$

where[4] $\delta(\underline{e}) = \sqrt{\underline{e}^T S_k \underline{e}}$, $I_1 = 2|\dot{S}_{L-J}\underline{\xi}|/\delta(\underline{e})$ and $\sigma_1^2 = 4\|\dot{S}_{L-J}\underline{\xi}\|^2/\delta^2(\underline{e})$. A similar bound can be obtained for the MF-DFSE(T) receiver.

[4] $|\underline{y}| \triangleq \sum_i |y_i|$.

In the case of the SBC-MF-DFSE(S) receiver analyzed in Section 5.7, the error probability bound given by (5.27) can be further upper-bounded as

$$\Pr(\varepsilon) \leq \frac{\sigma_2^2}{2I_2^2}\left[\mathrm{Q}\left(\frac{\delta^2(\underline{e})-I_2}{\sqrt{2N_0\sigma_n^2}}\right)+\mathrm{Q}\left(\frac{\delta^2(\underline{e})+I_2}{\sqrt{2N_0\sigma_n^2}}\right)\right]+\left(1-\frac{\sigma_2^2}{I_2^2}\right)\mathrm{Q}\left(\frac{\delta^2(\underline{e})}{\sqrt{2N_0\sigma_n^2}}\right), \quad (5.33)$$

provided that

$$\delta^2(\underline{e}) - I_2 \geq \sqrt{6N_0\sigma_n^2}, \quad (5.34)$$

where $I_2 = 2|\check{S}^T\dot{S}_{L-J}\underline{\xi}|/\chi$, $\sigma_2^2 = 4\|\check{S}^T\dot{S}_{L-J}\underline{\xi}\|^2/\chi^2$ and $\sigma_n^2 = \delta^2(\underline{e}) - 2\|\dot{S}_{L-J}\underline{\xi}\|^2/\chi + \underline{\xi}^T\dot{S}_{L-J}^T S_{L-J}\dot{S}_{L-J}\underline{\xi}/\chi^2$.

Note that the matrix $\check{S}$ is given in terms of the sampled channel correlations and the normalization factor χ which depends on the noise spectral density $N_0/2$. The dependence on the noise spectral density means that the matrix $\check{S}$ has to be computed for each value of the signal-to-noise ratio (SNR). The extensive numerical computation can be avoided as the noise spectral density approaches zero. Thus, assuming high SNR, we use the approximation

$$\chi \approx \frac{1}{s(0)}\sum_{i=-L}^{L}|s(i)|^2. \quad (5.35)$$

The condition (5.34) is evaluated for the approximate value of χ although it does not guarantee that the condition is met for the actual value of χ. Using the approximate value of χ in the analysis, we, in fact, upper-bound the error probability for a SBC-MF-DFSE(S) receiver that employs the soft decision

$$\tilde{a}_n = \frac{z_n}{\frac{1}{s(0)}\sum_{i=-L}^{L}|s(i)|^2} \quad (5.36)$$

to cancel bias instead of the optimum linear soft decision (5.20).

In order to determine the union bound on the probability of symbol error, one must take an ensemble average over all possible error sequences $\underline{e} \in E'$ (4.99), (5.28). In order to apply the Glave bound, the corresponding conditions (5.32) and (5.34) must hold for all error sequences $\underline{e} \in E'$. Since the peak untreated interference I_1 and I_2 depend on the tail of the error sequence $\underline{\xi}$, it is not sufficient to check the conditions for the minimum distance sequences ($\underline{e}_{min} = \arg\min_{\underline{e}\in E'}\delta(\underline{e})$) only. In practice, the conditions have to be checked for a few of the higher distance sequences as well.

Glave's upper bound applies only at high SNR values and when the eye (due to the untreated interference) is open. Matthews [31] determined upper and lower bounds on the probability of error for a thresholding detector for the entire range of SNR. His bounds can also be applied to our case in a similar manner.

5.9 Bound evaluation

In this section, we describe a generating function method to evaluate the symbol error probability bounds for MF-DFSE, BC-MF-DFSE and SBC-MF-DFSE derived in Sections 4.10, 5.5 and 5.8, respectively for the case of standard matched filtering. Previously, the error probability of DFSE receivers was approximated by considering minimum distance error sequences and may be some higher distance sequences, which were found empirically. In Section 4.12, we described a generating function method that can be used for unbiased DFSE receivers. In [20], we proposed a generating function method to evaluate an approximate bound for the BC-MF-DFSE(S) receiver. This section includes treatment for the MF-DFSE(S), BC-MF-DFSE(S) and the SBC-MF-DFSE(S) receivers.

An error state diagram (ESD) enumerates the distance $\delta(\underline{e})$, the number of symbol errors $\mathrm{w}(\underline{e})$ and the *a priori* probability $p(\underline{e})$ of all error sequences $\underline{e}$ in the set of allowable sequences E'. Each path through the ESD corresponds to an error sequence in E'. As in Section 4.12, an error state is defined as the value of L consecutive error symbols: $\{e_{j-L}, e_{j-L+1}, \ldots, e_{j-1}\}$. There are $(2|\mathcal{A}|-1)^L$ error states or nodes connected to each other through branches. The nodes and branches that correspond to J or more consecutive zeros in the middle of the error path are expurgated as in the case of unbiased DFSE receivers. The modified error state diagram is shown in Fig. 5.1 for the case of binary symbol alphabet, channel memory $L = 3$ and memory order $J = 1$. The pairs of error states that are negative of each other have been combined. Each branch is labeled with a branch distance parameter λ_i and the number of symbol errors entailed by the transition as the exponent of a dummy variable I.

For MF-DFSE(S), BC-MF-DFSE(S) and SBC-MF-DFSE(S), the distance squared of an error path through the ESD is given by (4.115), where the branch distance is given by

$$b_j = \mathrm{Re}\left\{ e_j^* \left(s(0)e_j + 2\sum_{i=1}^{L} s(i)e_{j-i} \right) \right\} \tag{5.37}$$

which follows from (4.82). The branch distance parameters λ_i are listed in Table 5.1. The branch distance appears as the exponent of a dummy variable D.

Note that the difference between the ESD of Fig. 4.7 and that of Fig. 5.1 is that the tail branches (corresponding to the tail $\underline{\xi}$ (4.79) of an error sequence) have been expurgated in Fig. 5.1. This is because for biased and bias-compensated MF-DFSE receivers, the untreated and the residual interference components, respectively, depend on the tail of the error path.

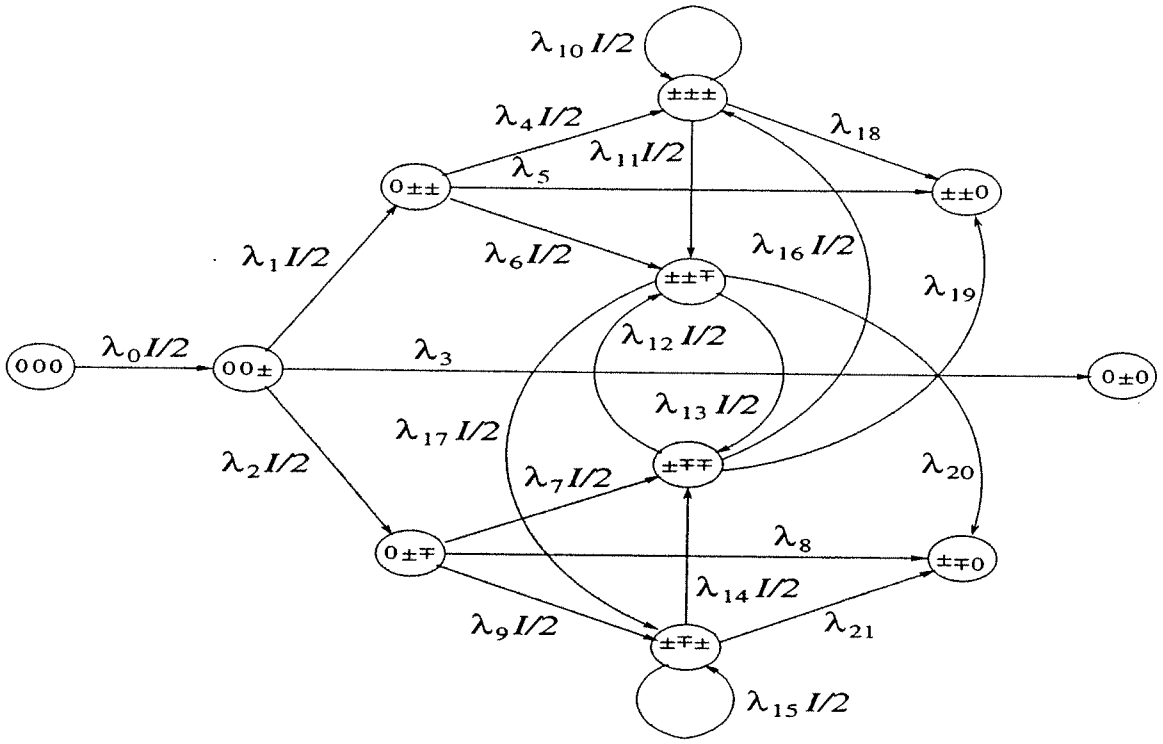

Figure 5.1: Error state diagram for MF-DFSE(S) ($L = 3, J = 1$).

Table 5.1: Branch distance parameters for MF-DFSE(S) ($L = 3, J = 1$)

$\lambda_0 = D^{4[s(0)]}$	$\lambda_1 = D^{4[s(0)+2s(1)]}$
$\lambda_2 = D^{4[s(0)-2s(1)]}$	$\lambda_4 = D^{4[s(0)+2s(1)+2s(2)]}$
$\lambda_6 = D^{4[s(0)-2s(1)-2s(2)]}$	$\lambda_7 = D^{4[s(0)+2s(1)-2s(2)]}$
$\lambda_9 = D^{4[s(0)-2s(1)+2s(2)]}$	$\lambda_{10} = D^{4[s(0)+2s(1)+2s(2)+2s(3)]}$
$\lambda_{11} = D^{4[s(0)-2s(1)-2s(2)-2s(3)]}$	$\lambda_{12} = D^{4[s(0)-2s(1)-2s(2)+2s(3)]}$
$\lambda_{13} = D^{4[s(0)+2s(1)-2s(2)-2s(3)]}$	$\lambda_{14} = D^{4[s(0)+2s(1)-2s(2)+2s(3)]}$
$\lambda_{15} = D^{4[s(0)-2s(1)+2s(2)-2s(3)]}$	$\lambda_{16} = D^{4[s(0)+2s(1)+2s(2)-2s(3)]}$
$\lambda_{17} = D^{4[s(0)-2s(1)+2s(2)+2s(3)]}$	$\lambda_3 = \lambda_5 = \lambda_8 = \lambda_{18-21} = 1$

In order to take an ensemble average over these components or apply the Glave bound, we have to enumerate the error paths that terminate in each tail sequence $\underline{\xi}$ separately. Noting that the interference term is insensitive to the sign of the tail sequence, we seek $(2|\mathcal{A}|-1)^{L-J-1}$ generating functions ($J < L$), in general, corresponding to the error paths that terminate with a given tail $\underline{\xi}$ such that the last component of $\underline{\xi}$, $e_{k-1-J} \neq 0$.

Let $T_j(D, I)$ be the generating function for the error paths which terminate in the tail $\underline{\xi}_j$ ($j = 1, 2, \ldots, 3^{L-J-1}$) found by solving the state equations simultaneously. Each generating function can be expanded in a series as

$$\frac{\partial}{\partial I} T_j(D, I)\Big|_{I=1} = \sum_l N_{j,l} D^{\delta_j^2(l)} \tag{5.38}$$

where $N_{j,l}$ is the number of error sequence pairs with distance $\delta_j(l)$ that terminate in the tail $\underline{\xi}_j$, per the number of symbol errors and the number of the corresponding input sequences. Then, the symbol error probability bound of (4.99) for MF-DFSE(S) can be computed as

$$P_s \leq \frac{2}{|\mathcal{A}|^{L-J}} \sum_{j=1}^{3^{L-J-1}} \sum_l \sum_{\underline{a} \in \mathcal{A}^{L-J}} N_{j,l} \mathrm{Q}\left(\frac{\delta_j(l) + \gamma\left(\underline{\xi}_j, \delta_j(l), \underline{a}\right)}{\sqrt{2N_0}} \right) \tag{5.39}$$

where we use the fact that the untreated interference $\gamma(\underline{e}, \underline{a})$ given by (4.83) depends on the error sequence $\underline{e}$ only through the tail of the error sequence $\underline{\xi}$ and the distance of the error sequence $\delta(\underline{e})$. The input symbols are considered i.i.d. equiprobable and the interference is averaged for all possible values of $L - J$ input symbols. When L is relatively large and J is small, it leads to several terms in the summation. In this case, the Glave bound can be employed which requires averaging for only three values of interference. Note that the parameters I_1 and σ_1^2 as given in Section 5.8 depend on the error sequence only through its distance and the tail sequence. Thus, the Glave bound for MF-DFSE(S) can be evaluated as

$$\begin{aligned} P_s \leq & \sum_{j=1}^{3^{L-J-1}} \sum_l N_{j,l} \left\{ \frac{\sigma_{1,j,l}^2}{I_{1,j,l}^2} \left[\mathrm{Q}\left(\frac{\delta_j(l) - I_{1,j,l}}{\sqrt{2N_0}} \right) + \mathrm{Q}\left(\frac{\delta_j(l) + I_{1,j,l}}{\sqrt{2N_0}} \right) \right] \right. \\ & \left. + \frac{1}{2}\left(1 - \frac{\sigma_{1,j,l}^2}{I_{1,j,l}^2}\right) \mathrm{Q}\left(\frac{\delta_j(l)}{\sqrt{2N_0}} \right) \right\}. \end{aligned} \tag{5.40}$$

where the subscripts l and j are for the lth error sequence with the jth tail in the ESD.

Similarly, the Glave bound for the SBC-MF-DFSE(S) receiver described in Section 5.8 can be evaluated as

$$P_s \leq \sum_{j=1}^{3^{L-J-1}} \sum_l N_{j,l} \left\{ \frac{\sigma_{2,j,l}^2}{2I_{2,j,l}^2} \left[\mathrm{Q}\left(\frac{\delta_j^2(l) - I_{2,j,l}}{\sqrt{2N_0\sigma_{n,j,l}^2}} \right) + \mathrm{Q}\left(\frac{\delta_j^2(l) + I_{2,j,l}}{\sqrt{2N_0\sigma_{n,j,l}^2}} \right) \right] \right.$$

$$+ \left(1 - \frac{\sigma_{2,j,l}^2}{I_{2,j,l}^2}\right) \mathrm{Q}\left(\frac{\delta_j^2(l)}{\sqrt{2N_0\sigma_{n,j,l}^2}}\right)\Bigg\}. \tag{5.41}$$

The approximate symbol error probability expression for BC-MF-DFSE(S) given by (5.13) can be computed as

$$P_s \lesssim 2 \sum_{j=1}^{3^{L-J-1}} \sum_{l} \sum_{\underline{t}} N_{j,l} \mathrm{Q}\left(\frac{\delta_j(l) + \gamma\left(\underline{\xi}_j, \delta_j(l), \underline{t}\right)}{\sqrt{2N_0}}\right) P_{\underline{t}} \tag{5.42}$$

where $\gamma\left(\underline{\xi}_j, \delta_j(l), \underline{t}\right)$ is the residual interference arising from tentative decision errors $\underline{t}$, given by (5.12). In order to compute (5.42), we assume that the sequence of tentative decision errors is an i.i.d. sequence which is independent of the sequence of main decision errors *unde* and has distribution

$$t_n = \begin{cases} 0 & 1-p \\ +1 & \frac{1}{2}p \\ -1 & \frac{1}{2}p \end{cases} \tag{5.43}$$

where p is the probability of tentative decision error which, in the case of a single-stage BC-MF-DFSE(S) receiver, is the symbol error probability of a conventional matched-filter (thresholding) detector.

As the noise is correlated, tentative decision errors are correlated with each other as well as with main decision errors. Our assumptions are thus optimistic because errors in the tentative detector will tend to occur in bursts, inducing errors in the main detector. Nevertheless, independence can be assumed in case noise correlations are small.

5.10 Performance results

In this section, we compare the performance of the various receivers described in this chapter and Chapter 4 via simulation and analysis. First, we we give some examples of equalization for BPSK modulated signaling on static time-dispersive AWGN channels. The receivers employ standard matched filtering and are assumed to have perfect knowledge of the symbol timing and the impulse response of the channel. Later, we give examples of multiuser detection for BPSK modulated signals on symbol-asynchronous DS-CDMA channels with AWGN. In the case of multiuser detection, the receiver has knowledge of the spreading codes, signal powers and the relative timing of all users.

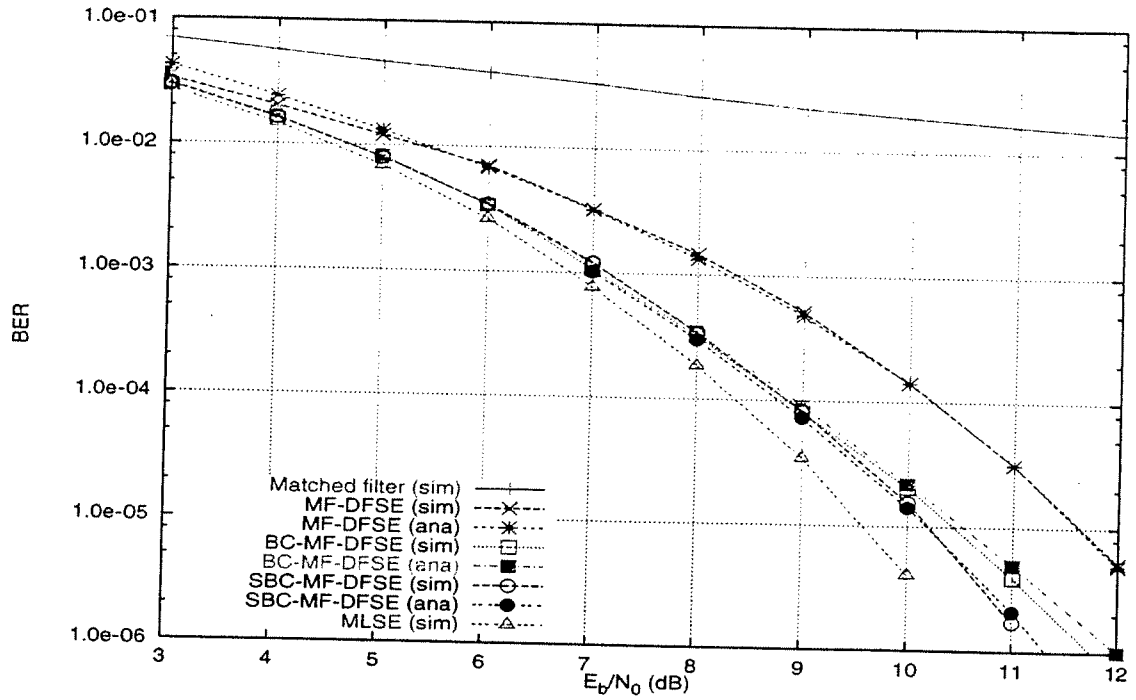

Figure 5.2: BER performance of various receivers in Example 1.

5.10.1 Equalization examples

We give four examples of equalization for a single user system. For our first example, we consider the symbol-spaced impulse response $f_1 = (0.9617, -0.2005, 0.1551, -0.1040)$. The channel has memory $L = 3$. Fig. 5.2 shows the bit-error rate (BER) of various receivers on channel 1. Each simulation was run for a count of 600 errors. The memory order J for the DFSE receivers is set to be one and final decisions are made at a lag G of 30 symbols. Note that the channel has much smaller ISI components than the channel in Fig. 4.8. As a result, the untreated interference in the case of MF-DFSE, given by (4.83), is small and the performance of MF-DFSE is not much worse than MLSE. Bias compensation using hard tentative decisions (BC-MF-DFSE) provides a gain of about a dB at moderate SNRs. Bias compensation using optimum linear soft tentative decisions (SBC-MF-DFSE) (5.20) shows improvement over compensation using hard tentative decisions at high SNR. This is because the mean square error after bias compensation is reduced and the effect is more significant as the noise diminishes.

The analytical results shown in Fig. 5.2 were obtained using the generating function method described in Section 5.9. The minimum error distance for the DFSE and MLSE

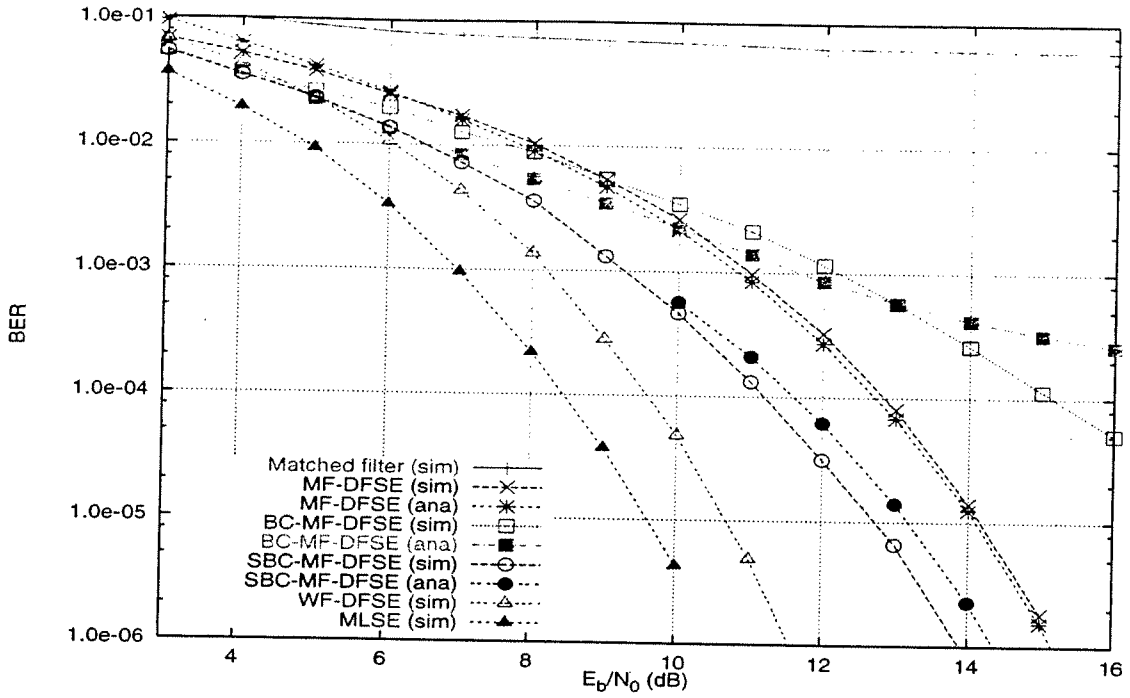

Figure 5.3: BER performance of various receivers in Example 2.

receivers in Fig. 5.2 is found to be one. For MF-DFSE, we evaluate the upper bound of (5.39), where we take ensemble average over the untreated interference components. For BC-MF-DFSE, we evaluate the semi-analytical bound of (5.42), where we assume independence between tentative and main decision errors and obtain the probability of tentative decision error, p in (5.43), from simulation (the matched filter detection curve in Fig. 5.2). For SBC-MF-DFSE, we evaluate the Glave bound of (5.41) using the approximate normalization factor of (5.35). For channel 1, the Glave bound holds for $E_b/N_0 > 6.6$ dB. All bounds in Fig. 5.2 are approximate in the sense that they do not consider error propagation inherent in DFSE receivers. However, error propagation is not significant for channels with moderate dispersion. All bounds are tight for the entire SNR range shown.

For our second example, the channel response is given by $f_2 = (0.84, -0.30, 0.40, 0.21)$. This channel also has memory $L = 3$ and the memory order for the DFSE receivers is chosen as one. The channel, is however, more dispersive than the channel in Example 1 (the sampled channel correlations s are larger in Example 2). The BER for various receivers is shown in Fig. 5.3. Bias compensation using hard tentative decisions (BC-MF-DFSE) actually deteriorates performance at moderate to high SNRs due to the lack of reliability of

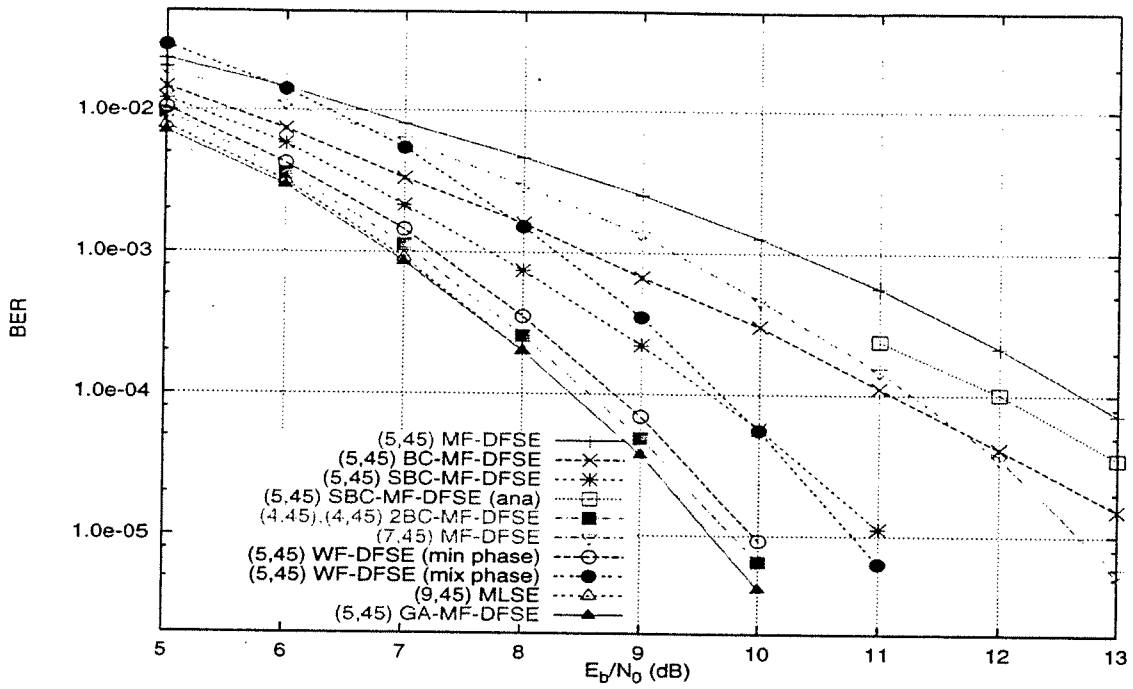

Figure 5.4: BER performance of various receivers in Example 3.

these decisions. However, by using optimum soft linear tentative decisions, SBC-MF-DFSE gains more than a dB over MF-DFSE. WF-DFSE, being an unbiased receiver, performs much better than the other DFSE receivers on the minimum phase channel as discussed in Chapter 4.

The analytical results shown in Fig. 5.3 were obtained in the same manner as described in Example 1. The Glave bound for SBC-MF-DFSE holds for $E_b/N_0 > 9.6$ dB for this channel. Notice that the semi-analytical approximate bound for BC-MF-DFSE does not seem to be consistent with the simulation curve. The simplifying assumptions used to obtain the semi-analytical expression are unrealistic when the sampled channel correlations are relatively large as in this case. The bounds for MF-DFSE and SBC-MF-DFSE are tight, the former being tighter as we performed ensemble averaging for the untreated interference components in the former case.

The channel for our third equalization example is a memory 9 minimum-phase channel with impulse response $f_{3,min} = (0.861, 0.258, -0.100, -0.274, 0.130, 0.100, -0.038, 0.112, -0.114, -0.228)$. A channel with the same magnitude response as $f_{3,min}$ but a mixed phase response is given by $f_{3,mix} = (0.5347, 0.6543, -0.1310, -0.2710, 0.0574, 0.0661, 0.1225, -0.1132,$

0.1566, −0.3679). Fig. 5.4 shows the BER performance of various detection schemes indexed with the memory order and the decision lag (J, G). Each simulation was run for a count of 1000 errors. Ideal noise whitening is assumed for WF-DFSE in the case of minimum-phase channel while transmit-matched filtering with Nyquist pulse-shaping at the transmitter is assumed in the case of mixed-phase channel.

Fig. 5.4 shows that BC-MF-DFSE (with hard tentative decisions) gains $1.0 - 1.5$ dB over MF-DFSE with memory order 5 in the SNR range shown. With linear optimum soft decisions, SBC-MF-DFSE gains further over MF-DFSE and the gains increase with increasing SNR. The two-stage scheme 2BC-MF-DFSE described in Section 5.2.1 closely approaches MLSE performance and obtains a gain of 4 dB over MF-DFSE at an error rate of 10^{-4}. Note that the combined number of states in the two stages of 2BC-MF-DFSE is kept the same as in $(5, 45)$ MF-DFSE. The schemes with soft and two-stage bias compensation even perform better than $(7, 45)$ MF-DFSE (with higher memory order but no bias compensation) for this channel. The performance of WF-DFSE for the minimum-phase channel is close to MLSE. However, it's worse for the mixed-phase channel. The performance of MF-DFSE and other receivers that operate on matched filter statistics, is insensitive to channel phase. Note that the delay incurred from anti-causal noise-whitening needed to obtain a minimum-phase channel for WF-DFSE can be compared to the delay of a two-stage BC-MF-DFSE scheme.

Fig. 5.4 shows the simulated BER for $(5, 45)$ GA-MF-DFSE which is slightly lower than MLSE due to the reasons discussed in Section 5.5.1. Also shown in Fig. 5.4 is the Glave bound for single error sequences in SBC-MF-DFSE, which is good for $E_b/N_0 > 11$ dB. Since the performance on this channel is dominated by single error sequences, considering only single error sequences in the analysis is well justified. In spite of this, we find that the bound is very loose. This can be explained by noting that the channel has a large memory – 9. In the analysis in Section 5.8, the distribution of a linear combination of interference components that appear as an argument to the Q function in (5.27), is replaced by the worst case interference distribution concentrating at the three points of no interference, peak constructive interference and peak destructive interference (5.33). With the large number of significant interference components in this example: $3L - J = 22$, the worst-case distribution leads to quite pessimistic results.

For our last equalization example, the channel impulse response is taken from [12, Ex-

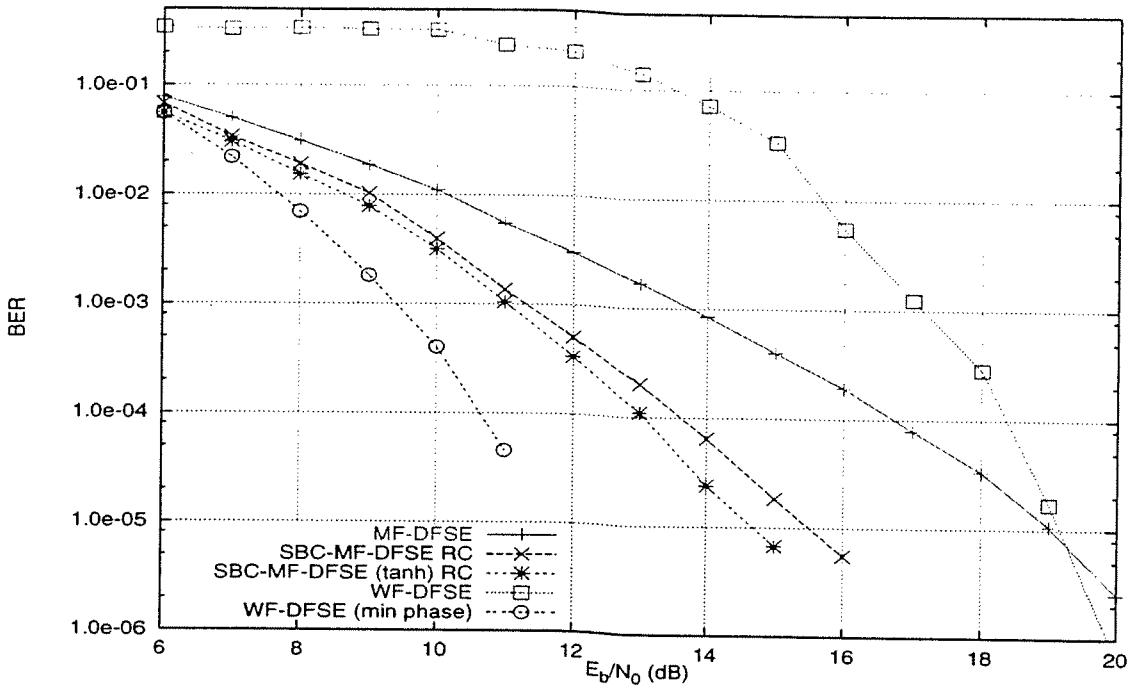

Figure 5.5: BER performance of various receivers in Example 4.

ample B]. The channel has memory 14 and is highly dispersive. Fig. 5.5 shows simulation results for various schemes with memory order 5 and decision lag 45 after a count of 600 errors. The performance of WF-DFSE is highly sensitive to channel phase. On this channel, symbol-by-symbol decisions are highly unreliable as the eye opening is -200%. Still, by using linear soft tentative decisions to cancel bias, significant performance improvement is obtained over MF-DFSE. Further improvement is obtained by using the following soft decision

$$\tilde{a}_n = \tanh\left(\frac{z_n}{\frac{N_0}{2} + \zeta s(0)}\right). \tag{5.44}$$

where ζ is a scale factor which is selected empirically. We found that the MMSE estimator of (5.19) which was obtained by assuming the interference as Gaussian, did not perform as well as the linear optimum estimator for any of the example channels considered in this section. In this example, $\zeta = 5.0$ while $\frac{1}{|s(0)|^2}\sum_{i\neq 0}|s(i)|^2 = 1.94$, which is the corresponding factor for the MMSE estimator of (5.19).

The bias compensation schemes shown in Fig. 5.5 use the reduced computation (RC) form of the bias term (5.4) which is independent of the state. In case of binary signaling, only two bias terms need to be computed at each recursion regardless of the trellis size. Thus,

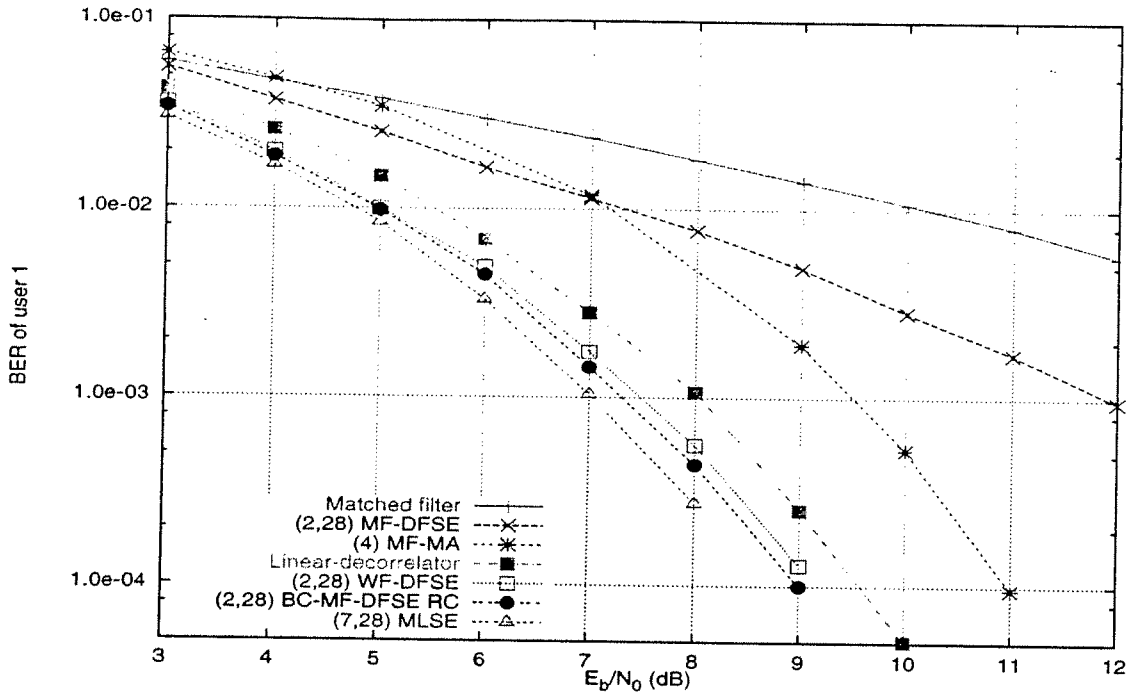

Figure 5.6: BER performance of various detection schemes for DS-CDMA channel 1.

the added complexity is very low for moderate trellis sizes. We found that the performance loss due to the approximation of the bias term was not more than a fraction of a dB for any of the channels considered in this section.

5.10.2 Multiuser detection examples

We simulate a BPSK modulated asynchronous DS-CDMA system on an AWGN channel with eight users whose signature waveforms are derived from Gold sequences of length 31. The spreading codes are short i.e. symbol-length. The relative delays of users are fixed for the simulation and are in an increasing order. All receivers have a bank of filters each of which is matched to the spreading code of a user followed by a synchronized symbol-rate sampler. The multiuser channel is static and has the spectrum

$$S(D) = \frac{1}{31}\begin{bmatrix} 31 & 8-D & 7 & 6+D & -3+2D & -6+5D & -3+2D & -2+D \\ 8-D^{-1} & 31 & -D & 9-2D & -6-3D & -7-2D & -D & 9-2D \\ 7 & -D^{-1} & 31 & -D & -1 & -D & -1 & -2+D \\ 6+D^{-1} & 9-2D^{-1} & -D^{-1} & 31 & -D & -1 & -D & -1 \\ -3+2D^{-1} & -6-3D^{-1} & -1 & -D^{-1} & 31 & -D & -1 & -D \\ -6+5D^{-1} & -7-2D^{-1} & -D^{-1} & -1 & -D^{-1} & 31 & -D & -1 \\ -3+2D^{-1} & -D^{-1} & -1 & -D^{-1} & -1 & -D^{-1} & 31 & -D \\ -2+D^{-1} & 9-2D^{-1} & -2+D^{-1} & -1 & -D^{-1} & -1 & -D^{-1} & 31 \end{bmatrix}$$

Fig. 5.6 shows the BER of user 1 for various detection schemes when all users have identical SNR. Each simulation was run for a count of 500 errors. It is evident that even with ideal power control, the performance of the conventional matched filter detector that makes symbol-by-symbol decisions independently for all users, is significantly worse than optimum MLSE. With a four state trellis, MF-DFSE, that operates on the matched filter statistic of all users jointly, provides some improvement over the matched filter detector. The four-path MF-MA is $2-3$ dB worse than MLSE. The linear-decorrelator[5], that nulls out all multiple-access interference, loses about $0.5-1.0$ dB compared to MLSE due to noise enhancement. WF-DFSE that operates on the equivalent whitened minimum-phase channel obtains near MLSE performance. Not shown in Fig. 5.6, WF-MA with four survivor paths is also found to obtain near MLSE performance. However, WF-DFSE, WF-MA and the linear-decorrelator require multiuser channel inversion and/or factorization which has complexity quadratic in the number of users. The M-algorithm receivers require sorting of survivor paths at each recursion which is not needed by the DFSE schemes as they are trellis based.

The single-stage BC-MF-DFSE receiver which employs hard tentative decisions to cancel bias, obtains the best performance on this channel (next to MLSE). With four states only, BC-MF-DFSE closely approaches the performance of MLSE which requires 128 states in the Viterbi algorithm. Bias approximation in this case does not result in any appreciable loss of performance.

Fig. 5.7 shows the BER of user 1 versus the SNR of the rest of the users. The SNR of

[5]The linear-decorrelator comprises a zero-forcing filter followed by a thresholding device.

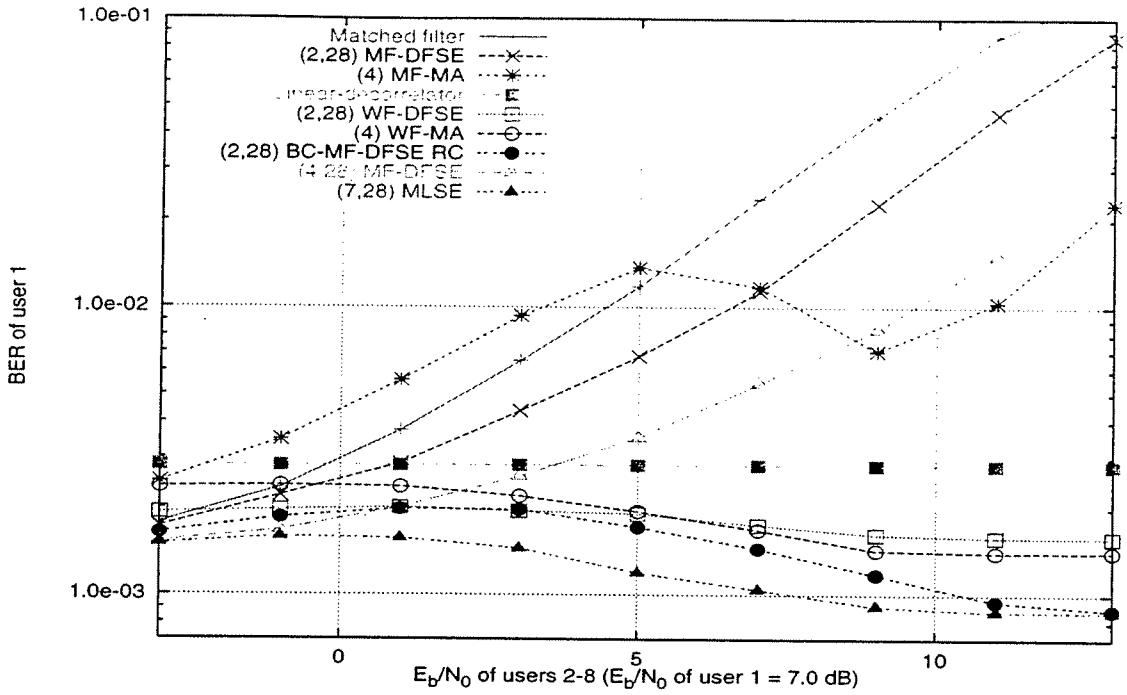

Figure 5.7: Near-far performance of various detection schemes for DS-CDMA channel 1.

user 1 is held constant at 7.0 dB. It can be seen that the matched filter detector, MF-DFSE and MF-MA do not perform well in a near-far situation. Such a situation occurs as an example when interfering users are closer to the base station than the desired user in the uplink and can thus get most of their signal power through to the base station in the absence of a (good) power control algorithm. In this case, the untreated interference dominates the performance of the sub-optimal matched filter type receivers as the ratio of the interference-to-desired signal power increases. However, WF-DFSE, WF-MA and the linear-decorrelator perform well as they do not suffer from untreated interference components.

Note that although the symbols of the desired user are not detected reliably by the matched filter detector, the symbols of the interfering users are detected quite reliably as their SNR increases. Thus, even in the severe near-far situation, the untreated interference (that affects MF-DFSE) is removed reliably by means of hard tentative decisions. As a result, BC-MF-DFSE outperforms all other methods, including MF-DFSE with higher memory order, and converges to MLSE in high SNR of interfering users, for this system.

For our second multiuser detection example, we consider another eight-user BPSK-modulated DS-CDMA system with short Gold spreading codes of length 31. The multiuser

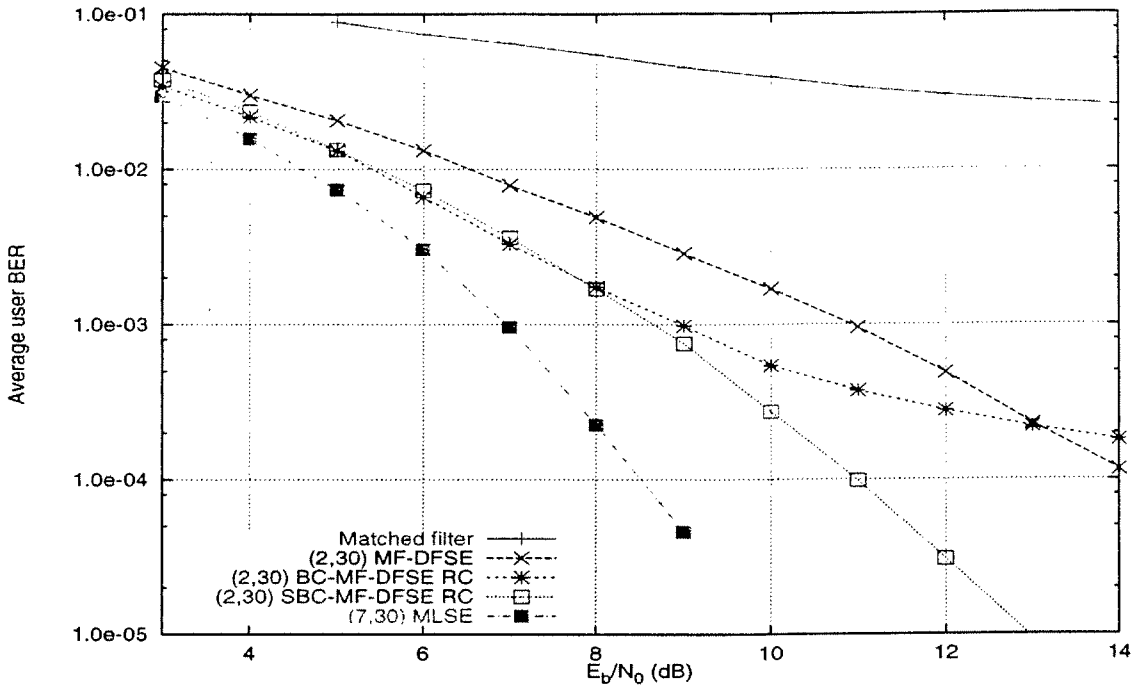

Figure 5.8: BER performance of various detection schemes for DS-CDMA channel 2.

channel spectrum is given by

$$S(D) = \frac{1}{31}\begin{bmatrix} 31 & -D & -9 & 6+D & 5-6D & 4+3D & -5+4D & -2+D \\ -D^{-1} & 31 & -D & 3+4D & -6-3D & -1 & 10-3D & 1-2D \\ -9 & -D^{-1} & 31 & -2+D & -1 & -D & 7 & -2+D \\ 6+D^{-1} & 3+4D^{-1} & -2+D^{-1} & 31 & -D & -7-2D & 6+D & -5-4D \\ 5-6D^{-1} & -6-3D^{-1} & -1 & -D^{-1} & 31 & -10+D & -3+2D & -6-3D \\ 4+3D^{-1} & -1 & -D^{-1} & -7-2D^{-1} & -10+D^{-1} & 31 & -D & 3+4D \\ -5+4D^{-1} & 10-3D^{-1} & 7 & 6+D^{-1} & -3+2D^{-1} & -D^{-1} & 31 & 8-D \\ -2+D^{-1} & 1-2D^{-1} & -2+D^{-1} & -5-4D^{-1} & -6-3D^{-1} & 3+4D^{-1} & 8-D^{-1} & 31 \end{bmatrix}$$

Fig. 5.8 shows the average simulated BER of users for various detection schemes when all users have identical SNR. Note that the spreading codes in this system have higher partial correlations than the system in Example 1. The conventional matched filter detector does not perform very well. As a result, bias compensation using hard tentative decisions provides

some gain at moderate SNR, but causes a loss at high SNR. By using linear MMSE estimates for bias compensation in SBC-MF-DFSE, the loss can be converted to a significant gain at high SNR.

The multiuser detection results presented in this section were obtained for DS-CDMA systems with short (symbol-length) spreading codes. In current DS-CDMA systems, long spreading codes are generally employed which have periods much longer than the symbol interval. Long codes are preferable over short codes as they have better autocorrelation and cross-correlation properties. However, long codes are difficult to deal with for multiuser detection schemes that perform some kind of linear filtering like zero-forcing or noise-whitening. This is because the multiuser channel changes every symbol interval in the presence of long codes. Even with short codes, the multiuser channel changes with user arrival and departure. These variations in the channel are difficult, if not impossible, to track for a linear filter. Symbol-asynchronism also poses a problem. However, it is quite easy to generate user code partial correlations at the base station by means of a bank of on-line correlators that are properly synchronized to each user's code. The tracking of the medium responses of users has become a standard for Rake receivers used in conventional DS-CDMA receivers. These are the only requirements for a multiuser receiver like MF-DFSE that operates on joint matched filter statistics. Thus, MF-DFSE with hard or soft bias compensation is quite attractive for asynchronous DS-CDMA systems with short or long spreading codes.

5.11 Conclusions

In this chapter, we considered bias compensation (cancellation of untreated interference components) for reduced trellis and tree search algorithms that operate on matched filter statistics. Our main emphasis was on bias-compensated matched-filter decision feedback sequence estimation (BC-MF-DFSE) receivers with standard matched filters. Cancellation of future interfering components is performed by using tentative decision feedback. We considered using hard and soft tentative decisions for this purpose as well as multistage schemes. As soft tentative decisions, we considered optimum symbol-by-symbol linear and non-linear MMSE estimates of symbols.

We examined the error-rate performance of MF-DFSE with and without bias compen-

sation by conducting a first event error analysis. We obtained union bounds on the symbol error probability of the various receivers and described a generating function method to evaluate the bounds. The bounds were evaluated for equalization examples for channels with relatively small memory and were found to be generally tight. Simulation results were provided for some example channels with large memory. It was found that bias compensation using soft tentative decisions provides significant gains over no compensation for most channels of practical interest. It was also found that a reduced-complexity scheme which compensates for the most significant interference components only, retains most of these gains.

We also compared the performance of various receivers for multiuser detection via simulation of BPSK-modulated asynchronous DS-CDMA systems. It was found that the bias-compensated MF-DFSE scheme performs very well, even in a severe near-far situation. The scheme is ideal for multiuser detection in the case of short as well as long spreading codes and asynchronous signals.

CHAPTER 6

Soft-output algorithms

6.1 Introduction

The various algorithms considered in the previous chapters generate hard decisions at the output. Such algorithms are fine as long as one is interested in minimizing the error rate for a single system. For concatenated systems with memory, however, the performance of the outer system can be significantly enhanced by providing it with soft decisions in the form of likelihoods, symbol *a-posteriori* probabilities (APP) or erasures. One example of such a system is error control coding for intersymbol interference (ISI) channels. Another example is multiuser demodulation for a direct-sequence CDMA (DS-CDMA) system with error control coding and interleaving. In order to make the most of the code, the demodulator must provide soft information to the decoders. Unfortunately, most multiuser detection algorithms ignore the possibility of generating this reliability information and concentrate instead on minimizing the demodulated error rate.

Recently, a considerable amount of work has been done in symbol-by-symbol detection techniques for channels with ISI [1,3,21,23,25,28]. Li *et al.* [28] showed that optimum soft-output equalization can be performed with a forward-only recursion with complexity that grows exponentially with the channel memory. An earlier algorithm proposed by Abend *et al.* [1] requires complexity which is exponential in the decision lag, which is generally chosed to be much larger than the channel memory. The optimum soft-output algorithm (OSA) of Li *et al.* operates on discrete-time statistics containing white noise. On the other hand, the optimal symbol-by-symbol detection (OSSD) algorithm of Hayes *et al.* [23] operates on standard matched filter statistics. They and other authors, however, over-

estimate the complexity of this algorithm. We derive a forward-recursive matched-filter optimum soft-output algorithm (MF-OSA) following their development. The complexity of this algorithm is at par with the OSA. The MF-OSA can be reduced to add-compare-select operations mostly like the sub-optimum soft-output algorithm (SSA) of [28], resulting in the MF-SSA.

The OSA can be applied to the problem of multiuser estimation, but this requires noise whitening. Despite the strides made in the noise-whitening technique [47], it requires sizable complexity and is not very suitable for long spreading sequences and dynamic channels. The algorithm of Verdú [42] operates on standard matched-filter statistics like the MF-OSA. However, it has high latency as it requires a backward-forward recursion like the BCJR algorithm [3]. The MF-OSA is, thus, attractive in this case. It is an optimum demodulator for a coded multiuser DS-CDMA system with ideal interleaving, in the sense that without exploiting any information about coding in the demodulation process, it supplies each individual decoder with as much information as possible about the sequence of modulator-input symbols for the corresponding user while suppressing the irrelevant information about other user's sequences. This is called user-separating demodulation in [36].

Bayesian Conditional Decision Feedback Estimation (BCDFE) proposed in [25] for ISI channels is a reduced-complexity symbol-by-symbol estimation technique that employs an efficient method for trellis memory reduction like the DFSE algorithm. The scheme is designed to produce symbol APP estimates to enhance outer decoding. However, we note that while the scheme is capable of providing good hard decisions on symbols, it fails to deliver reliable estimates of symbol APPs. Fortunately, this can be fixed by a modification of the algorithm. The modified BCDFE algorithm recursively updates conditional symbol APP estimates (conditioned on the reduced state) and averages them over the state at a smoothing lag to obtain reliable symbol APP estimates.

The chapter is organized as follows. Sections 6.2 and 6.3 describe the MF-OSA and MF-SSA respectively. The modified BCDFE algorithm is derived in Section 6.4. We compare the complexity of the various algorithms in Section 6.5. The algorithms are considered for soft-output multiuser estimation with error control coding in Section 6.6. Simulation is undertaken to compare the performance of the various algorithms with the soft-output Viterbi algorithm (SOVA) [21] for a DS-CDMA system with four asynchronous users. Simulation results are presented in Section 6.7.

6.2 A matched-filter optimum soft-output algorithm

In this section, we derive an optimal forward-recursive soft-output algorithm that operates on standard matched filter statistics. We consider the system model of Section 2.2. The baseband received signal is given by (2.3). The algorithm finds the set of symbol *a-posteriori* probabilities (APP) $\{p(\alpha_n|y(t))\}_{n=0}^{N-1}$, for $\alpha_n \in \mathcal{A}$. From the log-likelihood function given by (2.6), it follows that

$$p(\underline{\alpha}_N, y(t)) = C \exp\left[-\frac{1}{2N_0}\int_{t\in I}\left|y(t) - \sum_{n=0}^{N-1}\alpha_n h(t-nT;t)\right|^2 dt\right] p(\underline{\alpha}_N) \tag{6.1}$$

where $\underline{\alpha}_N = [\alpha_0, \alpha_1, \ldots, \alpha_{N-1}]^T$ is a sequence of hypothesized symbols which is assumed to be independent and identically distributed with probability $p(\underline{\alpha}_N) = \prod_{n=0}^{N-1}\alpha_n$ and C is a constant independent of the sequence hypothesis. From (2.6), (2.11) and (2.18), it follows that

$$p(\underline{\alpha}_N, y(t)) = C_1 \exp\left[\Lambda(\underline{z}_N, \underline{\alpha}_N)/2N_0\right] p(\underline{\alpha}_N) \tag{6.2}$$

where $\underline{z}_N = [z_0, z_1, \ldots, z_{N-1}]^T$ is the sequence of standard matched statistics given by (2.14) and C_1 is another constant independent of the sequence hypothesis. The log-likelihood metric[1] $\Lambda(\underline{z}_N, \underline{\alpha}_N)$ is given by

$$\Lambda(\underline{z}_N, \underline{\alpha}_N) = \sum_{n=0}^{N-1}\Gamma_n(z_n, \alpha_n, \sigma_n) \tag{6.3}$$

where the branch metric $\Gamma_n(z_n, \alpha_n, \sigma_n)$ corresponding to the state $\sigma_n : \alpha_{n-1}, \alpha_{n-2}, \ldots, \alpha_{n-L}$ and the input symbol α_n is given by

$$\Gamma_n(z_n, \alpha_n, \sigma_n) = \mathrm{Re}\left\{\alpha_n^*\left[2z(n) - s(0;n)\alpha_n - 2\sum_{l=1}^{L}s(l;n)\alpha_{n-l}\right]\right\}. \tag{6.4}$$

For $n = 0, 1, \ldots, N-1$, $0 \le i \le n-L-1$ and $\alpha \in \mathcal{A}$, define

$$\Omega(\underline{z}_n, \sigma_n) \triangleq \sum_{\underline{\alpha}_{n-L}} \exp\left[\Lambda(\underline{z}_n, \underline{\alpha}_n)/2N_0\right] p(\underline{\alpha}_n), \tag{6.5}$$

$$\Omega_i(\underline{z}_n, \sigma_n, \alpha) \triangleq \sum_{\underline{\alpha}_{n-L}|\alpha_i=\alpha} \exp\left[\Lambda(\underline{z}_n, \underline{\alpha}_n)/2N_0\right] p(\underline{\alpha}_n), \tag{6.6}$$

where[2] $\underline{x}_n = [x_0, x_1, \ldots, x_{n-1}]^T$. Then, for $0 \le i \le n-L$, we have

$$\Omega_i(\underline{z}_{n+1}, \sigma_{n+1}, \alpha) = \sum_{\underline{\alpha}_{n-L+1}|\alpha_i=\alpha} \exp\left[\frac{\Lambda(\underline{z}_n, \underline{\alpha}_n) + \Gamma_n(z_n, \alpha_n, \sigma_n)}{2N_0}\right] p(\underline{\alpha}_{n+1})$$

[1]The notation is modified slightly to indicate the functional dependencies.

[2]The notation single bar | means 'given'.

$$= \sum_{\alpha_{n-L}|\alpha_i=\alpha} \exp\left[\frac{\Gamma_n(z_n,\alpha_n,\sigma_n)}{2N_0}\right] p(\alpha_n) \sum_{\underline{\alpha}_{n-L}|\alpha_i=\alpha} \exp\left[\frac{\Lambda(\underline{z}_n,\underline{\alpha}_n)}{2N_0}\right] p(\underline{\alpha}_n)$$

$$= \sum_{\alpha_{n-L}|\alpha_i=\alpha} \exp\left[\Gamma_n(z_n,\alpha_n,\sigma_n)/2N_0\right] p(\alpha_n)\Omega_i(\underline{z}_n,\sigma_n,\alpha) \tag{6.7}$$

where the first equality follows from (6.3) and the second equality follows from the fact that the branch metric $\Gamma_n(z_n,\alpha_n,\sigma_n)$ is independent of the hypothetical symbols $\underline{\alpha}_{n-L}$. In (6.7), it is understood that $\Omega_{n-L}(\underline{z}_n,\sigma_n,\alpha) = \Omega(\underline{z}_n,\tilde{\sigma}_n)$, where $\tilde{\sigma}_n = \sigma_n|\alpha_{n-L} = \alpha$. Similarly, it can be shown that

$$\Omega(\underline{z}_{n+1},\sigma_{n+1}) = \sum_{\alpha_{n-L}} \exp\left[\Gamma_n(z_n,\alpha_n,\sigma_n)/2N_0\right] p(\alpha_n)\Omega(\underline{z}_n,\sigma_n). \tag{6.8}$$

By substituting (6.5) and (6.6) in (6.2), note that

$$p(\sigma_N, y(t)) = \sum_{\underline{\alpha}_{N-L}} p(\underline{\alpha}_N, y(t)) = C_1\Omega(\underline{z}_N,\sigma_N) \tag{6.9}$$

and for $0 \le i \le N-L-1$,

$$p(\sigma_N, a_i = \alpha, y(t)) = \sum_{\underline{\alpha}_{N-L}|\alpha_i=\alpha} p(\underline{\alpha}_N, y(t)) = C_1\Omega_i(\underline{z}_N,\sigma_N,\alpha). \tag{6.10}$$

Thus, for $0 \le i \le N-L-1$, we get the symbol APPs as

$$p(a_i = \alpha|y(t)) = \frac{\sum_{\sigma_N}\Omega_i(\underline{z}_N,\sigma_N,\alpha)}{\sum_{\sigma_N}\Omega(\underline{z}_N,\sigma_N)}. \tag{6.11}$$

The last L symbols are assumed known at the receiver. Equations (6.8), (6.7) and (6.11) complete the recursion of the matched-filter optimal soft-output algorithm (MF-OSA) with forward-only recursion. The algorithm was first derived in [18] for soft-output multiuser detection using a bank of matched filters. In [18], the algorithm is referred to as optimal soft-output multiuser estimation (OSOME).

It is not necessary to observe the entire signal in order to obtain close to optimum estimates of symbol APPs. In general, good estimates can be obtained at a sufficient decision lag as in the case of an MLSE algorithm. For a decision lag $G \ge L$, the MF-OSA(G) algorithm consists of the following steps. For each time $n = 0,1,\ldots,N-1$, compute and store the state metrics given by (6.8). For each $n \ge L$, $i = n-G,\ldots,n-L$ and[3] $\alpha \in \mathcal{A}'$, compute and store the symbol metrics given by (6.7). For each $n \ge G$ and $\alpha \in \mathcal{A}'$, estimate symbol APPs as

$$p(a_{n-G} = \alpha|y(t)) = \frac{\sum_{\sigma_{n+1}}\Omega_{n-G}(\underline{z}_{n+1},\sigma_{n+1},\alpha)}{\sum_{\sigma_{n+1}}\Omega(\underline{z}_{n+1},\sigma_{n+1})}. \tag{6.12}$$

[3] $\mathcal{A}'$ is the set of all but one symbol (say α') in the alphabet $\mathcal{A}$.

$$p(a_{n-G} = \alpha' | y(t)) = 1 - \sum_{\alpha \in \mathcal{A}'} p(a_{n-G} = \alpha | y(t)). \tag{6.13}$$

Note that the symbol *a priori* probabilities $p(\alpha_n)$ can be dropped from all computations if the symbols are equally likely *a priori*.

6.3 A matched-filter sub-optimum soft-output algorithm

The MF-OSA algorithm described in the previous section requires a large number of multiplication and exponentiation operations which lead to high implementation complexity. In this section, we simplify the MF-OSA algorithm so that it requires mostly add-compare-select operations, like an MLSE algorithm. For this purpose, we define

$$\Omega'(\underline{z}_n, \sigma_n) \stackrel{\Delta}{=} \max_{\underline{\alpha}_{n-L}} \left[\Lambda(\underline{z}_n, \underline{\alpha}_n)/2N_0 + \log(p(\underline{\alpha}_n))\right], \tag{6.14}$$

$$\Omega'_i(\underline{z}_n, \sigma_n, \alpha) \stackrel{\Delta}{=} \max_{\underline{\alpha}_{n-L} | \alpha_i = \alpha} \left[\Lambda(\underline{z}_n, \underline{\alpha}_n)/2N_0 + \log(p(\underline{\alpha}_n))\right]. \tag{6.15}$$

A derivation similar to (6.7) can be used to show that for $0 \leq i \leq n-L$,

$$\Omega'_i(\underline{z}_{n+1}, \sigma_{n+1}, \alpha) = \max_{\alpha_{n-L} | \alpha_i = \alpha} \left[\Gamma_n(z_n, \alpha_n, \sigma_n)/2N_0 + \Omega'_i(\underline{z}_n, \sigma_n, \alpha)\right] + \log(p(\alpha_n)) \tag{6.16}$$

and

$$\Omega'(\underline{z}_{n+1}, \sigma_{n+1}) = \max_{\alpha_{n-L}} \left[\Gamma_n(z_n, \alpha_n, \sigma_n)/2N_0 + \Omega'(\underline{z}_n, \sigma_n)\right] + \log(p(\alpha_n)). \tag{6.17}$$

Note that (6.17) is similar to the recursion of the MLSE receiver of Section 2.4. By substituting (6.14) in (6.2), we see that

$$\max_{\underline{\alpha}_{N-L} | \alpha_i = \alpha} p(\underline{\alpha}_N, y(t)) = C_1 \exp\left[\Omega'_i(\underline{z}_N, \sigma_N, \alpha)\right]. \tag{6.18}$$

Comparing the above equation with (6.10), note that the sum of exponentials of positive quantities is dominated by the term with the largest exponent. Thus, symbol APPs can be approximated as

$$p(a_i = \alpha | y(t)) \approx \frac{\sum_{\sigma_N} \exp\left[\Omega'_i(\underline{z}_N, \sigma_N, \alpha)\right]}{\sum_{\sigma_N, x \in \mathcal{A}} \exp\left[\Omega'_i(\underline{z}_N, \sigma_N, x)\right]}. \tag{6.19}$$

For a decision lag $G \geq L$, the matched-filter sub-optimal soft-output algorithm MF-SSA(G) consists of the following steps. For each time $n = 0, 1, \ldots, N-1$, recursively compute and store the state metrics given by (6.17). For each $n \geq L$, keep the history of the best surviving path $\hat{\alpha}_{n-G}(\sigma_n), \ldots, \hat{\alpha}_{n-L}(\sigma_n)$ leading to each state σ_n, as in the Viterbi algorithm. For each

$n \geq L$, $i = n-G, \ldots, n-L$ and $\alpha \neq \hat{\alpha}_i(\sigma_n)$, compute and store the symbol metrics given by (6.16) (note that $\Omega'_i(\underline{z}_n, \sigma_n, \hat{\alpha}_i(\sigma_n)) = \Omega'(\underline{z}_n, \sigma_n)$, so there is no need to compute and store it separately). For each $n \geq G$ and $\alpha \in \mathcal{A}$, estimate symbol APPs as

$$p(a_{n-G} = \alpha | y(t)) \approx \frac{\sum_{\sigma_{n+1}} \exp\left[\Omega'_{n-G}(\underline{z}_{n+1}, \sigma_{n+1}, \alpha)\right]}{\sum_{\sigma_{n+1}, x \in \mathcal{A}} \exp\left[\Omega'_{n-G}(\underline{z}_{n+1}, \sigma_{n+1}, x)\right]}. \tag{6.20}$$

Note that the above algorithm avoids the multiplication operations of the MF-OSA(G) algorithm of Section 6.2. Exponentiation operations are needed, however, in the last step. The algorithm was proposed in [18] for multiuser detection, where we refer to it to as sub-optimal soft-output multiuser estimation (SSOME). A variation of the above algorithm estimates symbol APPs as

$$p(a_{n-G} = \alpha | y(t)) \approx \frac{\exp\left[\Omega'_{n-G}(\underline{z}_{n+1}, \sigma^*_{n+1}, \alpha)\right]}{\sum_{x \in \mathcal{A}} \exp\left[\Omega'_{n-G}(\underline{z}_{n+1}, \sigma^*_{n+1}, x)\right]}. \tag{6.21}$$

where $\sigma^*_n = \arg \max_{\Omega'(\underline{z}_n, \sigma_n)}$. This algorithm requires only two exponentiation operations in the last step. The algorithm is referred to as SSOME1 in [18]. It is similar in construction to the sub-optimal soft-output algorithm (SSA) of [28].

6.4 A reduced-state soft-output algorithm

In this section, we describe a forward-recursive reduced-state soft-output algorithm which operates on whitened-matched filter statistics. The algorithm can be considered as a reduced-complexity alternative to the optimal soft-output algorithm (OSA) of Li *et al.* [28]. It was obtained by modifying the algorithm of Lee *et al.* [25], which is referred to as Bayesian conditional decision feedback equalization (BCDFE). The BCDFE algorithm does not produce good soft outputs. The modified algorithm derived here was first proposed in [18] where we refer to it as modified BCDFE (MBCDFE).

The algorithm operates on whitened-matched filter statistics which may be obtained by applying the noise-whitening filter to the discrete-time matched filter statistics $\underline{z}_N$. The equivalent whitened discrete-time system model is given by

$$y_n = \sum_{i=0}^{L} f(i;n) a_{n-i} + w_n \tag{6.22}$$

where w_n is a sample of a complex white Gaussian noise process with mean zero and variance N_0 and $f(i;n)$ are whitened channel coefficients (possibly time-varying in index n).

Let (J, G) be the memory order and the decision lag for the algorithm, respectively chosen arbitrarily in the range $0 \leq J \leq L \leq G$. Let $\underline{y}_n = [y_0, y_1, \ldots, y_{n-1}]^T$ be the sequence of statistics received up to time $n-1$ and $\beta_n : \alpha_{n-1}, \alpha_{n-2}, \ldots, \alpha_{n-J}$ represent the reduced state at time n. The algorithm recursively estimates the probabilities $p(\beta_n|\underline{y}_n)$ and $p(a_{n-i} = \alpha|\underline{y}_n, \beta_n)$ for $J+1 \leq i \leq G$ and $\alpha \in \mathcal{A}$. For this it employs the recursive relations:

$$p(\beta_{n+1}|\underline{y}_{n+1}) = \frac{\sum_{\alpha_{n-J}} p(\beta_{n+1}, \alpha_{n-J}, y_n|\underline{y}_n)}{\sum_{\alpha_{n-J}, \beta_{n+1}} p(\beta_{n+1}, \alpha_{n-J}, y_n|\underline{y}_n)}, \tag{6.23}$$

$$p(a_{n-J} = \alpha|\underline{y}_{n+1}, \beta_{n+1}) = \frac{p(\beta_{n+1}, a_{n-J} = \alpha, y_n|\underline{y}_n)}{\sum_{\alpha_{n-J}} p(\beta_{n+1}, \alpha_{n-J}, y_n|\underline{y}_n)} \tag{6.24}$$

and

$$\begin{aligned} p(a_{n-i} = \alpha|\underline{y}_{n+1}, \beta_{n+1}) &= \sum_{\alpha_{n-J}} p(a_{n-i} = \alpha|\underline{y}_{n+1}, \beta_{n+1}, \alpha_{n-J}) p(\alpha_{n-J}|\underline{y}_{n+1}, \beta_{n+1}) \\ &\approx \sum_{\alpha_{n-J}} p(a_{n-i} = \alpha|\underline{y}_n, \beta_n) p(\alpha_{n-J}|\underline{y}_{n+1}, \beta_{n+1}) \end{aligned} \tag{6.25}$$

for $J+1 \leq i \leq G$, where in (6.25) we assume that given $\underline{y}_n$ and β_n, the symbols a_{n-i} $(J+1 \leq i \leq G)$ are conditionally independent of the statistic y_n and the input symbol a_n. The assumption is true for $J = L$, i.e., a full-state algorithm. The probability $p(\beta_{n+1}, \alpha_{n-J}, y_n|\underline{y}_n)$ is given by

$$p(\beta_{n+1}, \alpha_{n-J}, y_n|\underline{y}_n) = p(y_n|\underline{y}_n, \alpha_n, \beta_n) p(\beta_n|\underline{y}_n) p(\alpha_n) \tag{6.26}$$

where using the assumption following (6.25), the probability $p(y_n|\underline{y}_n, \alpha_n, \beta_n)$ is given by

$$p(y_n|\underline{y}_n, \alpha_n, \beta_n) = \sum_{\{\alpha_{n-i}\}_{i=J+1}^{L}} p\left(y_n \left| \alpha_n, \beta_n, \{\alpha_{n-i}\}_{i=J+1}^{L} \right.\right) p\left(\{\alpha_{n-i}\}_{i=J+1}^{L} \left| \underline{y}_n, \beta_n \right.\right) \tag{6.27}$$

which is approximated by the Gaussian density

$$p(y_n|\underline{y}_n, \alpha_n, \beta_n) \approx p\left(y_n \left| \alpha_n, \beta_n, \{\hat{a}_{n-i}(\beta_n)\}_{i=J+1}^{L} \right.\right) \tag{6.28}$$

where $\{\hat{a}_{n-i}(\beta_n)\}_{i=J+1}^{L}$ are conditional decisions (conditioned on state β_n) obtained as

$$\hat{a}_{n-i}(\beta_n) = \arg\max_{\alpha_{n-i}} p(\alpha_{n-i}|\underline{y}_n, \beta_n). \tag{6.29}$$

The modified BCDFE (J, G) algorithm consists of the following steps. For each time $n = 0, 1, \ldots, N-1$, compute and store the state probabilities for each reduced state β_n using (6.23), (6.26) and (6.28). For each $n \geq J$, $J+1 \leq i \leq G$ and $\alpha \in \mathcal{A}$, compute and

Algorithm	Compare	Add	Multiply	Divide	Exp	Storage
MF-OSA	1	$2^L(2A_\Gamma + G - L + 3)$	$2^{L+1}(G - L + 1)$	1	2^{L+1}	$2^L[f + f(G - L)]$
MF-SSA	$2^L(G - L + 1)$	$2^L(2A_\Gamma + 2G - 2L + 4)$	0	1	2^{L+1}	$2^L[f + (f + 1)(G - L)]$
MF-SSA1	$2^L(G - L + 2)$	$2^L(2A_\Gamma + 2G - 2L + 2)$	0	1	1	$2^L[f + (f + 1)(G - L)]$
SOVA	$2^L(G - L + 2)$	$2^L(2A_\Gamma + 3e + 4)$	$2^{L+1}(e)$	2^L	2^L	$2^L[f + (f + 1)(G - L)]$
BCDFE	$2^{J+1}(G - J) + 1$	$2^J(2A_\Gamma + 4)$	$2^J(3)$	2^{J+1}	2^{J+1}	$2^J(f + G - J)$
MBCDFE	$2^J(L - J) + 1$	$2^J(2A_\Gamma + G - J + 4)$	$2^J(2G - 2J + 3)$	2^{J+1}	2^{J+1}	$2^J[f(G - J + 1) + L - J]$

Table 6.1: Complexity in number of operations per iteration (f = #bits required to store a floating point number, e = #places where the hypothesized symbols of two merging paths differ.)

store the conditional symbol APPs using (6.24), (6.25), (6.26) and (6.28). For each $n \geq J$ and $J \leq i \leq L - 1$, obtain and store conditional decisions using

$$\hat{a}_{n-i}(\beta_{n+1}) = \arg\max_{\alpha_{n-i}} p(\alpha_{n-i}|\underline{y}_{n+1}, \beta_{n+1}). \tag{6.30}$$

Note that these decisions will be used in (6.28) in the next recursion. Finally, for each $n \geq G$, estimate symbol APPs using

$$p(a_{n-G} = \alpha|\underline{y}_{n+1}) = \sum_{\beta_{n+1}} p(a_{n-G} = \alpha|\underline{y}_{n+1}, \beta_{n+1}) p(\beta_{n+1}|\underline{y}_{n+1}). \tag{6.31}$$

The number of multiplication and exponentiation operations required in the above algorithm can be cut drastically by operating in the log domain as in the algorithm described in Section 6.3.

Note that the BCDFE algorithm proposed in [25] recursively obtains conditional hard decisions instead of conditional symbol APPs in the modified algorithm (6.25). This results in a significant loss of the soft information. The modified algorithm uses conditional hard decisions in (6.28) only to truncate the state, in the same manner as in DFSE. This does not have much effect on the quality of soft decisions as we observe from simulation.

6.5 Complexity comparison

Table 6.1 compares the complexity of the various algorithms discussed in this chapter for binary symbol alphabet. It is assumed that A_Γ add operations are needed to compute the branch metric $\Gamma_n(.)$ in (6.8) (or the Gaussian density (6.28) for the BCDFE algorithms).

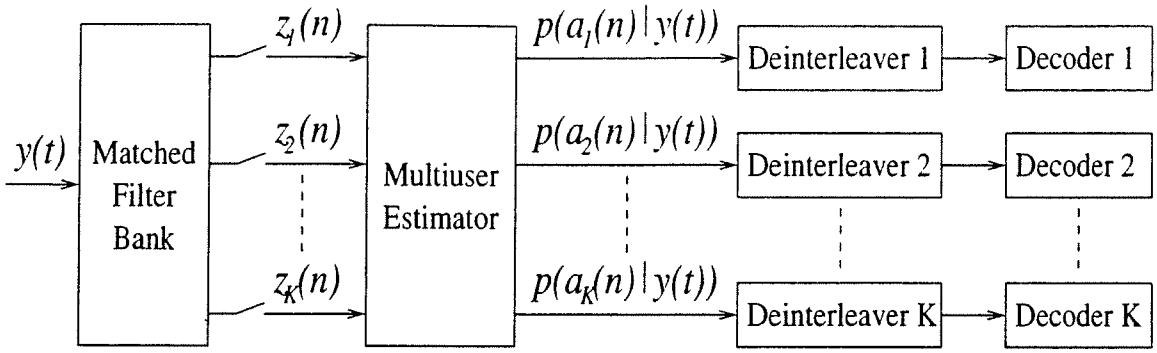

Figure 6.1: Multiuser receiver for a coded DS-CDMA system.

Note that the complexity of MF-OSA(G), where G is the decision lag, is on the order of $2^L(G-L)$. MF-SSA does not require any multiplication operations. However exponentiation operations are needed for soft-output generation. MF-SSA1 avoids most of the exponentiation operations as well. The complexity of MBCDFE(J,G), where J is the memory order chosen, is on the order of $2^J(G-J)$. The modified algorithm requires some extra storage and computational complexity as compared to the original algorithm.

6.6 Application to multiuser estimation

The algorithms described in this chapter are considered for multiuser estimation with error control coding. Fig. 6.1 shows a multiuser receiver for a coded asynchronous DS-CDMA system. The multiuser estimator operates on the discrete-time matched-filter statistics of all users jointly and produces *a-posteriori* probabilities for the coded symbols of all users at the output. These soft outputs are de-interleaved for each user and then fed into the soft-decision decoder for each user separately. The original and modified BCDFE algorithms operate on whitened-matched filter statistics. The corresponding receiver is similar to the receiver of Fig. 6.1 except that it includes a noise-whitening filter which follows the matched filter bank.

6.7 Simulation results

We simulated an asynchronous DS-CDMA system with four users that employ BPSK modulation and rate $\frac{1}{2}$, memory 4 convolutional encoding over an AWGN channel. Code

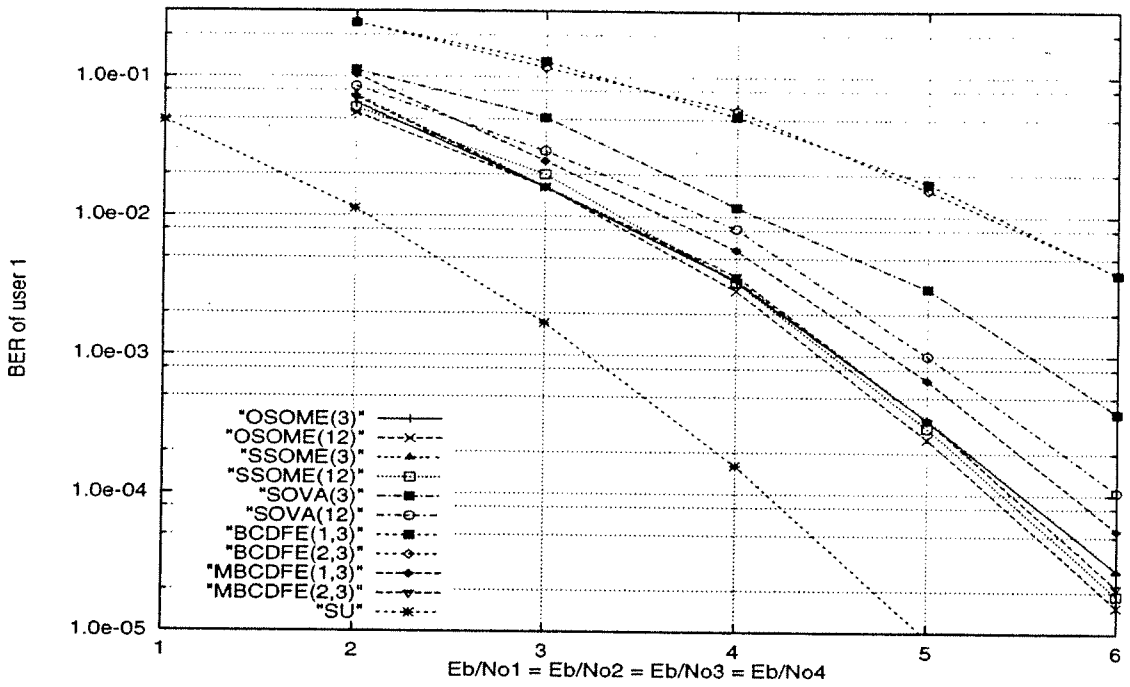

Figure 6.2: BER performance of various algorithms in ideal power control.

symbol sequences of all users are interleaved by a 30×30 interleaver. Each user is assigned a short Gold spreading sequence with 7 chips/coded symbol. The relative delays of users are arbitrarily chosen in an increasing order and are fixed for the simulation. The multiuser channel has the spectrum

$$S(D) = \frac{1}{7}\begin{bmatrix} 7 & -4-D & 1+2D & -D \\ -4-D^{-1} & 7 & -4-D & 3 \\ 1+2D^{-1} & -4-D^{-1} & 7 & -2+D \\ -D^{-1} & 3 & -2+D^{-1} & 7 \end{bmatrix} \tag{6.32}$$

Fig. 6.2 shows the BER of user 1 versus the signal-to-noise ratio (E_b/N_0) in perfect power control. Each simulation was run for a count of 500 errors. It can be seen that the BER curves of OSOME(3), OSOME(12), SSOME(3), SSOME(12) and MBCDFE(2,3) lie in a band of width 0.2 dB. The OSOME(12) algorithm loses about 1.2 dB over coded single user performance. SSOME(3) achieves a $0.4 - 0.5$ dB gain over SOVA(12) in the range $3 - 6$ dB. Note that SSOME(3) requires only state metrics (and no symbol metrics) to be computed. We have not plotted the BER performance for SSOME1 because SSOME1(3)

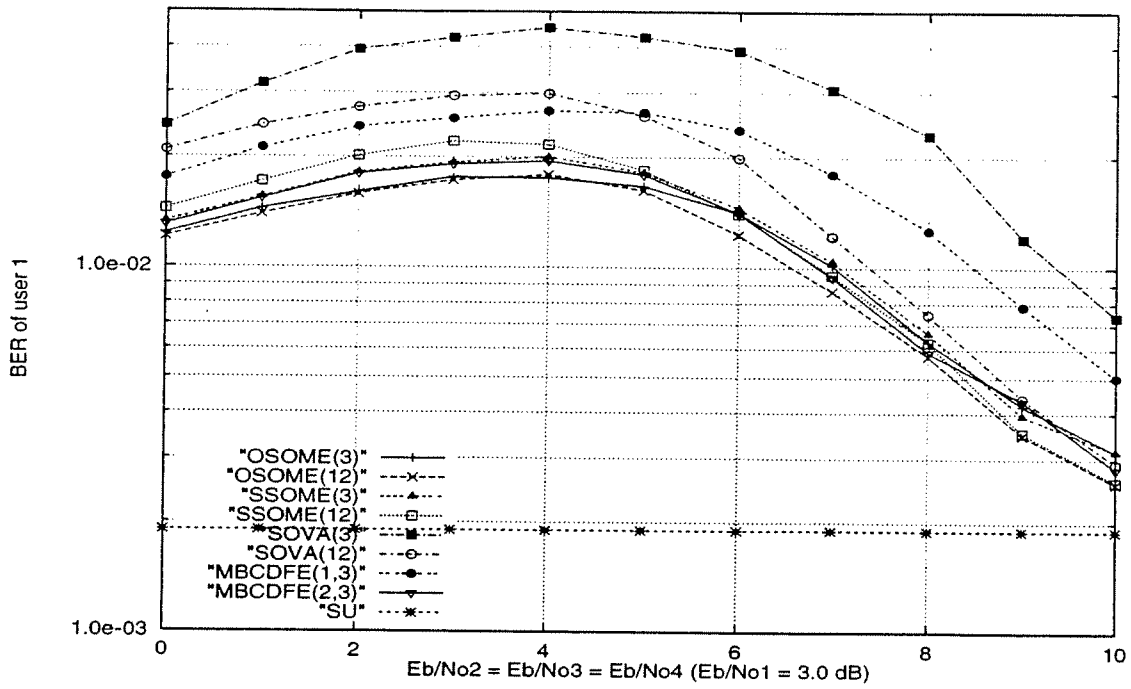

Figure 6.3: BER performance of various algorithms in near-far situation.

(the case of no symbol metrics) is identical to SOVA(3) and SSOME1(12) approaches the performance of SSOME(12). This shows that for small smoothing lags, it is beneficial to average the output symbol soft information over the states in the trellis, as in the case of SSOME. However, for large lags, it is sufficient to obtain the soft information from the most likely state in the trellis, as in SSOME1. The modified BCDFE algorithm with reduced-state trellises gains $1.0-2.0$ dB over the original BCDFE algorithm because the soft outputs of the later are no better than hard decisions.

Fig. 6.3 shows the BER of user 1 versus E_b/N_0 of interfering users (with E_b/N_0 of user 1 fixed at 3.0 dB). 10^5 data symbols were used for each simulation. The BER curves of all schemes tend to single user performance under extreme conditions of multiple-access interference. Thus, Fig. 6.2 depicts almost worst case performance for user 1 given its E_b/N_0. Note that MBCDFE(1,3) outperforms SOVA(12) under power control in moderate E_b/N_0. Although the application of MBCDFE requires noise-whitening, its performance/complexity tradeoff is highly desirable.

6.8 Conclusions

In this chapter, we derived soft-output algorithms for channels with memory which operate on standard matched-filter statistics. The new optimum and sub-optimum soft-output algorithms (MF-OSA and MF-SSA respectively) are similar in structure and complexity to the OSA and the SSA proposed earlier for whitened statistics. The algorithms have low latency as they employ a forward-only recursion. They were considered for multiuser detection in the presence of error control coding. The algorithms are especially suitable for asynchronous DS-CDMA systems with long spreading sequences. Adaptive complexity reduction techniques like the T-algorithm and T-algorithm with soft-limiting, can be applied to reduce the exponential complexity of these algorithms.

We also derived a reduced-state forward-recursive soft-output algorithm that operates on whitened matched-filter statistics. The algorithm generates good quality soft information with reduced complexity. It is obtained by modifying an algorithm proposed earlier which fails to generate good soft information.

CHAPTER 7

Conclusions

In this thesis, we have considered optimal and reduced-complexity techniques for equalization and multiuser detection. New techniques were developed, motivated by analysis of existing techniques and spurred by practical applications. One problem that was tackled was optimal[1] equalization for a wireless communication system with excess signal bandwidth and a fast time-varying medium. A new receiver was proposed which comprises a filter matched to the transmit pulse-shaping filter followed by a fractional-rate sampler and an adaptive Viterbi algorithm. The front-end filter is non-adaptive which is desirable for implementation. The receiver is insensitive to sampler timing phase due to fractional sampling. The Viterbi algorithm exploits the knowledge of the pulse-shaping filter to account for the correlation in the sampled statistics and requires only one-step prediction for medium-response coefficients.

We have presented a unified analysis of decision feedback sequence estimation (DFSE) and M-algorithm receivers for systems with finite memory that examines the effect of the receive filter and the branch metric of the reduced trellis or tree search algorithm. We considered receivers with a front-end filter matched to the overall channel response (standard matched filter) or the transmit filter response (transmit matched filter) and a symbol or fractional-rate sampler. An event error analysis indicates that interference components (bias) arise if there is a mismatch between the receive filter and the branch metric. These components can not be resolved by the trellis or tree search algorithm in a biased receiver and severely limit its error-rate performance. We have shown that an unbiased receiver consists of a standard or transmit matched filter followed by the appropriate noise-whitening

[1] Optimal in the sense of a known time-varying channel.

or zero-forcing filter and a reduced trellis or tree search algorithm with the appropriate metric.

We have compared various trellis-based techniques on the basis of the distance of a given error sequence which characterizes the probability of the associated error event. Our definition of the error distance includes the effect of noise enhancement which is inherent in trellis-based techniques operating on statistics containing non-white noise. This allowed us to compare trellis-based techniques with various receive filters on a fair basis. We showed that whitening filter DFSE (WF-DFSE) has higher error distance than zero-forcing filter DFSE (ZF-DFSE) and truncated-memory MLSE (TM-MLSE) with pre-filtering. Matched filter DFSE (MF-DFSE), in the case of standard matched filtering, achieves the same error distance as an MLSE receiver. Unfortunately, matched-filter type receivers belong to the class of biased receivers. Thus, their error-rate performance is dominated by untreated interference components for most channels in spite of their excellent error distance. After identifying the anti-causal interference components affecting MF-DFSE, we proposed several schemes that utilize tentative decisions to cancel these components. For this purpose, we considered hard and soft tentative decisions obtained in a symbol-by-symbol fashion as well as a multistage configuration.

We have obtained union bounds on the symbol error probability of the various receivers assuming no error propagation. In the case of MF-DFSE, with and without linear soft-input bias-compensation, we applied a Chebyshev technique for upperbounding the error probability in the presence of untreated or residual interference. We have outlined modified generating function methods to evaluate the union bounds. Simulation and analytical results were presented for equalization of inter-symbol interference and multiuser detection for direct-sequence code-division multiple-access (DS-CDMA) systems. The bounds were found to be tight in general for channels with relatively small memory. It was found that soft bias compensation enhances the performance of MF-DFSE for all channels of practical interest. Compensation of just the dominant bias term for MF-DFSE, obtains most of the gain without increasing complexity significantly. The scheme does not require any processing filters like the noise-whitening or zero-forcing filter and is insensitive to channel phase. These attributes make it attractive for multiuser detection for asynchronous DS-CDMA systems and bidirectional equalization for the GSM system.

We have derived soft-output algorithms for channels with memory which operate on

standard matched-filter statistics. The new optimum and sub-optimum algorithms employ a forward-only recursion and have complexity which is exponential in the channel memory only. These algorithms are suitable for soft-output demodulation for a coded multiuser DS-CDMA system. We have also derived a reduced-state soft-output algorithm which operates on whitened statistics. The algorithm provides reliable soft decisions with an adjustable performance/complexity tradeoff. It was obtained by modifying the BCDFE algorithm which fails to provide reliable soft decisions, as we find by means of simulation of a coded DS-CDMA system.

APPENDICES

APPENDIX A

Analysis of the alternative DFSE receiver

Consider the DFSE receiver of Fig. 4.4. Following the treatment given in Section 4.6.1, we see that a first event error occurs at time 0 in the reduced trellis search algorithm of Fig. 4.4 if

$$2\mathrm{Re}\{\underline{\bar{a}}_k^H C_k^H (P^{-1})_k \underline{x}'_k\} - \underline{\bar{a}}_k^H C_k^H R'_k Q'_k C_k \underline{\bar{a}}_k > 2\mathrm{Re}\{\underline{a}_k^H C_k^H (P^{-1})_k \underline{x}'_k\} - \underline{a}_k^H C_k^H R'_k Q'_k C_k \underline{a}_k \tag{A.1}$$

where $\underline{x}'_k = [x'(0), x'(1), \ldots, x'(k-1)]^T$ and the matrices C_k, R'_k and Q'_k are principal submatrices of dimension k of the matrices C, R' and Q' respectively. Using (4.28), (A.1) can equivalently be written as

$$\begin{aligned} 2\mathrm{Re}\{\underline{e}_k^H C_k^H (P^{-1})_k P_{k\times N} \underline{u}'\} \;>\; & \underline{e}_k^H C_k^H R'_k Q'_k C_k \underline{e}_k + 2\mathrm{Re}\{\underline{e}_k^H C_k^H R'_k Q'_k C_k \underline{a}_k\} \\ & - \; 2\mathrm{Re}\{\underline{e}_k^H C_k^H (P^{-1})_k P_{k\times N} \Phi C \underline{a}\} \end{aligned} \tag{A.2}$$

which is the condition for the error event ε defined in Section 4.6.1. The unbiasedness condition for this receiver can then be written as

$$C_k^H (P^{-1})_k P_{k\times N} \Phi C = C_k^H R'_k Q'_k C_k [I_k | O_{k\times N-k}] \quad \forall\, 1 \le k < N \tag{A.3}$$

or equivalently using the fact that $R'_k Q'_k = Q'^H_k R'^H_k$:

$$(P^{-1})_k P_{k\times N} = Q'^H_k (Q'^{-H})_{k\times N} \quad \forall\, 1 \le k < N \tag{A.4}$$

where the matrix $(Q'^{-H})_{k\times N}$ comprises the top k rows of the matrix Q'^{-H}. It follows from (A.2) and (A.3) that the probability of the error event ε for an unbiased DFSE receiver with the front-end filter matched to the transmit filter response, is given by

$$\Pr(\varepsilon) = \mathrm{Q}\left(\frac{\underline{e}_k^H C_k^H R'_k Q'_k C_k \underline{e}_k}{2\sqrt{N_0 \underline{e}_k^H C_k^H R'_k Q'_k (\Phi^{-1})_k R'_k Q'_k C_k \underline{e}_k}} \right). \tag{A.5}$$

An upper bound on the first event error probability is given by (4.62) with the error distance $\delta(\underline{\epsilon})$ in this case defined as

$$\delta(\underline{\epsilon}) \triangleq \frac{\underline{\epsilon}_k^H C_k^H R_k' Q_k' C_k \underline{\epsilon}_k}{\sqrt{\underline{\epsilon}_k^H C_k^H R_k' Q_k' (\Phi^{-1})_k R_k' Q_k' C_k \underline{\epsilon}_k}}. \tag{A.6}$$

APPENDIX B

Filters that satisfy unbiasedness

Let Y be an $N \times N$ Toeplitz matrix with elements

$$y(i,j) = \begin{cases} 1 & i = j \\ y(i-j) & 0 < |i-j| \leq L_y \\ 0 & \text{otherwise} \end{cases} \tag{B.1}$$

Let P^{-1} be the $N \times N$ Toeplitz matrix defined in (4.19) with the diagonal element $p'(0)$ set to 1. Assume that the inverses of the submatrices Y_k and $(P^{-1})_k$ exist for all $k \leq N$.

Proposition B.0.1 *Let* $\max(L_y, l_f, l_p) + 1 < N < \infty$. *If*

$$(P^{-1})_k P_{k\times N} = Y_k (Y^{-1})_{k\times N} \quad \forall\, k = 1, 2, \ldots, N-1 \tag{B.2}$$

then

$$P = Y^{-1}. \tag{B.3}$$

In order to prove the above proposition, we make use of the following lemma [5]:

Lemma B.0.1 *Let* T *be an* $m \times m$ *invertible Toeplitz matrix subdivided into* $k \times k$, $k \times (m-k)$, $(m-k) \times k$ *and* $(m-k) \times (m-k)$ *submatrices* T_{11}, T_{12}, T_{21} *and* T_{22} *as shown below. Then* $S = T^{-1}$ *is partitioned similarly into* S_{11}, S_{12}, S_{21} *and* S_{22}*:*

$$T = \begin{bmatrix} T_{11} & T_{12} \\ T_{21} & T_{22} \end{bmatrix}, \quad S = \begin{bmatrix} S_{11} & S_{12} \\ S_{21} & S_{22} \end{bmatrix},$$

where, assuming T_{11} is invertible.

$$\begin{aligned} S_{11} &= T_{11}^{-1} + T_{11}^{-1}T_{12}(T_{22} - T_{21}T_{11}^{-1}T_{12})^{-1}T_{21}T_{11}^{-1}, \\ S_{12} &= -T_{11}^{-1}T_{12}(T_{22} - T_{21}T_{11}^{-1}T_{12})^{-1}, \\ S_{21} &= -(T_{22} - T_{21}T_{11}^{-1}T_{12})^{-1}T_{21}T_{11}^{-1}, \\ S_{22} &= (T_{22} - T_{21}T_{11}^{-1}T_{12})^{-1}. \end{aligned}$$

Let the matrices P^{-1} and Y be subdivided into $k \times k$, $k \times (N-k)$, $(N-k) \times k$ and $(N-k) \times (N-k)$ submatrices P'_{11}, P'_{12}, P'_{21} and P'_{22} and Y_{11}, Y_{12}, Y_{21} and Y_{22} respectively as shown below

$$P^{-1} = \begin{bmatrix} P'_{11} & P'_{12} \\ P'_{21} & P'_{22} \end{bmatrix}, \quad Y = \begin{bmatrix} Y_{11} & Y_{12} \\ Y_{21} & Y_{22} \end{bmatrix}, \tag{B.4}$$

for $k = 1, 2, \ldots, N-1$. Then, using Lemma B.0.1, (B.2) can be broken into two equations concerning the first k and the last $N-k$ columns of the $k \times N$ matrices on either side of (B.2), given by

$$\begin{aligned} &P'_{11}[P'^{-1}_{11} + P'^{-1}_{11}P'_{12}(P'_{22} - P'_{21}P'^{-1}_{11}P'_{12})^{-1}P'_{21}P'^{-1}_{11}] = \\ &\quad Y_{11}[Y_{11}^{-1} + Y_{11}^{-1}Y_{12}(Y_{22} - Y_{21}Y_{11}^{-1}Y_{12})^{-1}Y_{21}Y_{11}^{-1}] \end{aligned} \tag{B.5}$$

and

$$P'_{11}[-P'^{-1}_{11}P'_{12}(P'_{22} - P'_{21}P'^{-1}_{11}P'_{12})^{-1}] = Y_{11}[-Y_{11}^{-1}Y_{12}(Y_{22} - Y_{21}Y_{11}^{-1}Y_{12})^{-1}] \tag{B.6}$$

respectively for $k = 1, 2, \ldots, N-1$. Substituting (B.6) into (B.5) and simplifying, we get

$$P'_{21}P'^{-1}_{11} = Y_{21}Y_{11}^{-1}. \tag{B.7}$$

Let $k = 1$, then $P'_{11} = Y_{11} = 1$ and (B.7) implies that the first column of the matrix P^{-1} is equal to the first column of the matrix Y. Since P^{-1} and Y are Toepltiz matrices, all elements in the lower triangle of P^{-1} are equal to the corresponding elements of Y, i.e. $P'_{21} = Y_{21}$ for all $k = 1, 2, \ldots, N-1$. Thus, (B.7) implies that

$$P'_{11} = Y_{11} \tag{B.8}$$

for all $k = 1, 2, \ldots, N-1$. Since $N > \max(L_y, l_f, l_p) + 1$, (B.8) involves all non-zero elements of the matrices P^{-1} and Y. Thus,

$$P = Y^{-1}. \tag{B.9}$$

Note that the diagonal elements of the matrices P^{-1} and Y were set to 1 to factor out a scaling factor. In general, we have

$$P = cY^{-1} \tag{B.10}$$

where c is a constant scaling factor.

APPENDIX C

Error distance for ZF-DFSE

Let the matrices S and S^{-1} be subdivided into $k \times k$, $k \times (N-k)$, $(N-k) \times k$ and $(N-k) \times (N-k)$ submatrices S_{11}, S_{12}, S_{21} and S_{22} and S^I_{11}, S^I_{12}, S^I_{21} and S^I_{22} respectively as shown below

$$S = \begin{bmatrix} S_{11} & S_{12} \\ S_{21} & S_{22} \end{bmatrix}, \quad S^{-1} = \begin{bmatrix} S^I_{11} & S^I_{12} \\ S^I_{21} & S^I_{22} \end{bmatrix}. \tag{C.1}$$

Then, using Lemma B.0.1, we get

$$\begin{aligned} S_k(S^{-1})_k S_k &= S_k + S_{12}(S_{22} - S_{21}S_{11}^{-1}S_{12})^{-1}S_{21} \\ &= S_k + S_{12}S^I_{22}S_{21}. \end{aligned} \tag{C.2}$$

For $k \geq L$, we have

$$S_k(S^{-1})_k S_k = S_k + \begin{bmatrix} 0_{k-L} & 0 \\ 0 & \dot{S}^H(S^I_{22})_L\dot{S} \end{bmatrix}. \tag{C.3}$$

Note that for $N \gg L$, S^{-1} is near Toeplitz in the middle of the matrix. Thus, we can replace the matrix $(S^I_{22})_L$ in (C.3) by the principal submatrix S'_L of an $N \times N$ Toeplitz matrix S' with elements $s'(i,j) = s'(i-j)$, given by the inverse z-transform of $1/S(z)$. Thus, for an error sequence $\underline{e} \in E'$ with tail $\underline{\xi}$ as defined in (4.79), we have

$$\underline{e}^H S_k(S^{-1})_k S_k \underline{e} \approx \underline{e}^H S_k \underline{e} + \underline{\xi}^H \dot{S}^H_{L-J} S'_{L-J} \dot{S}_{L-J} \underline{\xi}. \tag{C.4}$$

The error distance for ZF-DFSE(S) given by (4.76) can then be approximated as

$$\delta(\underline{e}) \approx \frac{\underline{e}^H S_k \underline{e}}{\sqrt{\underline{e}^H S_k \underline{e} + \underline{\xi}^H \dot{S}^H_{L-J} S'_{L-J} \dot{S}_{L-J} \underline{\xi}}}. \tag{C.5}$$

The above expression is approximate for error events occurring near the edges of the data burst where the noise correlation is not the same as in the middle, while it is exact for short error events occurring toward the middle of the burst.

Similarly, it can be shown that the error distance for ZF-DFSE(T) given by (4.77) can be approximated as

$$\delta(\underline{e}) \approx \frac{\underline{e}^H C_k^H \Phi_k C_k \underline{e}}{\sqrt{\underline{e}^H C_k^H \Phi_k C_k \underline{e} + \underline{\xi}^H (\ddot{C}_{L_d \times L-J})^H \ddot{\Phi}^H (\Phi')_{L_d} \ddot{\Phi} \ddot{C}_{L_d \times L-J} \underline{\xi}}} \tag{C.6}$$

where Φ' is an $N \times N$ Toeplitz matrix with elements $\phi'(i,j) = \phi'(i-j)$ obtained from the inverse z-transform of $1/\Phi(z)$ (where $\Phi(z)$ is the z-transform of $\{\phi(i)\}$).

APPENDIX D

Error probability of two-stage BC-MF-DFSE(S)

In this appendix, we derive expressions for the probability of a particular error event in a two-stage BC-MF-DFSE receiver with standard matched filtering. The first stage of the receiver is MF-DFSE(S) with memory order J_1 and the second stage is BC-MF-DFSE(S) with memory order J_2. The second stage uses the final decisions of the first stage to cancel bias. A valid error sequence in the first (second) stage does not have J_1 (J_2) consecutive zeros in the middle of the sequence and has J_1 (J_2) consecutive zeros at the end of the sequence. Let E_1 (E_2) be the set of all valid error sequences in the first (second) stage.

It follows from (4.78) that an error event beginning at time l_1 and ending at time l_2 (corresponding to the error sequence $\underline{t} = [t_{l_1}, t_{l_1+1}, \ldots, t_{l_2-1}]^T \in E_1$, $l = l_2 - l_1$) occurs in the first stage (assuming no error propagation from previous error events) if

$$2\mathrm{Re}\{\underline{t}^H \underline{u}'\} > \underline{t}^H S_l \underline{t} - 2\mathrm{Re}\{\underline{t}'^H \dot{S}_{L-J}^H \underline{a}'\} \tag{D.1}$$

where $\underline{u}' = [u_{l_1}, \ldots, u_{l_2-1}]^T$, $\underline{t}' = [t_{l_2-L}, \ldots, t_{l_2-J_1-1}]^T$ and $\underline{a}' = [a_{l_2}, \ldots, a_{l_2+L-J_1-1}]^T$. Given errors $\underline{t}'' = [t_k, \ldots, t_{k+L-J_2-1}]^T$ in the first stage, an error event occurs between times 0 and k (corresponding to the error sequence $\underline{e} = [e_0, e_1, \ldots, e_{k-1}]^T \in E_2$) in the second stage if

$$2\mathrm{Re}\{\underline{e}^H \underline{u}''\} > \underline{e}^H S_k \underline{e} + 2\mathrm{Re}\{\underline{e}''^H \dot{S}_{L-J}^H \underline{t}''\}. \tag{D.2}$$

where $\underline{u}'' = [u_0, \ldots, u_{k-1}]^T$ and $\underline{e}'' = [e_{k-L}, \ldots, e_{k-J_2-1}]^T$. Note that the sequence of tentative decision errors $\underline{t}''$ can be the result of several contiguous error events[1] in the first stage. We assume that $\underline{t}''$ can result from at most one error event in the first stage. This assumption is actually true for $J_1 \geq L - J_2 - 1$.

[1] Error events in the first stage are separated by at least J_1 consecutive correct decisions.

Let T be the set of all error sequences $\underline{t} \in E_1$ that include $\underline{t}''$ as a subsequence. Let $X = 2\mathrm{Re}\{\underline{e}^H \underline{u}''\}$ and $Y = 2\mathrm{Re}\{\underline{t}^H \underline{u}'\}$. Given $\underline{e} \in E_2$, $\underline{t} \in T$ and $\underline{a}' \in \mathcal{A}^{L-J_1}$, X and Y are jointly Gaussian random variables with means zero, variances $\sigma_X^2 = 4N_0 \underline{e}^H S_k \underline{e}$ and $\sigma_Y^2 = 4N_0 \underline{t}^H S_l \underline{t}$ respectively, and covariance

$$\mathrm{E}[XY^*] = \sum_{n=0}^{k-1} \sum_{m=l_1}^{l_2-1} 4N_0 \mathrm{Re}\{e_n^* s(n-m) t_m\}. \tag{D.3}$$

The joint probability of occurrence of $\underline{e} \in E_2$ and $\underline{t} \in T$ is given by

$$\Pr(\underline{e}, \underline{t}) = \sum_{\underline{a}' \in \mathcal{A}^{L-J_1}} \left[\int_{x_1}^{\infty} \int_{y_1}^{\infty} f_{XY}(x,y) dx dy \right] P_{\underline{a}'} \tag{D.4}$$

where $x_1 = \underline{e}^H S_k \underline{e} + 2\mathrm{Re}\{\underline{e}''^H \dot{S}_{L-J}^H \underline{t}''\}$ and $y_1 = \underline{t}^H S_l \underline{t} - 2\mathrm{Re}\{\underline{t}'^H \dot{S}_{L-J}^H \underline{a}'\}$. The probability that the error event ε: $\underline{e} \in E_2$ occurs in the second stage is thus given by

$$\Pr(\varepsilon) = \mathrm{Q}\left(\frac{1}{2} \sqrt{\frac{\underline{e}^H S_k \underline{e}}{N_0}} \right) \Pr(\underline{t}'' = \underline{0}) + \sum_{\underline{t} \in T'} \Pr(\underline{e}, \underline{t}) \tag{D.5}$$

where T' is a subset of the set T which includes all error sequences in T except those for which $\underline{t}'' = \underline{0}$. Note that $\Pr(\underline{t}'' = \underline{0})$ can be over-bounded by 1[2]. Thus, we get

$$\Pr(\varepsilon) \leq \mathrm{Q}\left(\frac{1}{2} \sqrt{\frac{\underline{e}^H S_k \underline{e}}{N_0}} \right) + \sum_{\underline{t} \in T'} \Pr(\underline{e}, \underline{t}). \tag{D.6}$$

Assuming independence between errors occurring in the two stages (i.e. independent X and Y), we get

$$\begin{aligned} \Pr(\varepsilon) \tilde{\leq} \; & \mathrm{Q}\left(\frac{1}{2} \sqrt{\frac{\underline{e}^H S_k \underline{e}}{N_0}} \right) + \sum_{\underline{t} \in T'} \sum_{\underline{a}' \in \mathcal{A}^{L-J_1}} \mathrm{Q}\left(\frac{\underline{e}^H S_k \underline{e} + 2\mathrm{Re}\{\underline{e}''^H \dot{S}_{L-J}^H \underline{t}''\}}{2\sqrt{N_0 \underline{e}^H S_k \underline{e}}} \right) \\ & \mathrm{Q}\left(\frac{\underline{t}^H S_l \underline{t} - 2\mathrm{Re}\{\underline{t}'^H \dot{S}_{L-J}^H \underline{a}'\}}{2\sqrt{N_0 \underline{t}^H S_l \underline{t}}} \right) P_{\underline{a}'}. \end{aligned} \tag{D.7}$$

[2]The bound becomes asymptotically tight at high signal-to-noise ratio.

BIBLIOGRAPHY

BIBLIOGRAPHY

[1] K. Abend and B. D. Fritchman, "Statistical detection for communication channels with intersymbol interference," *Proceedings of the IEEE*, vol. 58, no. 5, pp. 778–795, May 1970.

[2] J. B. Anderson and S. Mohan, "Sequential coding algorithms: A survey cost analysis," *IEEE Transactions on Communications*, vol. 32, pp. 169–176, February 1984.

[3] L. Bahl, J. Cocke, F. Jelinek, and J. Raviv, "Optimal decoding of linear codes for minimizing symbol error rate," *IEEE Transactions on Information Theory*, vol. IT-20, no. 3, pp. 284–287, March 1974.

[4] J. W. M. Bergmans, *Digital Baseband Transmission and Recording*, Boston: Kluwer Academic Publishers, 1996.

[5] A. Bjorck, *Large Scale Matrix Problems*, New York: Elsevier North Holland, 1981.

[6] G. E. Bottomley and S. Chennakeshu, "Unification of MLSE receivers and extension to time-varying channels," *IEEE Transactions on Communications*, vol. 46, no. 4, pp. 464–472, April 1998.

[7] A. Duel and C. Heegard, "Delayed decision feedback sequence estimation for QAM and trellis coded systems," *Conference on Information Siences and Systems*, vol. 20, pp. 367–372, March 1986.

[8] A. Duel and C. Heegard, "Delayed decision-feedback sequence estimation," *IEEE Transactions on Communications*, vol. 37, no. 5, pp. 428–436, May 1989.

[9] A. Duel-Hallen, *Detection algorithms for Intersymbol Interfence Channels*, PhD thesis, Cornell University, August 1987.

[10] V. M. Eyuboglu and S. U. H. Qureshi, "Reduced-state sequence estimation with set partitioning and decision feedback," *IEEE Transactions on Communications*, vol. 36, no. 1, pp. 13–20, January 1988.

[11] V. M. Eyuboglu and S. U. H. Qureshi, "Reduced-state sequence estimation for coded modulation on intersymbol interference channels," *IEEE Journal on Selected Areas in Communications*, vol. 7, no. 6, pp. 989–995, August 1989.

[12] D. D. Falconer and F. R. Magee Jr., "Adaptive channel memory truncation for maximum likelihood sequence estimation," *Bell Systems Technical Journal*, vol. 52, pp. 1541–1562, November 1973.

[13] G. D. Forney, "Maximum-likelihood sequence estimation of digital sequences in the presence of intersymbol interference," *IEEE Transactions on Information Theory*, vol. IT-18, no. 3, pp. 363–378, May 1972.

[14] G. J. Foschini, "A reduced state variant of maximum likelihood sequence detection attaining optimum performance for high signal-to-noise ratios," *IEEE Transactions on Information Theory*, vol. 23, pp. 605–609, September 1977.

[15] T. Frey and M. Reinhardt, "Signal estimation for interference cancellation and decision feeedback equalization," *IEEE Vehicular Technology Conference*, pp. 155–159, 1997.

[16] F. E. Glave, "An upper bound on the probability of error due to intersymbol interference for correlated digital signals," *IEEE Transactions on Information Theory*, vol. IT-18, pp. 356–363, May 1972.

[17] A. Hafeez and W. E. Stark, "Decision feedback sequence estimation for unwhitened ISI channels," *Annual Allerton Conference on Communication, Control and Computing*, vol. 35, pp. 493–502, September 1997.

[18] A. Hafeez and W. E. Stark, "Soft-output multiuser estimation for asynchronous CDMA channels," *IEEE Vehicular Technology Conference*, vol. 47, pp. 465–469, May 1997.

[19] A. Hafeez and W. E. Stark, "Decision feedback sequence estimation for unwhitened ISI and multiuser CDMA channels," *IEEE Vehicular Technology Conference*, pp. 424–429, May 1998.

[20] A. Hafeez and W. E. Stark, "Decision feedback sequence estimation for unwhitened ISI channels with applications to multiuser detection," *IEEE Journal on Selected Areas in Communications*, vol. 16, no. 9, pp. 1785–1795, December 1998.

[21] J. Hagenauer and P. Hoeher, "A Viterbi algorithm with soft-decision outputs and its applications," *Proceedings of Globecom*, vol. 3, pp. 47.1.1–47.1.7, November 1989.

[22] K. Hamied and G. L. Stuber, "A fractionally spaced MLSE receiver," *IEEE International Conference on Communication*, pp. 7–11, 1995.

[23] J. F. Hayes, T. M. Cover, and J. B. Riera, "Optimal sequence detection and optimal symbol-by-symbol detection: Similar algorithms," *IEEE Transactions on Communications*, vol. COM-30, no. 1, pp. 152–157, January 1982.

[24] H. Kubo, K. Murakami, and T. Fujino, "An adaptive maximum-likelihood sequence estimator for fast time-varying intersymbol interference channels," *IEEE Transactions on Communications*, vol. 42, pp. 1872–1880, Feb./Mrach/April 1994.

[25] G. Lee, S. B. Gelfand, and M. P. Fitz, "Bayesian decision feedback techniques for deconvolution," *IEEE Journal on Selected Areas in Communications*, vol. 13, no. 1, pp. 155–165, January 1995.

[26] W. U. Lee and F. S. Hill Jr., "A maximum likelihood sequence estimator with decision feedback equalization," *IEEE Transactions on Communications*, vol. COM-25, pp. 971–980, September 1977.

[27] A. Leon-Garcia, *Probability and Random Processes for Electrical Engineering*, Reading: Addison-Wesley, 2nd edition, 1994.

[28] Y. Li, B. Vucetic, and Y. Sato, "Optimum soft-output detection for channels with intersymbol interference," *IEEE Transactions on Information Theory*, vol. IT-41, no. 3, pp. 85–96, May 1995.

[29] S. Lin and D. J. Costello Jr., *Error Control Coding: Fundamentals and Applications*, New Jersey: Prentice-Hall, 1983.

[30] Q. Liu and Y. Wan, "A unified MLSE detection technique for TDMA digital cellular radio," *IEEE Vehicular Technology Conference*, pp. 265–268, 1993.

[31] J. W. Matthews, "Sharp error bounds for intersymbol interference," *IEEE Transactions on Information Theory*, vol. IT-19, pp. 440–447, July 1973.

[32] P. J. McLane, "A residual interference error bound for truncated-state Viterbi detectors," *IEEE Transactions on Information Theory*, vol. IT-26, pp. 549–553, September 1980.

[33] K. Okanoue, A. Ushirokawa, H. Tomita, and Y. Furuya, "New MLSE receiver free from sample timing and input level controls," *IEEE Vehicular Technology Conference*, pp. 408–411, 1993.

[34] S. U. H. Qureshi, "Adaptive equalization," *Proceedings of the IEEE*, vol. 73, no. 9, pp. 1349–1387, September 1985.

[35] S. U. H. Qureshi and E. E. Newhall, "An adaptive receiver for data transmission over time-dispersive channels," *IEEE Transactions on Information Theory*, vol. IT-19, pp. 448–457, July 1973.

[36] M. Rupf, F. Turkoy, and J. L. Massey, "User-separating demodulation for code-division multiple-access systems," *IEEE Journal on Selected Areas in Communications*, vol. 12, no. 5, pp. 786–795, June 1994.

[37] C. Schlegel, "The receiver filter influence on reduced-state trellis decoding on channels with ISI," *IEEE Transactions on Vehicular Technology*, 1995. Under revision.

[38] N. Seshadri, "Joint data and channel estimation using blind trellis search algorithms," *IEEE Transactions on Communications*, vol. 42, pp. 1000–1011, Feb./Mrach/April 1994.

[39] W. Sheen and G. L. Stuber, "Error probability for reduced-state sequence estimation," *IEEE Journal on Selected Areas in Communications*, vol. 10, no. 3, pp. 571–578, April 1992.

[40] G. Ungerboeck, "Adaptive maximum-likelihood receiver for carrier-modulated data-transmission systems," *IEEE Transactions on Communication Technology*, vol. COM-22, no. 5, pp. 624–636, May 1974.

[41] H. L. VanTrees, *Detection, Estimation and Modulation Theory Part III: Radar-Sonar Signal Processing and Gaussian Signals in Noise*, New York: John Wiley & Sons, 1968.

[42] S. Verdú. *Optimum multiuser signal detection*. PhD thesis, University of Illinois at Urbana-Champaign, August 1984.

[43] S. Verdú, "Minimum probability of error for asynchronous gaussian multiple-access channels," *IEEE Transactions on Information Theory*, vol. IT-32, no. 1, pp. 85–96, January 1986.

[44] S. Verdú, *Multiuser Detection*, New York: Cambridge University Press, 1998.

[45] F. L. Vermeulen and M. E. Hellman, "Reduced state Viterbi decoders for channels with intersymbol interference," *IEEE International Conference on Communication*, pp. 37B–1–37B–4, 1974.

[46] A. Viterbi and J. K. Omura, *Principles of Digital Communication and Coding*, McGraw-Hill, 1979.

[47] L. Wei and L. K. Rasmussen, "A near ideal noise whitening filter for an asynchronous time-varying CDMA system," *IEEE Transactions on Communications*, vol. 44, no. 10, pp. 1355–1361, October 1996.

[48] L. Wei, L. K. Rasmussen, and R. Wyrwas, "Near optimum tree-search detection schemes for bit-synchronous multiuser CDMA systems over gaussian and two-path rayleigh-fading channels," *IEEE Transactions on Communications*, vol. 45, no. 6, pp. 691–700, June 1997.

[49] K. Wesolowski, "An efficient DFE & ML suboptimum receiver for data transmission over dispersive channels using two-dimensional signal constellations," *IEEE International Symposium on Information Theory*, pp. 23–28, June 1985.

[50] K. Wesolowski, R. Krenz, and K. Das, "Efficient receiver structure for GSM mobile radio," *International Journal on Wireless Information Networks*, vol. 3, no. 2, pp. 117–122, 1996.

[51] Z. Xie, C. Rushforth, R. Short, and T. K. Moon, "Joint signal detecetion and parameter estimation in multiuser communications," *IEEE Transactions on Communications*, vol. 41, pp. 1208–1215, August 1993.